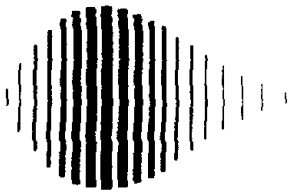

NATIONAL CENTER FOR EARTHQUAKE
ENGINEERING RESEARCH
State University of New York at Buffalo

MODELING OF R/C BUILDING STRUCTURES WITH FLEXIBLE FLOOR DIAPHRAGMS (IDARC2)

by

A. M. Reinhorn, S. K. Kunnath and N. Panahshahi
Department of Civil Engineering
State University of New York at Buffalo
Buffalo, New York 14260

Technical Report NCEER-88-0035

September 7, 1988

This research was conducted at State University of New York at Buffalo and was partially supported by the National Science Foundation under Grant No. ECE 86-07591.

NOTICE

This report was prepared by State University of New York at Buffalo as a result of research sponsored by the National Center for Earthquake Engineering Research (NCEER). Neither NCEER, associates of NCEER, its sponsors, State University of New York at Buffalo or any person acting on their behalf:

a. makes any warranty, express or implied, with respect to the use of any information, apparatus, method, or process disclosed in this report or that such use may not infringe upon privately owned rights; or

b. assumes any liabilities of whatsoever kind with respect to the use of, or the damage resulting from the use of, any information, apparatus, method or process disclosed in this report.

50272-101

REPORT DOCUMENTATION PAGE	1. REPORT NO. NCEER 88-0035	2.	3. Recipient's Accession No. PB89-207153/AS
4. Title and Subtitle: Modeling of R/C Building Structures with Flexible Floor Diaphragms (IDARC2)			5. Report Date: September 7, 1988 6.
7. Author(s): A.M. Reinhorn, S.K. Kunnath and N. Panahshahi			8. Performing Organization Rept. No.
9. Performing Organization Name and Address			10. Project/Task/Work Unit No. 11. Contract(C) or Grant(G) No. (C) 87-1005, ECE 86-07591 (G)
12. Sponsoring Organization Name and Address: National Center for Earthquake Engineering Research, State University of New York at Buffalo, Red Jacket Quadrangle, Buffalo, NY 14261			13. Type of Report & Period Covered: Technical Report 14.

15. Supplementary Notes

This research was conducted at the State University of New York at Buffalo and was partially supported by the National Science Foundation under Grant No. 86-07591.

16. Abstract (Limit: 200 words)

An analytical modeling scheme has been developed to include the effects of inelastic in-plane diaphragm flexibility in the analysis of reinforced concrete building structures. The floor-slab model has been incorporated into the existing framework of a computer code for Inelastic Damage Analysis of Reinforced Concrete frame shear-wall structures, IDARC. The revised computer code (IDARC2) has been used in parametric and correlation studies primarily to design a shaking table study of a single story 1:6 scale micro-concrete model.

The results of the preliminary analytical studies indicates that the in-plane floor flexibility can be a dominant factor on seismic response (i.e., overall dynamic characteristics and lateral force distribution) for rectangular shear-wall-frame buildings. The inplane deflections of the floor diaphragms impose larger strength and ductility demands on the columns of the flexible frames than is usually provided in such columns. The assumption of rigid floor diaphragms results in a non-conservative design of flexible frames. This can cause severe damage in these frames which eventually can lead to loss of vertical load carrying capacity of the columns with disastrous consequences. A user guide for the revised computer program is included to enable use of this program for other applications.

17. Document Analysis a. Descriptors

b. Identifiers/Open-Ended Terms

COMPUTER CODES	FLEXIBLE DIAPHRAGMS	STATIC ANALYSIS
DAMAGE ANALYSIS	FLOORS	SHAKING TABLE TESTS
DYNAMIC RESPONSE ANALYSIS	HYSTERESIS MODELS	SEISMIC RESPONSE
EARTHQUAKE ENGINEERING	REINFORCED CONCRETE	
c. COSATI Field/Group	SEQUENTIAL FAILURE MODE ANALYSIS	

18. Availability Statement	19. Security Class (This Report)	21. No. of Pages
Release Unlimited	Unclassified	129
	20. Security Class (This Page) Unclassified	22. Price A07

N O T I C E

THIS DOCUMENT HAS BEEN REPRODUCED FROM THE BEST COPY FURNISHED US BY THE SPONSORING AGENCY. ALTHOUGH IT IS RECOGNIZED THAT CERTAIN PORTIONS ARE ILLEGIBLE, IT IS BEING RELEASED IN THE INTEREST OF MAKING AVAILABLE AS MUCH INFORMATION AS POSSIBLE.

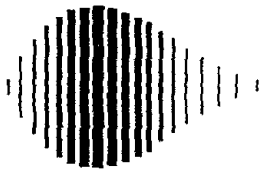

MODELING OF R/C BUILDING STRUCTURES WITH FLEXIBLE FLOOR DIAPHRAGMS (IDARC2)

by

Andrei M. Reinhorn[1], Sashi K. Kunnath[2] and Nader Panahshahi[3]

September 7, 1988

Technical Report NCEER-88-0035

NCEER Contract Number 87-1005

NSF Master Contract Number ECE 86-07591

1 Associate Professor, Department of Civil Engineering, State University of New York at Buffalo
2 Graduate Research Assistant, Department of Civil Engineering, State University of New York at Buffalo
3 Research Associate, Department of Civil Engineering, State University of New York at Buffalo

NATIONAL CENTER FOR EARTHQUAKE ENGINEERING RESEARCH
State University of New York at Buffalo
Red Jacket Quadrangle, Buffalo, NY 14261

PREFACE

The National Center for Earthquake Engineering Research (NCEER) is devoted to the expansion and dissemination of knowledge about earthquakes, the improvement of earthquake-resistant design, and the implementation of seismic hazard mitigation procedures to minimize loss of lives and property. The emphasis is on structures and lifelines that are found in zones of moderate to high seismicity throughout the United States.

NCEER's research is being carried out in an integrated and coordinated manner following a structured program. The current research program comprises four main areas:

- Existing and New Structures
- Secondary and Protective Systems
- Lifeline Systems
- Disaster Research and Planning

This technical report pertains to Program 1, Existing and New Structures, and more specifically to system response investigations.

The long term goal of research in Existing and New Structures is to develop seismic hazard mitigation procedures through rational probabilistic risk assessment for damage or collapse of structures, mainly existing buildings, in regions of moderate to high seismicity. The work relies on improved definitions of seismicity and site response, experimental and analytical evaluations of systems response, and more accurate assessment of risk factors. This technology will be incorporated in expert systems tools and improved code formats for existing and new structures. Methods of retrofit will also be developed. When this work is completed, it should be possible to characterize and quantify societal impact of seismic risk in various geographical regions and large municipalities. Toward this goal, the program has been divided into five components, as shown in the figure below:

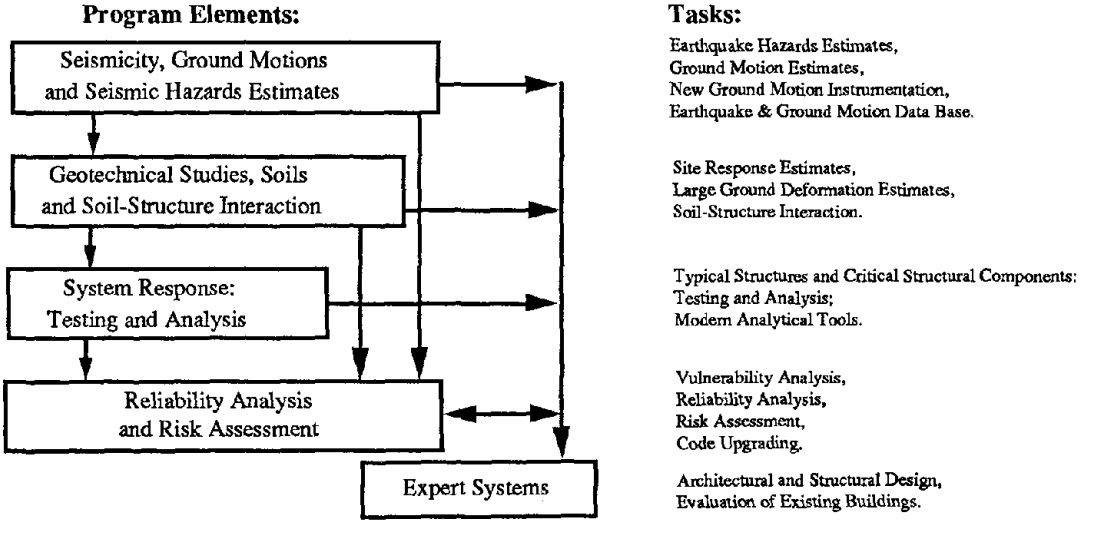

System response investigations constitute one of the important areas of research in Existing and New Structures. Current research activities include the following:

1. Testing and analysis of lightly reinforced concrete structures, and other structural components common in the eastern United States such as semi-rigid connections and flexible diaphragms.
2. Development of modern, dynamic analysis tools.
3. Investigation of innovative computing techniques that include the use of interactive computer graphics, advanced engineering workstations and supercomputing.

The ultimate goal of projects in this area is to provide an estimate of the seismic hazard of existing buildings which were not designed for earthquakes and to provide information on typical weak structural systems, such as lightly reinforced concrete elements and steel frames with semi-rigid connections. An additional goal of these projects is the development of modern analytical tools for the nonlinear dynamic analysis of complex structures.

This report describes one phase of an experimental and analytical research project on flexible floor diaphragms. The computer program IDARC was extended to include a nonlinear in-plane floor flexibility macro-model, and it was used to study the inelastic response of reinforced concrete building frames. The model considers three-dimensional effects, in-plane shear, bending, and out-of-plane bending. The effect of floor deformation was found to be significant; for example, the distribution of forces to parallel frames. The program was used to plan a shaking table test of a three-dimensional frame with a flexible floor.

ABSTRACT

An analytical modeling scheme has been developed to include the effects of inelastic in-plane diaphragm flexibility in the analysis of R/C building structures. The floor-slab model has been incorporated into the existing framework of a computer code for Inelastic Damage Analysis of Reinforced Concrete frame shear-wall structures, IDARC [17].

The revised computer code (IDARC2) has been used in parametric and correlation studies primarily to design a shaking table study of a single story 1:6 scale micro-concrete model.

A generalized technique for the evaluation of the flexural capacity of floor slabs is also developed. The analytical strength envelope is modified, based on observed experimental data, to fit a trilinear curve which enables the subsequent hysteretic component modeling. Shear capacity computations are derived from empirical models originally developed for shear walls. Inelastic bending and shear are modeled using the *three-parameter hysteretic model* [17].

The assembled macro-models of the floor-slab system along with the rest of the super structure are analysed in a four step process: (a) static analysis for dead and live loads to establish initial stress states in the system; (b) sequential failure mode analysis under monotonic lateral loading where progressive structural yielding may be monitored; (c) step-by-step dynamic response analysis with single-step force equilibrium check; and (d) qualitative damageability analysis using a normalized damage index.

Preliminary analytical predictions of the response to seismic excitations are reported for the scaled model designed for experimental studies. Subsequently, the influence of diaphragm flexibility on the redistribution of stresses to the vertical supporting system is studied. Numerical examples are presented as part of the response evaluation studies. A user guide for the revised computer program is included to enable use of this program for other applications.

The results of the preliminary analytical studies indicates that the in-plane floor flexibility can be a dominant factor on seismic response (i.e., overall dynamic characteristics and lateral force distribution) for rectangular shear-wall-frame buildings. The in-plane deflections of the floor diaphragms impose larger strength and ductility demands on the columns of the flexible frames than is usually provided in such columns. The assumption of rigid floor diaphragms results in a non-conservative design of flexible frames. This can cause severe damage in these frames which eventually can lead to loss of vertical load carrying capacity of the columns with disastrous consequences.

Preceding page blank

ACKNOWLEDGEMENTS

This study was made possible in part by funding from the National Center for Earthquake Engineering Research (grant Nos. NCEER-86-3032 and 87-1005) which in turn is supported by NSF grant ECE-86-07591. The support is gratefully acknowledged.

The authors wish to express their sincere thanks to Dr. Young Park for his contribution during the initial phase of this project; to Mr. Lee Fang for carrying out the numerical testing of the sample structure in Chapter V; and to Mr. Hector Velasco for drafting the figures.

TABLE OF CONTENTS

TABLE OF CONTENTS (CONTINUED)

LIST OF ILLUSTRATIONS

LIST OF ILLUSTRATIONS (CONTINUED)

LIST OF TABLES

SECTION 1
INTRODUCTION

Floor slabs in multi-story buildings serve two important functions while acting integrally with the rest of the structure to resist vertical and lateral loads: (a) transmission of gravity loads to the vertical structural system in which the primary action in the slab is out-of-plane bending and (b) distribution of lateral loads to the vertical structural system, an action that is primarily controlled by the in-plane stiffness of the floor-slab system. Of these, the former problem has been studied extensively and the analytical tools necessary to predict out-of-plane slab behavior are readily available. In-plane action, however, has not yet been clearly understood and, therefore, forms the focus of the present analytical development.

When a building is subjected to severe lateral forces, such as an earthquake, the inertial forces generated in the floor slabs must be transferred to the vertical structural system through the *diaphragm action* of the slabs. In many structures, this distribution can be approximated by assuming that the slabs are infinitely rigid in their plane. However, for structures where the stiffness of the vertical system and the stiffness of the horizontal slab system does not differ greatly, the influence of diaphragm flexibility must be explicitly considered in analysis. Recent research has indicated that the distribution of lateral forces is greatly affected by diaphragm flexibility, especially when significant cracking and yielding occurs in the floor-slab system.

1.1 Modeling of In-Plane Flexibility of Slabs - A Review

The conventional assumption that floor slabs are rigid in their own plane has been questioned as early as 1961 [2]. Goldberg and Herness [7] used slope deflection equations to study mode shapes of multi-story buildings in which the slab elements were modeled as beams. The effects of diaphragm flexibility under combined bending and torsion was assessed by Coull and Adams [6]. Another simplified analysis using the force method was suggested by Karadogan [12]. Rutenberg [19] analysed a class of buildings with flexible floors using the analogy between shear and axial forces thereby allowing the in-plane effects to be studied using plane frame procedures. Analytical solutions based on differential equations of equilibrium have also been derived [9], however, due to the *closed-form* nature of the analytical procedure, the suitability of the technique for analysis of large building structures is limited.

Approximate schemes have been used extensively in combination with available computer programs - such as SAP IV, TABS80 and COMBAT to model in-plane effects of floor slabs in large building structures [3,4].

However, all of the above analyses have been performed in the linear elastic range, a state in which true effects of slab flexibility are not reflected.

Finite element schemes to model slabs have since become popular due to the three-dimensional nature of the loading and behavior of slabs. Unemori et al. [20] were among the first to use such a scheme though the analysis was carried out in the elastic range. His results indicate that slab flexibility should be taken into account for relatively short buildings, with five or less stories. Recently, Chen [5] extended the technique to the inelastic range and demonstrated the effectiveness of the method in analysing slab elements under monotonic and cyclic loading.

A comprehensive analytical and testing program to study effects of in-plane slab flexibility has been underway at Lehigh University. Recently published material [12,16,18] presented constitutive relations and finite element procedures in particular for beam-supported and ribbed slabs.

The state-of-the-art is, therefore, restricted to rigorous finite element techniques for independent slab elements or the comprehensive analysis of large building structures with approximate treatment of floor slabs. For reinforced concrete structures, general modeling schemes available for fully inelastic analysis are unavailable.

1.2 Scope and Objectives of Present Study

The primary objective of the study is to understand the effect of diaphragm flexibility on the redistribution of lateral forces to the vertical structural system after the floor slab system has undergone inelastic yielding. The prerequisite for such a study is the development of an analytical tool that is capable of analyzing inelastic building systems in which the effects of in-plane slab flexibility has been incorporated.

Recently, an enhanced computer code, IDARC, for the inelastic analysis of R/C buildings was developed [17]. Considering its suitability for the modeling of large frame-wall structural systems, it was decided that an inelastic flexible diaphragm element be incorporated into the framework of the modeling scheme of IDARC.

The present study comprises the following tasks:

1. Global modeling of building structures with *inelastic* flexible floor diaphragms in which consideration is given primarily to in-plane flexibility.

2. The establishment of flexural and shear envelopes for the hysteretic modeling of slab systems.

3. The definition and incorporation of flexible floor slab elements into the existing framework of the computer program IDARC.

4. Parametric and correlation studies of building systems to identify behavior patterns arising from the influence of diaphragm flexibility.

This study is the first phase of a comprehensive study on the influence of flexibility and inelastic behavior near collapse of slabs. The analytical model developed herein is used for the design of experimental models and the shaking table testing program using 1:6 scaled specimens. Consequently, the results of the shaking table study, in turn, will help calibrate the macro-models used in the proposed analytical schemes.

SECTION 2
STRUCTURE MODELING

The structural idealization of three-dimensional (3D) buildings forms the basis of the modeling capabilities of IDARC. IDARC is a computer program for two-dimensional analysis of 3D building systems in which a set of frames parallel to the loading direction are interconnected by transverse elements to permit flexural-torsional coupling. The structural model is capable of integrating ductile moment-resisting frames with shear wall models and out-of-plane elements, thereby enabling a realistic modeling of the overall structural system. Some of the highlights of IDARC, which represent a significant advance over other available computer programs for macro-modeling of R/C structures, are listed below:

- a **flexibility approach** to construct the element stiffness matrices which allows for the variation of the contraflexure point (within or outside the element);
- a **general hysteretic model** that is capable of accounting for the three main behavior patterns in R/C components: *stiffness degradation, strength deterioration and pinching*, respectively;
- the use of a **non-symmetric trilinear envelope curve** that distinguishes cracking and yielding;
- **in-core determination of the trilinear envelope parameters** based on identification studies. In fact, this feature alone makes this approach extremely attractive for interpretation of experimental data from monotonic or shaking-table testing where initial parametric studies have to be carried out before arriving at final model specifications;
- the **separation of shear and flexure** in floor slabs and walls, thereby allowing them to be modeled independently;
- the expression of response values in more meaningful quantities (i.e., *damage indices*) so that an interpretation of the damage sustained by the structure is possible.

The details of the development of the analytical schemes may be found in an earlier publication [17] though some of the essential details are presented in this report for clarity and completeness of the present study.

2.1 Modeling of Structural System

A reinforced concrete building is idealized as a series of plane frames linked together by flexible floor slabs and transverse beams. Each frame must lie in the same vertical plane. Consequently, a building is modeled using the following six element types:

(i) Floor Slabs
(ii) Beams
(iii) Columns
(iv) Shear Walls
(v) Edge Columns
(vi) Transverse Beams

A discretized section of a building using all of the above element types is shown in Fig.2.1. Beams and columns are modeled as continuous equivalent shear-flexure springs. Floor slabs and shear walls are modeled using a pair of shear and flexure springs connected in series. Edge column elements can be modeled separately using inelastic axial springs. Transverse elements which contribute to the stiffness of the building are assumed to have an effect on both the vertical and rotational deformation of the shear walls or main beams to which they are connected and are modeled using elastic linear and rotational springs.

Distributed Flexibility Model.- The inelastic single-component model used in the analysis of beams, columns, floor slabs and shear walls uses a distributed flexibility approach. The flexibility factor, $1/EI$, in this model is assumed to be linearly distributed along the member between the two critical sections at the ends and the point of contraflexure. The flexural factors at the critical sections are monitored throughout the analysis to keep updated the inelastic behavior of the components during the load history; an elastic property is given to the section at the contraflexure point.

2.2 NEW MODEL: Flexible Floor Slabs

Diaphragm action in floor slabs can be compared to the action of shear walls placed in a horizontal position. Hence, if a slab is modeled exactly as a shear wall in the horizontal plane, its response to in-plane loading must be reasonably adequate. However, a major difference arises: while the response of shear walls to vertical loads is in-plane compression/tension, the response

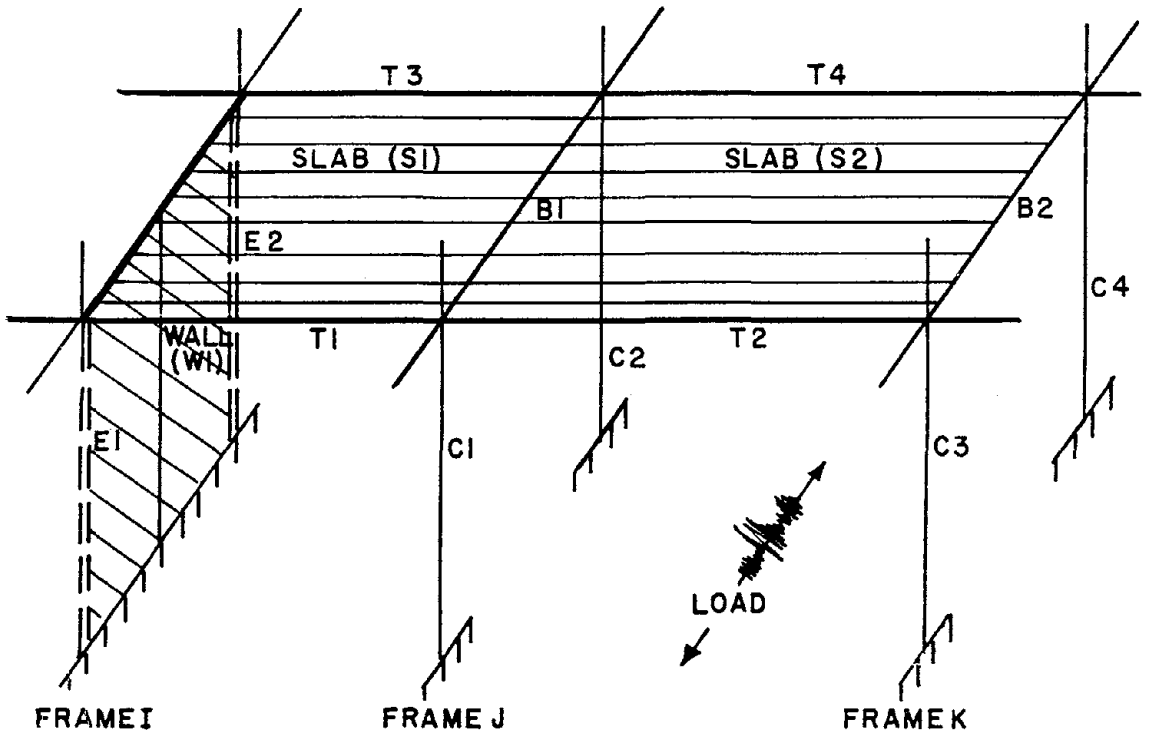

Notation and Degrees of Freedom:

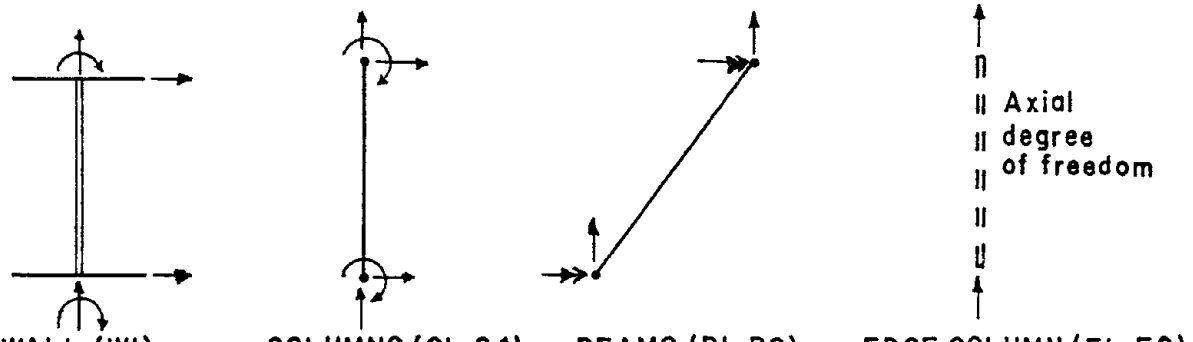

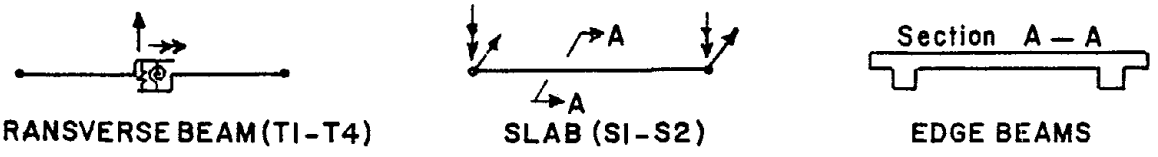

FIGURE 2-1 Typical Structure and Component Modeling

of floor slabs is primarily one of bending leading to a more complex three-dimensional response. In modeling the behavior of the slab system, no attempt has been made to account for such bi-axial bending. Instead, the response to pure in-plane loading is modified on the basis of observed experimental data [5] to account for the effects of out-of-plane loading. While such a technique is approximate for the present, it is expected that the correlation with observed experimental and shaking table studies will help calibrate the macro-model in an empirical way for future analytical response studies on flexible floor systems.

A typical floor slab element connecting two parallel frames is shown in Fig.2.2. Two degrees of freedom per node are assumed: an in-plane rotation and a lateral translation. A linear variation of flexibility is assumed in deriving the flexibility matrix. The incremental moment-rotation relationship is established from the integration of the M/EI diagram. Two possibilities arise, depending upon the location of the point of contraflexure (Fig.2.3). Hence:

$$\begin{pmatrix} \Delta\theta_a \\ \Delta\theta_b \end{pmatrix} = [k] \begin{pmatrix} \Delta M_a \\ \Delta M_b \end{pmatrix} \tag{2.1}$$

where:

$$[k] = L\begin{pmatrix} f_{11} & f_{12} \\ f_{21} & f_{22} \end{pmatrix} + \frac{1}{GA^*L}\begin{pmatrix} 1 & -1 \\ -1 & 1 \end{pmatrix}$$

where for the case that the contraflexure point lies within the element:

$$f_{11} = \frac{1}{12(EI)_a}(6\alpha - 4\alpha^2 + \alpha^3) + \frac{1}{12(EI)_b}(1 - 3\alpha + 3\alpha^2 - \alpha^3) + \frac{1}{12(EI)_o}(3 - 3\alpha + \alpha^2) \tag{2.1a}$$

$$f_{12} = f_{21} = \frac{1}{12(EI)_a}(-2\alpha^2 + \alpha^3) + \frac{1}{12(EI)_b}(-1 + \alpha + \alpha^2 - \alpha^3) + \frac{1}{12(EI)_o}(-1 - \alpha + \alpha^2) \tag{2.1b}$$

$$f_{22} = \frac{1}{12(EI)_a}\alpha^3 + \frac{1}{12(EI)_b}(3 - \alpha - \alpha^2 - \alpha^3) + \frac{1}{12(EI)_o}(1 + \alpha + \alpha^2) \tag{2.1c}$$

and, for the case that the point of contraflexure lies outside the element:

$$f_{11} = \frac{1}{4(EI)_a} + \frac{1}{12(EI)_b} \tag{2.2a}$$

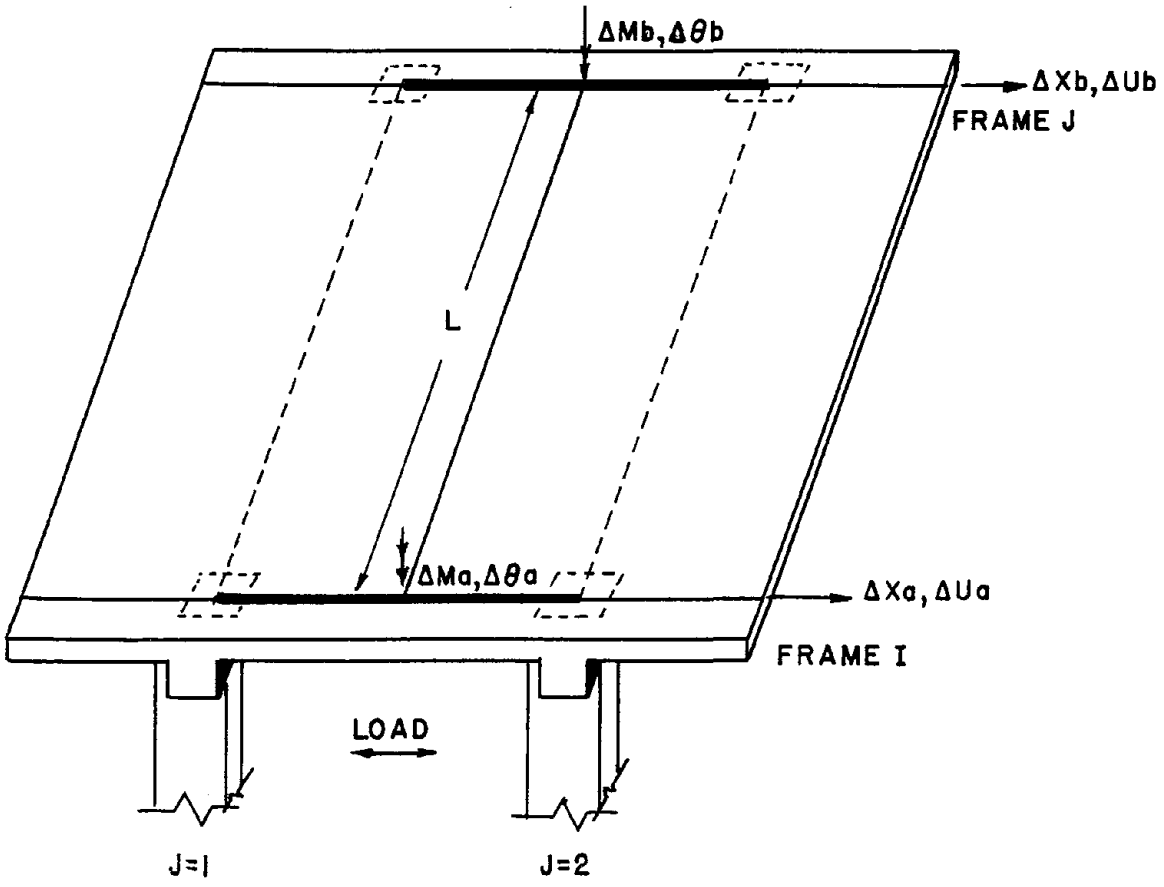

(a) Typical Floor Slab System

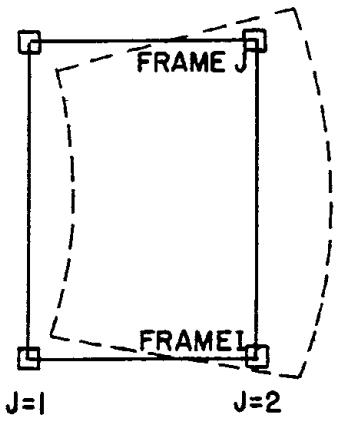

(b) Slab Distortion

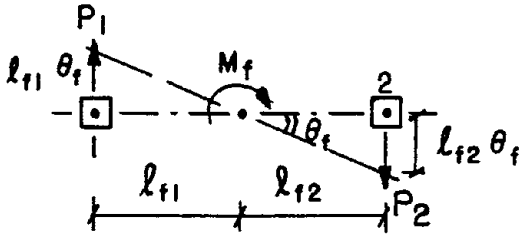

(c) Modeling of Torsion

FIGURE 2-2 Details of Slab Modeling

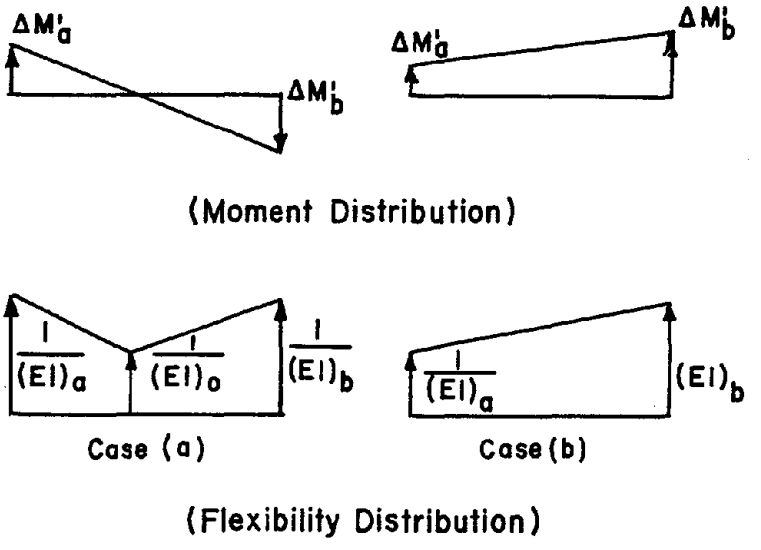

FIGURE 2-3 Distributed Flexibility Model

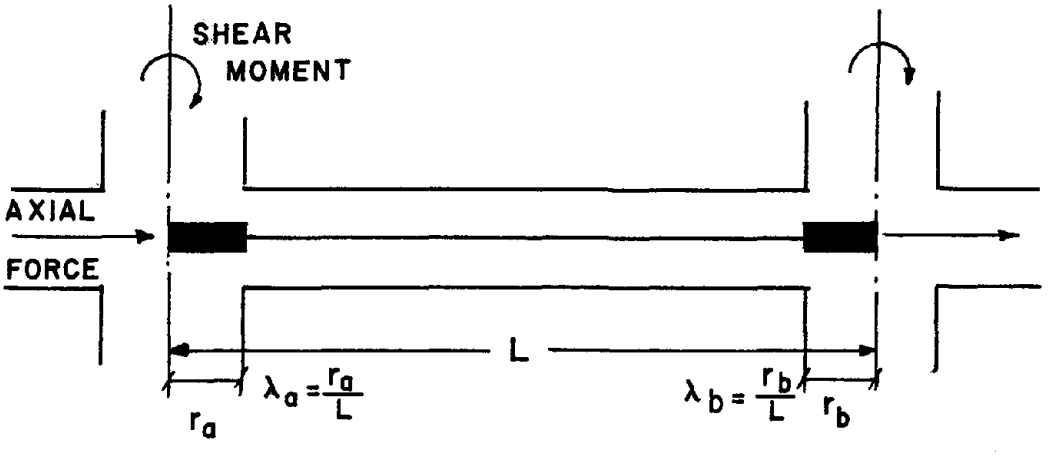

FIGURE 2-4 Typical Beam-Column Element with Degrees of Freedom

$$f_{12} = f_{21} = -\frac{1}{12(EI)_a} - \frac{1}{12(EI)_b} \tag{2.2b}$$

$$f_{22} = \frac{1}{12(EI)_a} + \frac{1}{4(EI)_b} \tag{2.2c}$$

where:

$$\alpha = \frac{\Delta M_a}{\Delta M_a + \Delta M_b} \tag{2.3}$$

2.2.1 Development of Stiffness Matrix

The $M-\theta$ relationship has an inverse form of the flexibility relation of Eq.(2.1):

$$\begin{pmatrix} \Delta M_a \\ \Delta M_b \end{pmatrix} = [k'] \begin{pmatrix} \Delta\theta_a \\ \Delta\theta_b \end{pmatrix} \tag{2.4}$$

in which $[k']$ is the inverted flexibility matrix.

From force-equilibrium:

$$\begin{pmatrix} \Delta X_a \\ \Delta M_a \\ \Delta X_b \\ \Delta M_b \end{pmatrix} = [\ R_s\ ] \begin{pmatrix} \Delta M_a \\ \Delta M_b \end{pmatrix} \tag{2.5}$$

where:

$$[\ R_s\ ] = \begin{pmatrix} \left(-\frac{1}{L}\right) & \left(-\frac{1}{L}\right) \\ 1 & 0 \\ \left(\frac{1}{L}\right) & \left(\frac{1}{L}\right) \\ 0 & 1 \end{pmatrix} \tag{2.6}$$

Hence, the stiffness equation for slab elements is:

$$\begin{pmatrix} \Delta X_a \\ \Delta M_a \\ \Delta X_b \\ \Delta M_b \end{pmatrix} = [\ K_S\ ] \begin{pmatrix} \Delta v_a \\ \Delta \theta_a \\ \Delta v_b \\ \Delta \theta_b \end{pmatrix} \tag{2.7}$$

where:

$$[\ K_S\ ] = [\ R_s\ ]\ [\ k'\ ]\ [\ R_s\ ]^T \tag{2.8}$$

is the element stiffness matrix.

2.2.2 Modeling of Frame Torsion

Any floor slab system that undergoes in-plane bending also experiences a certain amount of twisting due to differential movement of the slab edges (Fig.2.2b). The effect of the torsional resistance of the frames on the in-plane rotation of the slabs depends on the relative stiffness of the horizontal and vertical structural systems. Generally the effect of frames in restraining the floor slab system from inplane rotation is negligible and can be ignored. However, the influence of solid shear walls arranged in the perpendicular direction to the lateral loading can result in considerable rotational restraint for the floor slab which needs to be included in the analysis [15]. Modeling of the torsional restraint is achieved in the 2-dimensional scheme of IDARC in the following manner:

A rotation of the slab system is assumed to take place about the center of the frame axis. For a rotation θ_f about the center, the frame moment M_f is given by:

$$M_f = k_f \theta_f \tag{2.9}$$

The restraint provided by the columns due to the lateral deflection shown in Fig.2.2c is evaluated as:

$$P_i = 3\left(\frac{EI}{h^3}\right)_i l_i\ \theta_f \tag{2.10}$$

where EI and h refer to the flexural rigidity and height of the vertical element.

The stiffness coefficient is then determined for a unit rotation taking into account the total moment about the center of the frame axis:

$$k_f = \Sigma P_i l_i \tag{2.11}$$

where P_i is obtained from Eq.(2.10) by setting $\theta_f = 1$.

2.3 Summary of Other Models

Details of the element types that currently exist in the IDARC library can be found in the earlier manual. A brief summary of the element modeling is presented here for reference.

2.3.1 Beam-Columns

Main beam-column elements form a vertical plane in the axis of loading. They are modeled as simple flexural springs in which shear-deformation effects have been coupled by means of an equivalent spring. Details of the formulation are given in Park et al. [17]. A typical element with rigid panel zones is shown in Fig.2.4. The inclusion of rigid zones necessitates a transformation of the flexibility matrix as follows:

$$[\bar{k}] = [B][k'][B]^T \tag{2.12}$$

where:

$$[B] = \frac{1}{1-\lambda_a-\lambda_b}\begin{pmatrix} 1-\lambda_b & \lambda_a \\ \lambda_b & 1-\lambda_a \end{pmatrix} \tag{2.13}$$

Axial deformation effects are included in columns but ignored in beams. Interaction between bending moment and axial load is presently not considered directly in the step-by-step analysis, but the effect of axial load in the moment capacity computations is included.

2.3.2 Shear Walls

The modelling of shear wall elements is similar to that for floor slabs except for (1) the inclusion of axial effects and (2) the incorporation of edge columns at the ends of the wall. Walls may, however, be modeled with or without edge columns. Alternatively, the edge columns may be included only for strength computations in setting up envelope curves. The ability to treat each wall as an equivalent column with inelastic axial springs at the edges allows for the bending

deformation of the wall element to be caused by the vertical movements of the boundary columns. The motivation for such a modeling scheme is based on experimental studies conducted during the U.S.-Japan Research Program and was used in analytical studies reported by Kabeyasawa et al.[10].

2.3.3 Edge Columns and Transverse Beams

Studies on the behavior of columns subjected to axial load reversals are limited hence no attempt was made to develop a new model for the inelastic response of the axial spring of edge columns tied to shear walls. Instead, the model developed as part of the U.S.-Japan Research Program was implemented without modification. The details of the model are reported elsewhere [10].

To incorporate the effects of transverse elements on the in-plane response of the main frames, each transverse T-beam is modeled using elastic springs with one vertical and one rotational (torsional) degree-of-freedom as shown in Fig.2.1. Transverse elements are basically of two types: beams which connect to shear walls; and beams connected to the main beams in the direction of loading. Direct stiffness contributions arising from these springs are simply added to corresponding terms in the overall structure stiffness matrix. The purpose of modeling transverse beams in this fashion is to account for their restraining action due to two effects, should they become significant: (a) the axial movements of vertical elements, especially edge columns in shear walls; (b) flexural-torsional coupling with main elements.

SECTION 3
CONSTRUCTION OF ENVELOPE CURVES

The macro-modeling of reinforced concrete components involves the prescription of force-deformation curves and some associated rules for unloading and reloading. In the present study, a trilinear envelope is used to distinguish cracking and yielding of the component. This envelope is generally non-symmetric in compression and tension for T-beams but symmetric for columns, walls and slabs.

Strength and deformation are expressed as moment and curvature in the following discussion. For beams and columns, the modeling of the trilinear envelope for the equivalent inelastic spring is achieved through empirical relations based on calibrated experimental data. Floor slabs and shear walls are composed of two inelastic springs: flexure and shear. The latter is established through the use of empirical models while the former is determined using an analytical fiber model analysis. The next section describes the details of implementation of a generalized fiber model that fits a trilinear curve to the evaluated moment-curvature history under monotonic load.

3.1 Generalized Fiber Model Analysis for Flexural Springs

A general cross section of a floor slab system is shown in Fig.3.1. A shear wall section is a special case of this system with either one or up to three different subdivisions of cross sections (in the presence of edge columns or increased edge reinforcement).

A section may be sub-divided into any number of parts, depending upon the variation of the reinforcement or the presence of intersecting beams (as is the case with floor slab systems supported on beams or having close joists/ribs). Each part is then further discretized into *fibers* for the monotonic analysis. In the sample slab system shown, 7 sections have been defined. Each intersecting beam cross-section is divided into 6 fibers, the end-sections of the slab are divided into 6 fibers each while the two mid-sections have 16 fibers each.

From equilibrium under the applied axial load and moment we have:

$$\Delta N = \int E \; d\epsilon \; dA \tag{3.1}$$

$$\Delta M = \int E \; d\epsilon \; x \; dA \tag{3.2}$$

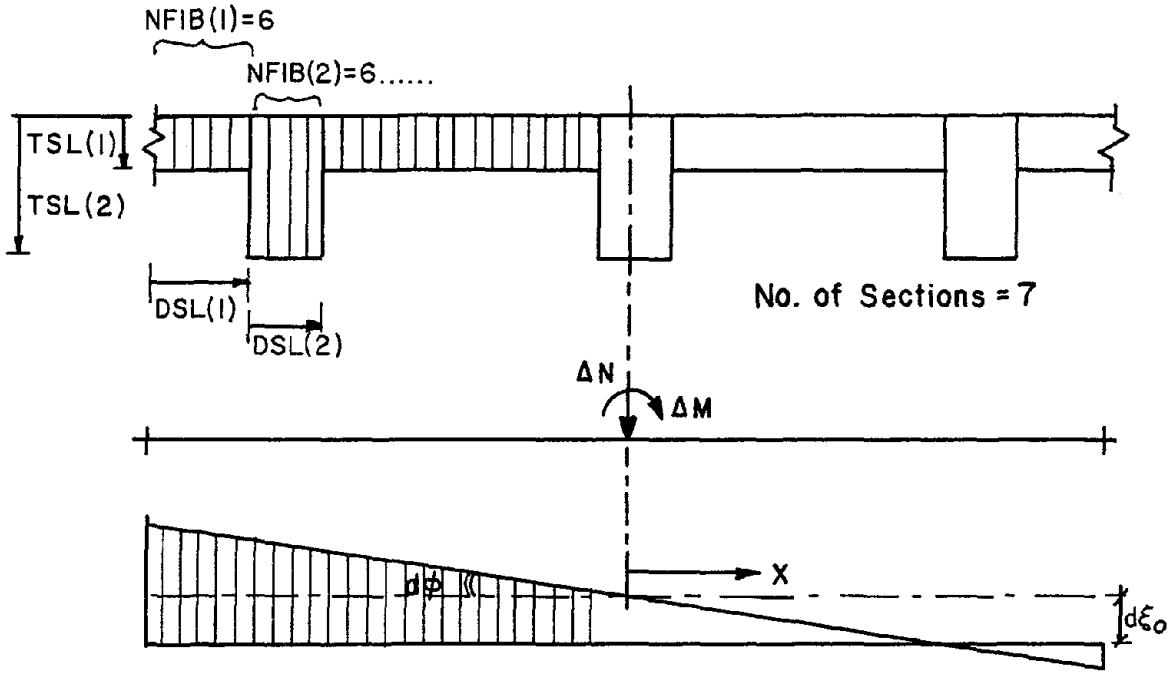

FIGURE 3-1 Modeling of Slab System for Fiber Model Analysis

where:

$$d\epsilon = d\epsilon_o + x d\phi \tag{3.3}$$

where:

$d\epsilon_o$ = central axial strain

$d\phi$ = curvature to be determined

Substituting Eq.3.3 into Eq.3.1 , the following is obtained in incremental form:

$$d\epsilon_o = \frac{\Delta N - (\Sigma E_i x_i A_i) d\phi}{\Sigma E_i A_i} \tag{3.4}$$

where:

E_i = mean modulus of fiber i

x_i = distance from center of fiber to center of section

A_i = area of cross-section of fiber

and the summation extends from 1 through the total number of fibers.

At the start of the analysis, the axial load is applied in full and a displacement controlled loading is applied in small increments. The procedure for establishing the corresponding moment history is adopted from Mander [14]:

Step 1: To the previous value of curvature apply a new increment of curvature.

Step 2: From the out-of-balance axial load and curvature increment (if any), determine the centroidal strain using Eq.3.4.

Step 3: Compute the revised strain profile using Eq.3.3, and calculate the new axial load and moment as follows:

$$N = \Sigma f_{ci} A_i + \Sigma f_{si} A_i \tag{3.5}$$

$$M = \Sigma f_{ci} A_i x_i + \Sigma f_{si} A_i x_i \tag{3.6}$$

where:

f_{ci} = stress in concrete at fiber i

f_{si} = stress in steel at fiber i

Step 4: Calculate the out-of-balance axial force and if this exceeds some specified tolerance, set the curvature increment to zero and return to Step 2.

The above procedure works well even in the presence of strain softening. However, it must be noted that the purpose of this analysis is merely to set up a trilinear envelope which defines cracking and yielding. Strength deterioration under cyclic loading is achieved through hysteretic modeling.

3.1.1 Floor Slabs

The hysteretic modeling of floor slabs has presently been established through the interpretation of available experimental data. The procedure described in Chapter 3.1 computes the complete moment-curvature envelope using a displacement-controlled loading. A sample envelope for an actual test specimen is shown in Fig.3.2a alongside the experimental curves. The two experimental curves represent the same slab specimen with and without superimposed dead and live load. It has been seen that the presence of vertical loading on the slab significantly reduces the in-plane load-carrying capacity while also changing the resulting shape of the strength-deformation envelope as shown clearly in Fig.3.2a. The objective of the slab modeling scheme is to fit the experimental envelope in the presence of vertical loads. Based on observed experimental data (of which the curves shown in Fig.3.2a. is a representative sample), the following scheme is developed:

- The yield capacity of floor slabs is assumed to be equal to the cracking strength predicted by the monotonic analysis under in-plane loading. This assumption is valid for nominally reinforced slabs which generally show abrupt yielding following cracking. Tests conducted at Lehigh [5] also confirm this fact. However, for heavily reinforced slabs, where the yield strength is much higher than cracking (as indicated by monotonic analysis under in-plane loads), it was decided to use an average value between the predicted cracking and yield strengths which is expected to represent the strength loss due to the presence of vertical loads.

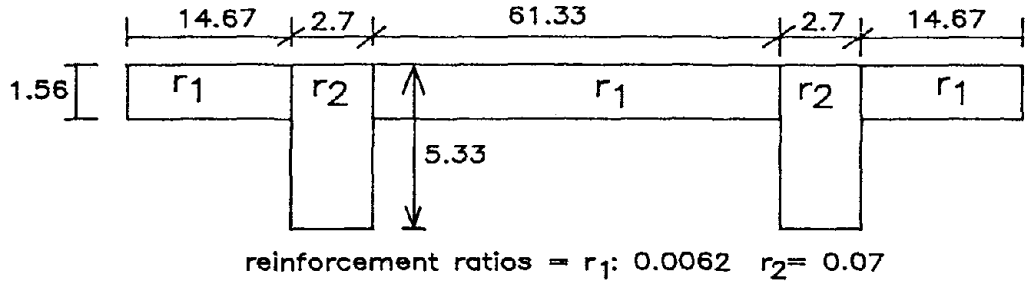

reinforcement ratios = r_1: 0.0062 r_2= 0.07

$f_c' = 4.0ksi$ $f_s = 68.0ksi$

$E_c = 3000ksi$ $E_s = 28000ksi$

$\epsilon_o = 0.003$

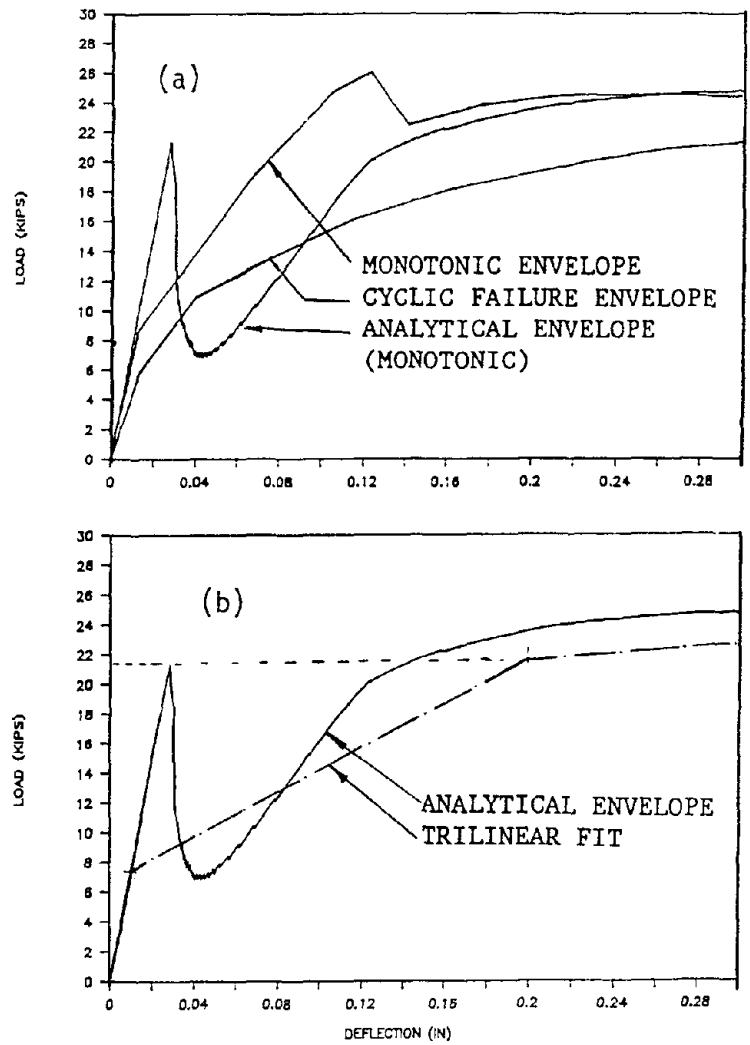

FIGURE 3-2 Envelope Curve Determination for Slabs

- Deviation from the initial elastic slope is observed to take place at approximately 1/3 of the yield strength when vertical loads were present in the slab element. Such an approximation is also reported in the finite element studies of Chen [5].

- Yield curvature is fixed at the smaller of the following two estimates:

(1) at a point along the moment-curvature envelope which yields a slope equal to 5% of the initial elastic slope.

(2) at 6 times the cracking curvature, as observed in most of the experimental testing.

The implementation of the technique for a sample slab that was tested at Lehigh [5] is shown in Fig.3.2b. Note that a displacement-controlled loading was used in the analysis, therefore the shape of the curve with marked strength-loss after cracking is not the likely path under actual loading conditions. The fitted trilinear curve accounts for all the experimental observations noted above on the behavior of floor slabs under both vertical and in-plane loads.

3.1.2 Shear Walls

The trilinear envelope for the flexural spring in shear walls is more straight-forward since the primary forces on the wall are in-plane. Hence, the estimates provided by the fiber model analysis are more reliable. The only approximation that is required is for the case of poorly reinforced walls in which cracking and yielding occur almost simultaneously. In such a case, the cracking strength is reduced by 20% to enable the construction of a realistic trilinear envelope.

A parametric study of flexural capacity envelopes using the fiber model analysis is shown in Fig.3.3a. The detail in the region of cracking is magnified in Fig.3.3b. The effect of varying the axial load on the wall shows a significant change in load carrying capacity. In this parametric study, a 1/6th scale model wall (details presented in Chapter 5) was analysed to study the influence of varying axial load. This phenomenon is important in coupled shear walls which experience alternating compression and tension under the action of earthquake forces. If such a consequence is not accounted for, the estimates provided by a fiber model analysis may be erroneous.

3.2 Envelope Curve Determination for Shear Springs

Modeling of the shear behavior of the slab and wall elements is accomplished independently thereby enabling a shear-type failure to be detected. This is done, as discussed earlier, by introducing a shear spring in series with the flexural spring.

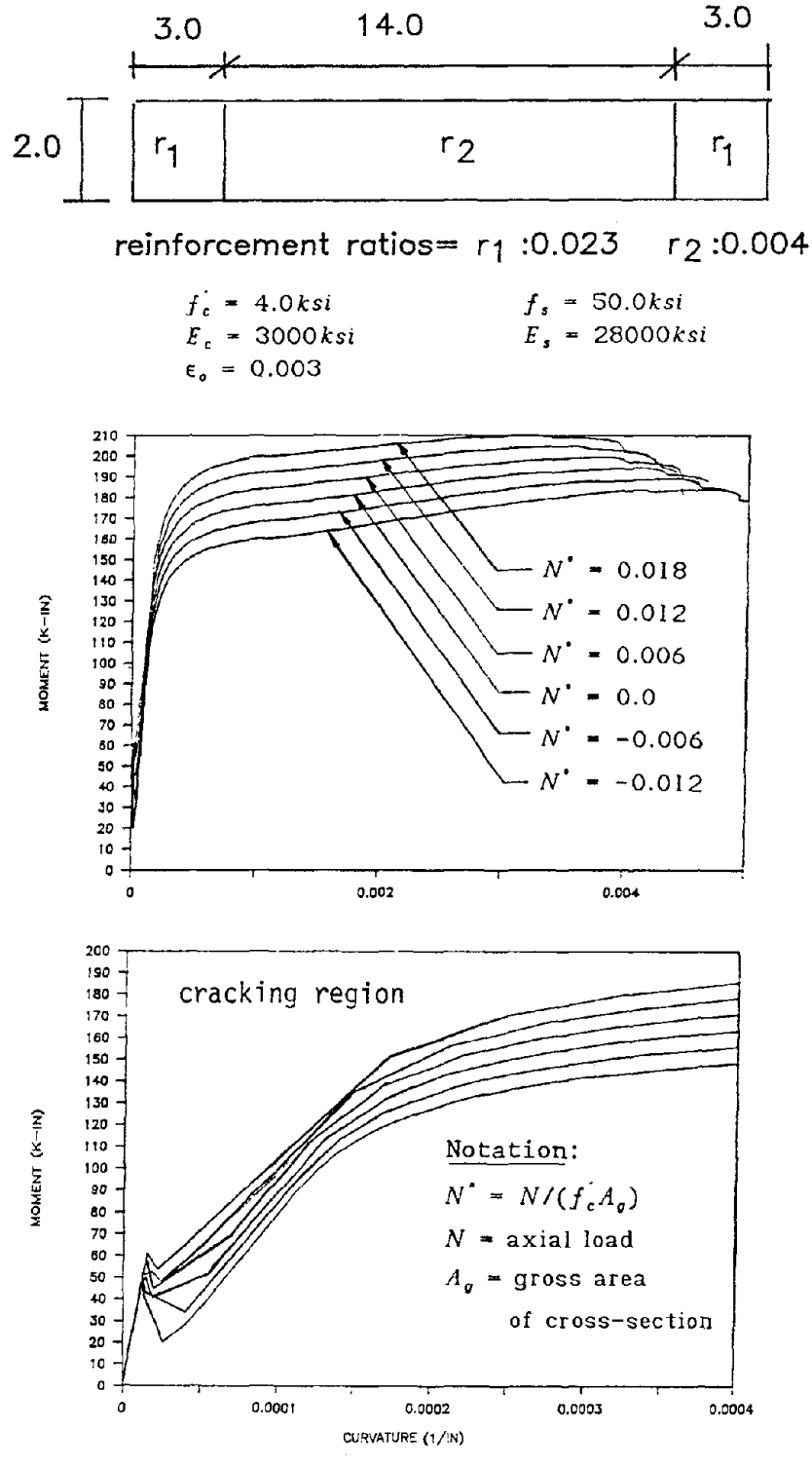

FIGURE 3-3 Moment-Curvature Envelopes for Walls, Influenced by Axial Loads

The shear envelope for slabs is developed along lines similar to walls since no other data is presently available. The original equation used in the IDARC Manual has been modified in this study:

The yield shear strength is calculated from:

$$Q_y = \left[\frac{0.0679 \rho_t^{0.23} (f_c' + 2.56)}{\sqrt{l_r + 0.12}} + 0.32 \sqrt{f_y p_w} \right] A' \tag{3.7}$$

$$A' = 0.875 B \left(D - \frac{d}{2} \right) \tag{3.8}$$

$$\rho_t = \frac{A_g}{B\left(D - \frac{d}{2}\right)} \tag{3.9}$$

where: B = equivalent web thickness taken as mean section thickness

D = total section depth

d = equivalent edge beam depth (D/6)

Ag= equivalent edge beam reinforcement

The yield shear deformation is still computed as a function of the shear span ratio by defining the secant yield stiffness [17].

For *shear walls* with edge columns, the equations listed in the previous section are used with actual data from the edge columns. However, in the absence of edge columns, an equivalent section equal to 1/4 the total wall section is defined at each end.

3.3 Equivalent Shear-Flexure Springs for Beam-Columns

The envelope curve used for beam-columns is formulated using empirical models based primarily on regression analysis of extensive experimental data. Details of the formulation may be found in the earlier report [17] though some of the essential features are presented here.

In specifying the cracking strength, it was necessary to consider a distinct transition from the elastic slope rather than use the conventional formulation of tensile concrete cracking at the extreme fiber so as to enable the development of the trilinear envelope. Consequently, the following equations were proposed based on the analysis of experimental data:

$$M_{cr} = 11.0\sqrt{f_c'}Z_e + \frac{Nd}{6} \tag{3.10}$$

where:

M_{cr} = cracking moment

f_c' = concrete compressive strength

Z_e = section modulus

N = axial load

d = depth of section

Details of the development of the yield moment parameter is reported elsewhere [17] in which the effect of axial stress and the inelasticity of concrete is taken into consideration. The ultimate strength is then expressed as a function of the yield strength:

$$M_u = (1.24 - 0.15p_t - 0.5n_o)M_y \tag{3.11}$$

where:

M_u = ultimate moment

p_t = tension steel ratio

n_o = normalized axial stress $\left(\frac{N}{bdf_c'}\right)$

b = width of section

d = depth of section

The scatter associated with Eq.(3.11) is relatively small with a coefficient of variation of about 12%.

The yield curvature is estimated as the cumulative effect of 4 components: flexural deformation ϕ_f, deformation due to bond-slip, ϕ_b, inelastic shear deformation, ϕ_s, and the elastic shear deformation, ϕ_e:

$$\phi_y = \phi_f + \phi_b + \phi_s + \phi_e \tag{3.12}$$

The possibility of prescribing different amounts of steel and different cross-sections for the flange and web of T-Beam sections enables the direct modeling of non-symmetric envelopes without need for special hysteretic rules to produce the biased loop behavior of typical T-sections.

The prescription of the envelope curves and the associated parameters for inelastic hysteretic modeling constitute the overall task of structural identification. The procedures described in this Section are based on empirical models derived from statistical analysis of experimental data, and through the use of mechanical models (fiber model). These equations are approximate but adequate to capture the behavior of components and their effect on overall structural response.

SECTION 4
RESPONSE EVALUATION

The analysis of the assembled macro-models involves the following sequence of operations: (a) estimation of strength-deformation parameters for all components using empirical or mechanical models; (b) computation of initial stress states in components under pre-loading; (c) estimation of fundamental natural period of structure; (d) failure/collapse mode analysis under monotonic lateral loading; (e) modification of component properties using revised shear spans following the monotonic analysis; (f) incremental dynamic response analysis using the 3-parameter hysteretic model [17]; and finally (g) determination of the state of damage of components and structure following the response analysis.

Steps (a) through (e) are part of a system identification procedure which is essential to set up parameters for strength and deformation for the hysteretic modeling prior to the inelastic dynamic analysis.

4.1 Structural Identification

A realistic representation of structural parameters is essential in describing trilinear force-deformation envelope curves for components. All of the empirical equations used in the present analytical procedure have been obtained from rigorous statistical analysis of available experimental data. It is also possible to replace the module-generated information with actual data from component testing.

In the present scheme, the first step involved an initial bilinear representation of force-deformation for all components. Hence only the initial elastic modulus and yield force level for each component is required. Prior to commencing the monotonic analysis, the initial stress state of the structure was established.

4.1.1 Initial Stress Under Dead and Live Loads

It is possible to estimate the initial stress states of members under equivalent dead and live loads that may exist in the structure prior to analysis for earthquake loads. The same initial state is assumed before the failure sequence analysis as well.

Loads are specified in two ways:

(a) Uniform loads on main beam elements
    (i.e., beams defined in the direction of load)
(b) Nodal moments at beam ends due to overhanging cantilevers
    (not otherwise considered in the analysis)

The assumed linear moment distribution in the flexibility matrix computations is expected to produce some errors though not significant if the force levels are well below cracking point.

Alternatively, the initial stresses may be computed by the user (from another 3D elastic program or actually measured prior to testing) and input as direct initial forces in the members. No additional loading need be specified since the effect will be cumulative.

4.1.2 Fundamental Natural Period

The fundamental natural frequency of the structural system is established using the Rayleigh quotient. The general form of the Rayleigh quotient is obtained by equating the maximum potential and kinetic energies of the system:

$$\omega^2 = \frac{\{\psi^T\}[K]\{\psi\}}{\{\psi^T\}[M]\{\psi\}} \tag{4.1}$$

where [K] and [M] are the stiffness and mass matrix of the system, respectively, ω is the fundamental frequency, and $\{\psi\}$ is the *shape* vector of fundamental mode of vibration of the system.

In the present analysis, the structure is loaded laterally in an inverse triangular form. The magnitude of the base of the triangle is obtained from the distribution of floor weights to respective frames using the tributary area concept. The deflected shape of the structure using this load pattern is assumed to be similar to the first mode shape. Therefore, the application of Eq.(4.1) is direct. In discrete form, for a multi-story building, this may be written as:

$$\omega^2 = \frac{\sum_{i=1}^{N}\sum_{j=1}^{M} k_{ij}\Delta u_{ij}^2}{\sum_{i=1}^{N} m_i u_i^2} \tag{4.2}$$

where N is the number of stories, M is the number of frames, u is the deflection, Δu is the relative story drift, and i,j refer to the story and frame number respectively.

The fundamental period is used primarily for assigning a constant viscous damping factor in the dynamic analysis. Since the effect of viscous damping is not fully known, no attempt is made to perform a sophisticated eigen value analysis. Moreover, in reinforced concrete structures, most of the damping is a result of hysteretic damping caused by inelastic loading reversals and the effect of viscous damping is negligible.

4.1.3 Collapse Mode Analysis

A collapse mode analysis is a simple and efficient technique to predict seismic response behavior prior to a full dynamic analysis. The method provides a means to assess design requirements and consequently change appropriate parameters to achieve a desired sequence of component yielding. The monotonic analysis involves an incremental solution procedure whereby the structure is loaded laterally in an **inverse triangular form.** The load increment for each step is evaluated from the base shear estimate. The force vector corresponding to each lateral degree-of-freedom is computed as follows:

$$f(i,j) = \bar{w}_b \frac{\Sigma w(i,j)}{\Sigma w(i,j)h(i)} w(i,j)h(i) \qquad (4.3)$$

where: w, h and $\bar{w}_b$ = the weight, height and factored base shear, respectively;

subscripts i, j = story and frame level respectively.

The stress state of each member is evaluated at the end of each step of load application. Stresses are determined at critical sections only, viz., the end sections, except for floor slabs and walls where shear type failure is also monitored. When element yielding is detected, the elastic slope is reduced to 1% of its initial value for that particular element section. Analysis proceeds till the deflection of the top of the structure exceeds 2% of the total building height.

4.1.4 Modified Properties and Dynamic Data Preparation

The completion of the monotonic analysis sets the stage for data preparation for the ensuing dynamic analysis. An estimate of the natural period is known and at the end of the montonic analysis, a better approximation of the critical shear spans is possible since weaker elements have yielded and stress-redistribution has taken place.

Since critical shear spans can be determined only after the failure analysis, the monotonic analysis had to be performed using a bilinear envelope curve for all elements. The following parameters are evaluated using the computed shear span ratios:

(a) Yield deformation for the equivalent springs in beams and columns.

(b) Yield deformation for the shear springs in floor slabs and walls.

(c) Ultimate deformation capacities for all components.

The determination of yield deformation is crucial to setting up the trilinear envelopes for the hysteretic modeling. Details of the empirical models that are used to complete the definition of the hysteretic modeling are reported in Park et al.[17].

4.2 Dynamic and Damage Analysis

The incremental dynamic analysis is carried out using a generalized hysteretic model for inelastic bending and shear. The rules governing hysteresis are described in the earlier manual [17] but the essential elements of the model are summarized in the next section. An attempt is then made to quantify the response statistics in a more meaningful way by using a normalized damage index [17]. The damage quantities computed are only qualitative indicators of structural damage. More calibration studies with experimental testing is in progress to define the physical meaning of these indices.

4.2.1 Three Parameter Hysteretic Model

The hysteretic model that was developed for the analysis uses three parameters in conjunction with a non-symmetric trilinear curve to establish the rules under which inelastic loading reversals take place. The general meaning and effect of the parameters is illustrated in Fig.4.1.

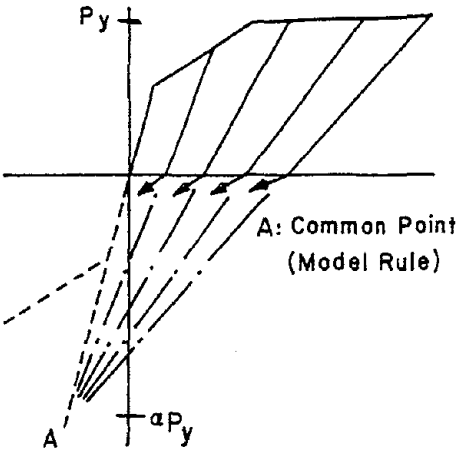

(a) Stiffness Degradation

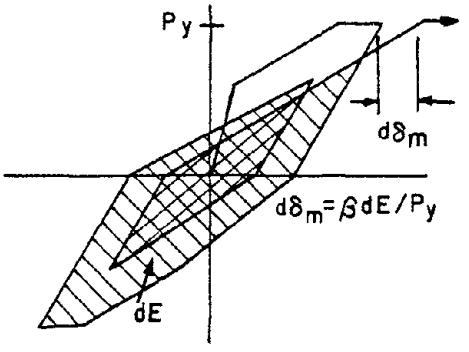

(b) Strength Deterioration

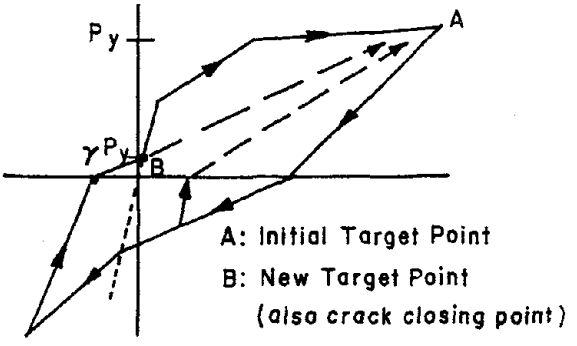

(Model Rule)

(c) Bond-Slip

FIGURE 4-1 Three Parameter Model

A variety of hysteretic properties can be achieved through the combination of the trilinear envelope and the three parameters, henceforth to be referred to as α, β and γ. The values of these parameters determine the properties of stiffness degradation, strength deterioration and pinching, respectively.

Stiffness degradation, represented by α is introduced by setting a common point on the extrapolated initial stiffness line and assumes that unloading lines target this point until they reach the x-axis (Fig.4.1a) after which they aim the previous maximum or minimum points (unless the previous maximum or minimum was still in the elastic range in which case the cracking point is targeted).

The parameter β specifies the rate of strength degradation as shown in Fig.4.1b. The same parameter is used in the definition of the damage index. This parameter gives the ratio of the incremental damage caused by the increase of the maximum response to the normalized incremental hysteretic energy as follows:

$$\beta = \left(\frac{d\delta_m}{\delta_u}\right) / \frac{dE}{(\delta_u P_y)} = \frac{d\delta_m}{dE/P_y} \tag{4.4}$$

Therefore, the incremental increase of the maximum deformation due to the dissipated hysteretic energy is expressed as:

$$d\delta_m = \beta \frac{dE}{P_y} \tag{4.5}$$

where the value of β is determined in-core using empirical relations reported in Park et al.[17].

Modification for Pinching. - The description for pinching has been modified from the originally assumed model in [17]. Pincking behavior is introduced as before by lowering the target maximum or minimum point to a straight level of γP_y along the previous unloading line. Reloading lines now aim this new point until they reach *the elastic slope line* (instead of the crack closing point described in the previous report) after which they target the previous maximum or minimum point (Fig.4.1c)

4.2.2 Numerical Implementation with Equilibrium Check

The incremental solution of the following dynamic equation of equilibrium:

$$[M]\{\Delta \ddot{u}_r\} + [C]\{\Delta \dot{u}_r\} + \{R(u_t)\} = \{F(t)\} \tag{4.6}$$

is established through the application of the Newmark-Beta algorithm [Bathe, 1976], in which:

$[M]$ is the lumped mass matrix

$[C]$ is the damping matrix

$\{R(u_t)\}$ is the restoring force vector at the start of the time step

u_r is the relative displacment

$\{F(t)\}$ is the effective load vector

In constructing the diagonal mass matrix, the effects of rotational inertia have been neglected. The solution is performed incrementally assuming that the properties of the structure do not change during the time step of analysis. However, since the stiffness of some elements is likely to change during some calculation step, the new configuration may not satisfy equilibrium. A compensation procedure is adopted to minimize this error by applying a one-step unbalanced force correction.

At the end of some given time step, t_i assume that the right hand side of Eq.(4.5) yields a total system force F_i which is not in equilibrium with the applied force in the previous step giving an unbalanced force ΔF as follows:

$$\Delta F = F_t - F_{t-1} \tag{4.7}$$

This corrective force is allowed to act for the next time step of analysis and then removed in the subsequent analysis step since allowing the corrective force to continue to act will produce cumulative error leading to a modification of the applied force history. Such a procedure was first adopted in DRAIN2D [11] since the total cost of performing an iterative nonlinear analysis would become prohibitive especially for large building systems.

4.2.3 Damageability Evaluation

The damage model implemented in the first version of IDARC is also used in the present study since, in keeping with the overall philosophy of the present modeling scheme, it remains the only calibrated model based on actual observed damage of reinforced concrete buildings. Until more experimental and post-damage verification is made, the authors believe that this model serves as a useful indicator in interpreting the overall damage sustained by the structure and its components.

Structural damage is expressed as a linear combination of the damage caused by peak deformation and that contributed by hysteretic energy dissipation due to repeated cyclic loading:

$$D = \frac{\delta_m}{\delta_u} + \frac{\beta}{P_y \delta_u} \int dE \tag{4.8}$$

where:

δ_m = maximum deformation under earthquake load

δ_u = ultimate deformation capacity under monotonic load

β = strength deterioration parameter defined in the earlier section

P_y = yield strength

ϵ = incremental absorbed energy

A story level damage index is next defined. Such an index is useful when analysing weak-column strong-beam type buildings where sudden shear drifts due to the formation of shear-panel mechanisms may trigger progressive collapse of the total structure. For the purpose of establishing the story-level damage index, a weighting factor is introduced based on the energy-absorbing capacity of elements:

$$D = \Sigma \lambda_i D_i \; ; \; \lambda_i = \frac{E_i}{\Sigma E_i} \tag{4.9}$$

where:

λ_i = energy weighting factor

E_i = total energy absorbed by component

In the case of strong-column weak-beam type buildings, it is necessary to extend the above concept to the entire structure. The overall damage index is obtained by performing a final weighted summation over all the stories of the building.

The damage index so defined will yield normalized values between 0 and unity. Theoretically, a damage index in the neighborhood of 1.0 signifies partial or complete collapse of the component. However, the calibration of the model based on observed damage to R/C structures following earthquakes shows that a damage index in the neighborhood of 0.4 corresponds to structural damage beyond repair [17].

For the present scheme, a new calibration is necessary since the weighting factors required to account for the importance of slab yielding has yet to be determined. It is expected that the monotonic testing of components and the shaking table study will provide adequate information on the calibration parameters that need to be built into the damage formulation.

Parameter Identification for Damage Evaluation. - Only two of the five parameters necessary to evaluate the damage index (see Eq.4.7) are component characteristics which need to be identified. They comprise the ultimate deformation capacity δ_u of the component and the strength deterioration parameter β. For beam-columns, the empirical equations required have already been reported [Park et al., 1985].

A new formulation has been derived for the ultimate deformation capacity of shear walls based on analysis of experimental data [Oh, 1988]:

$$\delta_u(\%) = 0.53 l_s^{1.23} d^{-0.23} \rho_h^{0.56} \rho_c^{-0.05} \rho_v^{-0.3} n_o^{0.09} (f_c')^{0.85} \qquad (4.10)$$

in which:

δ_u = ultimate deformation capacity

l_s = shear span

n_o = axial stress

ρ_h = horizontal reinforcement ratio $\geq 0.4\%$

ρ_c = edge column reinforcement ratio $\geq 0.2\%$

ρ_v = vertical reinforcement ratio

For slabs, a simple approximation is currently being used based on observed experimental results. The ultimate capacity is defined at a ductility of 3.0. Yield deformation is obtained from the fiber model analysis presented in Section 3.1.

SECTION 5

INFLUENCE OF DIAPHRAGMS IN A SINGLE STORY STRUCTURE WITH END WALLS

An example of the application of the program developed, IDARC2, is presented in this chapter. Recent experience and research have demonstrated that for sound seismic design of R/C structures, a realistic evaluation of the stiffness, strength, and ductility capacity of the structure is necessary. This chapter illustrates the importance of including the effect of in-plane behavior of floor slabs in such an evaluation, for narrow buildings with stiff end walls.

5.1 Description and Discretization of the Structure

A single story structure with multiple bays in the longitudinal direction and one bay in the transverse direction is considered for this study. The slab panels are supported along its four edges by monolithic concrete beam-column frames, and shear walls at the ends. Each bay measures 24 ft. in both directions with a 4 ft. overhanging slab on all non-continuous sides. The columns are 18 in. by 18 in., the beams are 22 in. deep and 12 in. wide, and the slab thickness is 7 inches.

The structure is designed for combined gravity and seismic loads. Service gravity loads consisted of self-weight plus a live load of 80 psf. The structure is designed to satisfy the requirements of current ACI Standard 318/83 [23]. The seismic design load is selected in accordance to the Zone 4 classification of Uniform Building Code [1]. Structure dimensions and critical member cross-sections used for the analysis are shown in Fig. 5.1a. The idealized structure used for the analysis is shown Fig. 5.1b. Concrete strength of 4000 psi and Grade 40 reinforcement is used. The floor dead load plus 25% of floor live load is lumped at each transverse frame in according to its tributary area. A critical damping ratio of 2% is specified.

The 1940 El Centro normalized earthquake accelerogram, N-S component, with a peak acceleration of 0.7g, shown in Fig. 5.2 is used as the input ground motion. The first 20 seconds of the earthquake are considered. The pertinent details of the structural information used in the analysis are listed in the output sample given in Appendix B.

5.2 Parameters Studied

A total of nine cases are analyzed. The main parameters considered are:

1) the number of bays spanning along the longitudinal direction, perpendicular to the direction of the ground motion.

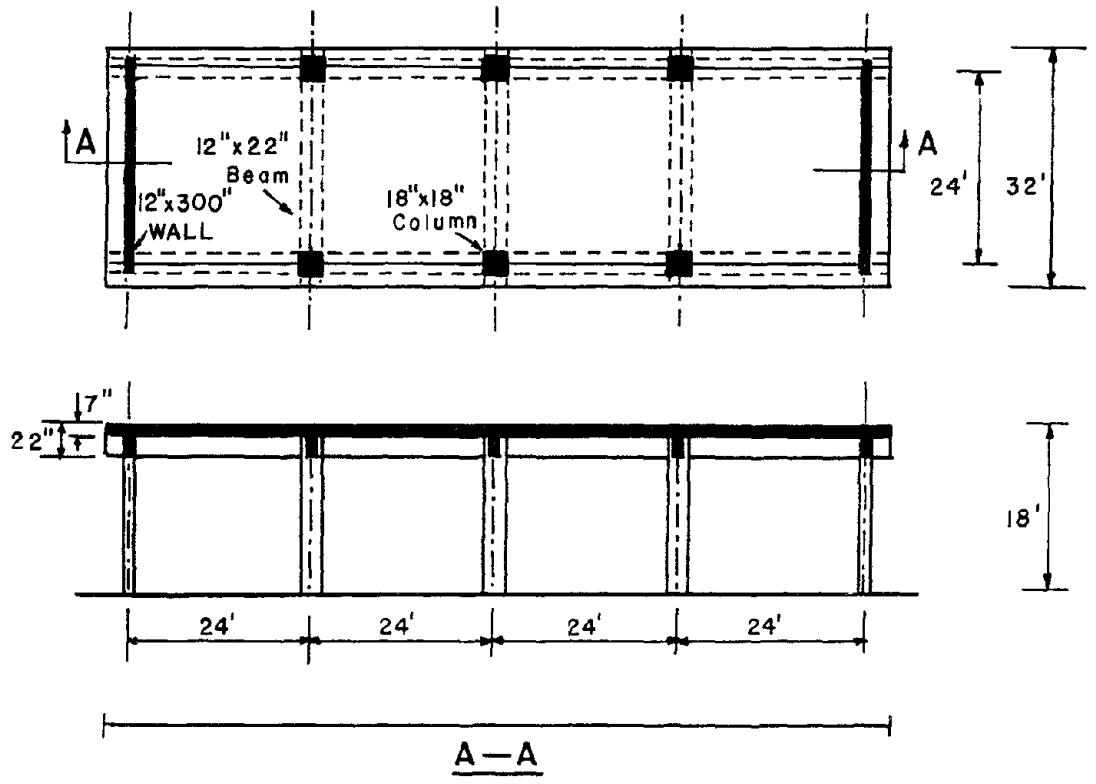

(a) Overall Geometry

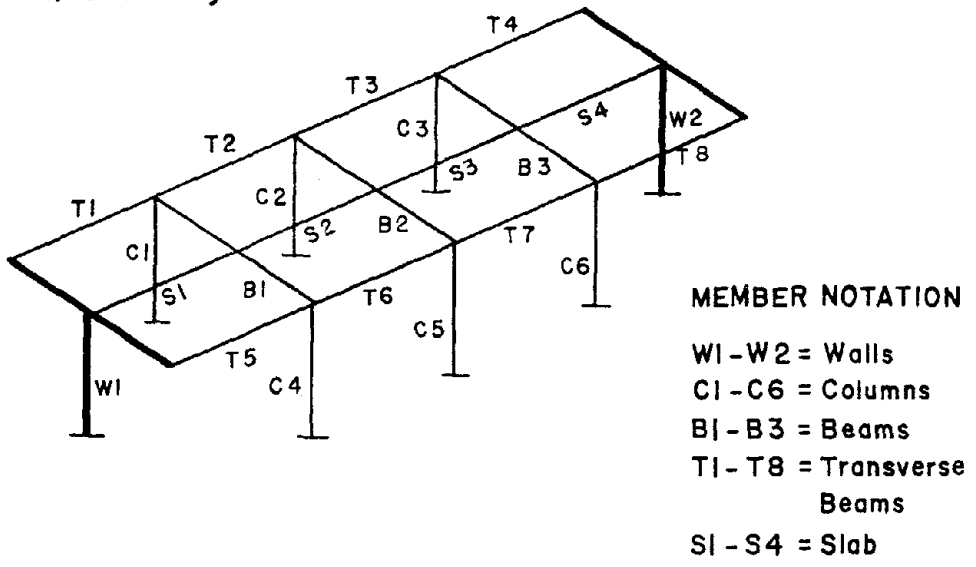

(b) Idealized Model Used in IDARC2 ANALYSIS

FIGURE 5-1 Typical Single Story Structure Used for the Parametric Study

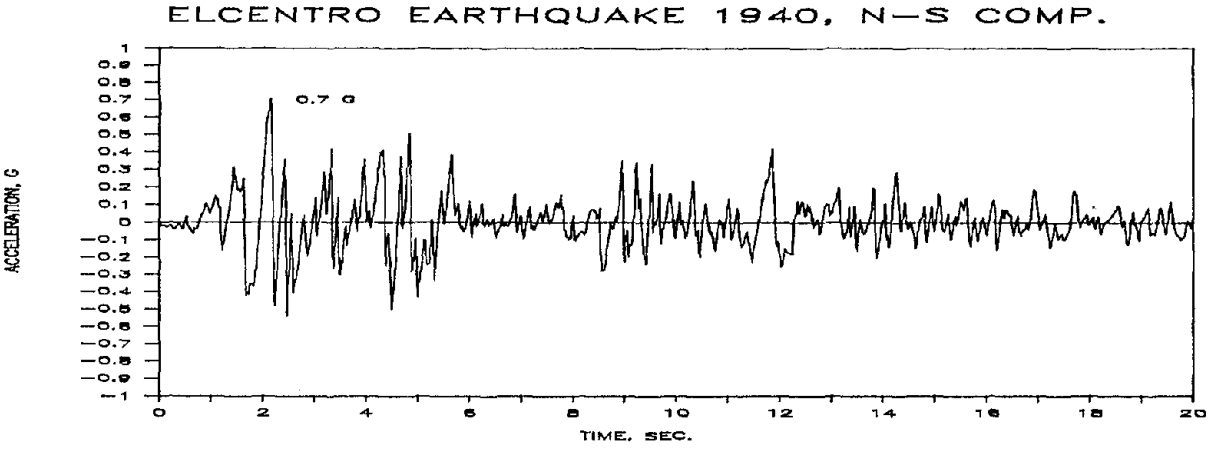

FIGURE 5-2 Input Ground Accelerogram Used for Analysis

2) the in-plane flexibility model used for the floor diaphragm.

For the present example, four, six, and eight span single story structures with floor diaphragm action modeled as either inelastic, elastic, or rigid slabs are considered. The results are presented and discussed in the following section.

5.3 Results and Discussion of the Seismic Response Analyses

The peak values of displacement of the middle frame and end frame (wall), total base shear for the structure, the base shear of the end wall and middle frame, in-plane slab shear and moment (normalized with respect to the yield values computed by the program) are tabulated for the nine cases analyzed in Table 5.1. The definition of displacement responses and internal base shear forces are shown in Fig. 5.3. The maximum slab shear occurred at the end panel, while the maximum slab moment is experienced at the interior panel next to the middle frame.

The maximum deformations of the end walls are kept by their rigidity to small values. The deflection of the rigid diaphragm (which has a large but not infinite rigidity) is almost identical to that of the walls (see Table 5.1 (2) and (3)). However, when the diaphragm is flexible either elastic or inelastic the deformations in the center are substantially larger (see Table 5.1 (3)). This imposes a large ductility demand on the middle frames which often may be beyond the design provisions. At the same time the total base shear in the structure is also increasing (see Table 5.1 (4)) when an elastic model is assumed instead of a rigid model. The increase is more accentuated for langer structures (i.e., 8 spans versus 6 and 4 spans).

The shear and the flexural moment in the diaphragm are also influenced by the behavior assumed for the diaphragm. While the shear response is usually smaller than the shear capacity of the diaphragms, the in-plane bending moment response exceeds the moment capacity (M_{ys}) provided by the design when rigid or elastic floors are assumed for long structures (see Table 5.1 (8)). However, if an inelastic model is assumed the resistance required exceeds the yielding value slightly. Thus, if slab is provided with sufficient ductility then such an exceedence can be acceptable.

The middle frame displacement history, plotted in Figs. 5.4-5.6 provides a convenient way of comparison of the overall response of the 4, 6, and 8 span structures analyzed by IDARC2 program using inelastic, elastic, and rigid slab models. The relative displacement between the middle frame and the end wall at the floor level (is referred as floor slab drift in this study, see Fig. 5.3) are compared for inelastic and elastic slab models in Fig. 5.7-5.9.

TABLE 5-1 Predicted Analytical Results of Single Story Structure

No.of	Slab	Max. Displacement, in.		Max. Base Shear, k			Max. Slab Response		T
Spans	Model	End Wall	Middle Frame	Structure	End Wall	Middle Frame	Vs	Ms/Mys	Sec/Cycl.
0	1	2	3	4	5	6	7	8	9
4	R	.014 (2.60)	.015 (2.21)	400.3 (2.21)	198.4 (2.21)	1.21 (2.60)	122.3 (2.21)	.63 (2.21)	.037
	FE	.018 (2.48)	.106 (2.48)	526.8 (2.48)	254.0 (2.48)	7.29 (2.48)	208.4 (2.48)	1.12 (2.48)	.059
	FI	.013 (2.50)	.244 (4.54)	402.6 (2.50)	185.6 (2.50)	14.74 (5.05)	123.1 (2.51)	.67 (2.51)	.059
6	R	.025 (2.47)	.028 (2.47)	711.2 (2.47)	350.1 (2.47)	2.23 (2.47)	256.3 (2.47)	1.78 (2.47)	.044
	FE	.025 (3.58)	.402 (3.57)	778.5 (3.58)	352.3 (3.58)	16.77 (3.57)	312.8 (3.57)	2.39 (3.57)	.106
	FI	.013 (2.15)	1.34 (4.58)	470.0 (2.65)	187.6 (2.15)	27.78 (4.58)	140.3 (2.19)	1.06 (2.22)	.106
8	R	.041 (2.47)	.046 (2.47)	885.8 (2.47)	430.4 (2.47)	3.67 (2.47)	340.8 (2.48)	3.16 (2.48)	.051
	FE	.068 (2.57)	1.28 (2.56)	1139. (2.57)	489.3 (2.57)	26.31 (2.55)	450.6 (2.55)	4.50 (2.56)	.159
	FI	.015 (2.15)	3.73 (2.23)	611.9 (2.15)	209.9 (2.15)	32.94 (2.23)	150.5 (2.16)	1.24 (2.23)	.159

(Numbe in parenthesis = Time at which the max. response is reached)

Notations:

FI --- Flexible inelastic slab;
FE --- Flexible elastic slab;
R --- Rigid slab;
Vs --- Maximum in-plane shear in the end panel slab;
Ms --- Maximum in-plane moment in the mid-panel slab;
Mys --- Yeild moment for the interior slab (Mys = 74838 k-in.)
T --- Fundamental period of the structure.

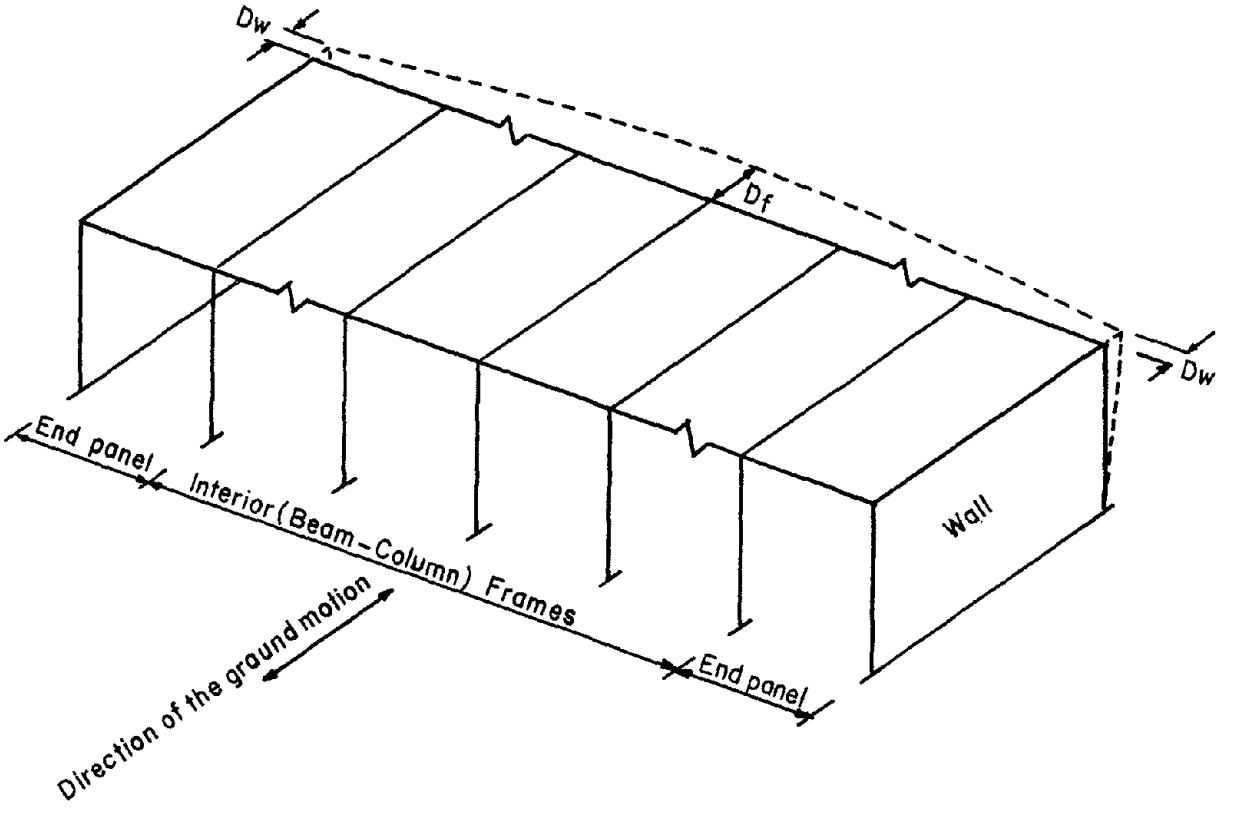

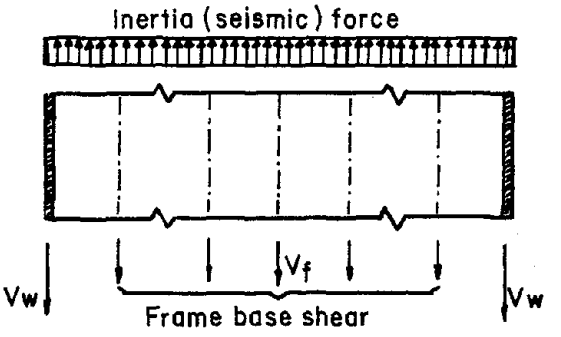

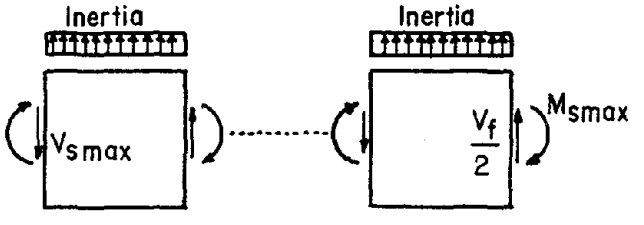

Notations:

Dw = End Frame Top Displ.
Df = Middle Frame Top Displ.
Vw = End Frame Base shear
Vf = Middle Frame Base Shear
Vs max.= Max. In-plane Slab Shear Force
Ms max.= Max. In-plane Slab Moment
Df-Dw = Slab Drift At Mid-frame

FIGURE 5-3 Definition of The Displacement Responses and Internal Forces

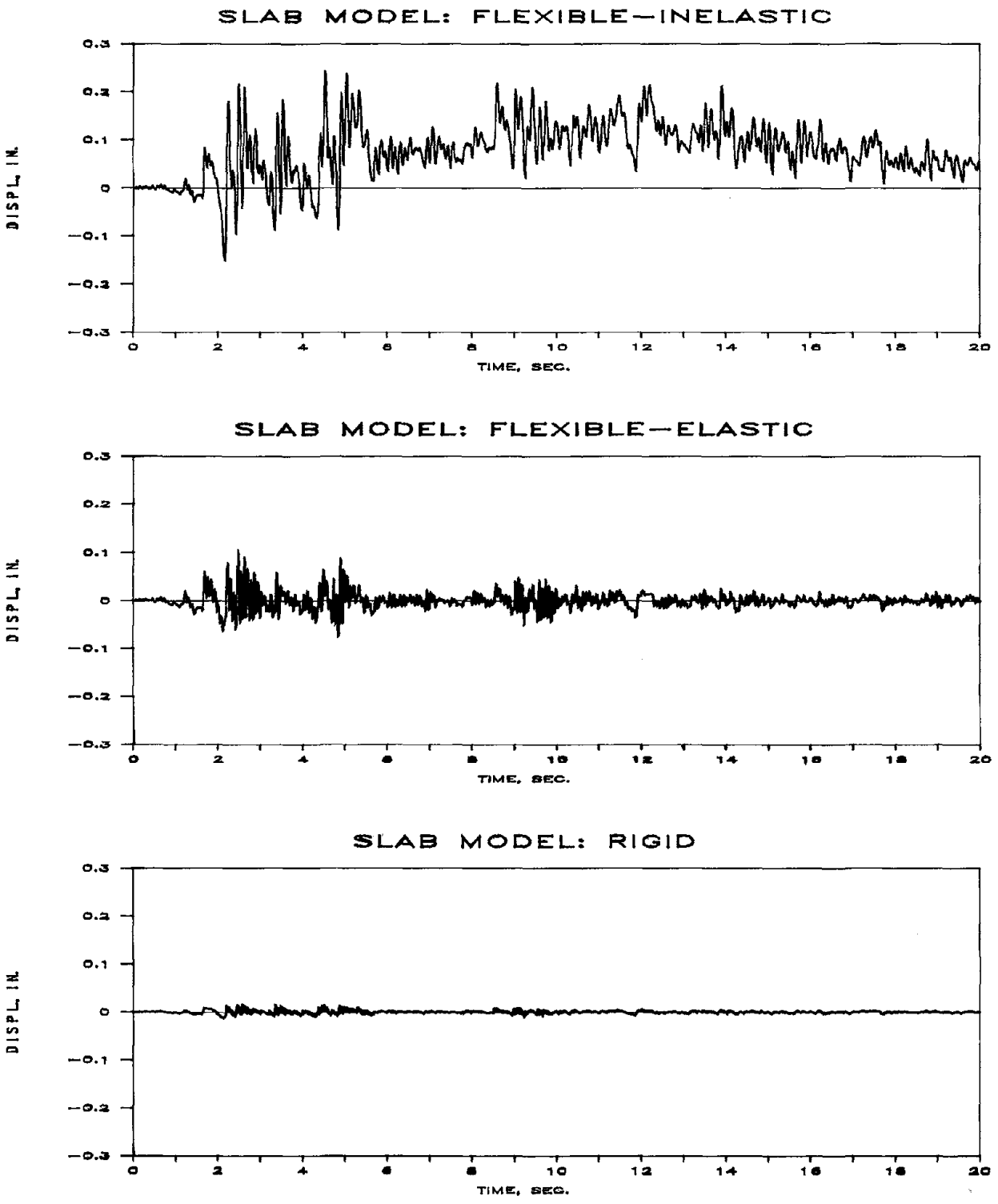

FIGURE 5-4 Lateral Displacement at the Middle Frame for 4 Span Structure

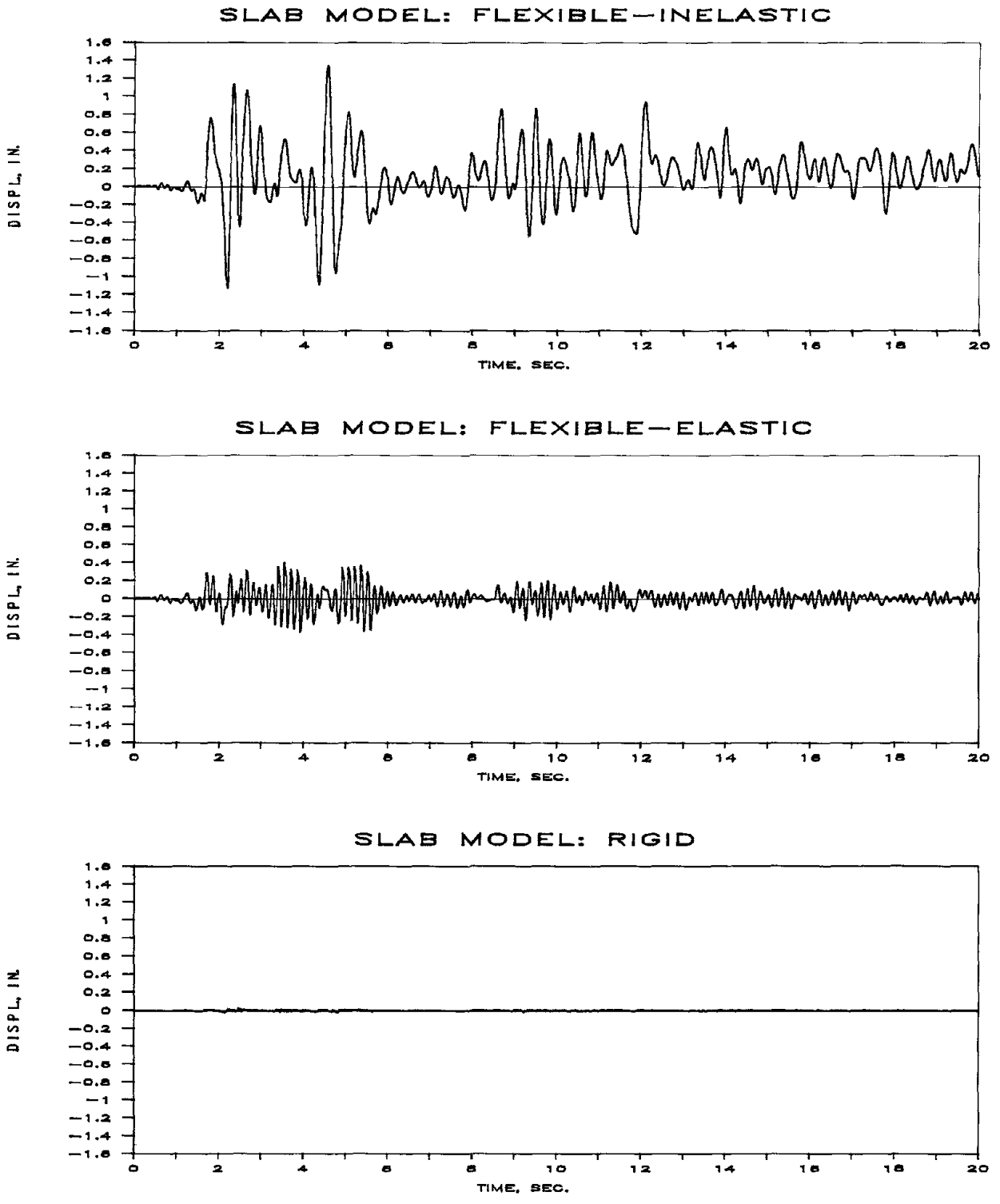

FIGURE 5-5 Lateral Displacement at the Middle Frame for 6 Span Structure

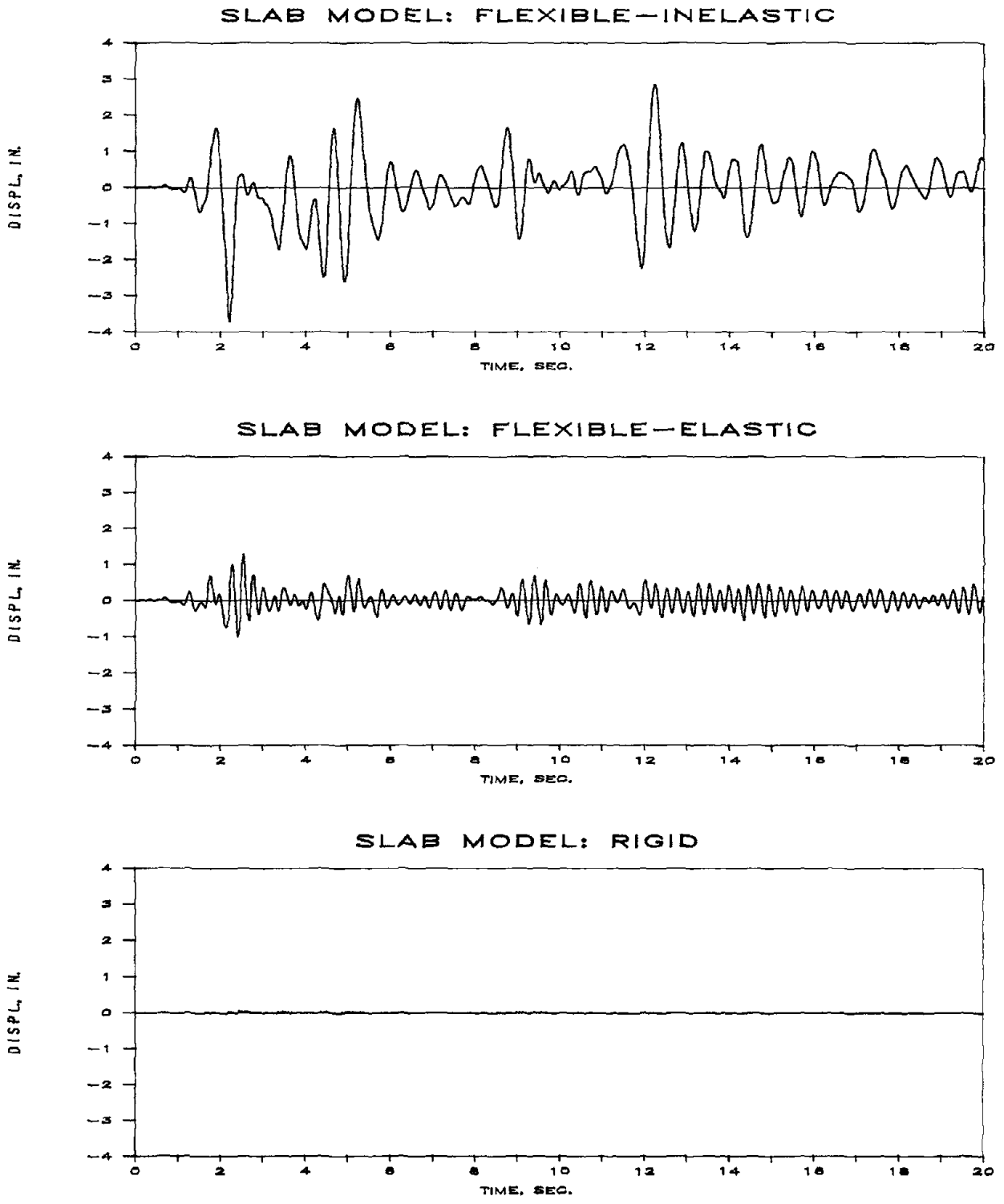

FIGURE 5-6 Lateral Displacement at the Middle Frame for 8 Span Structure

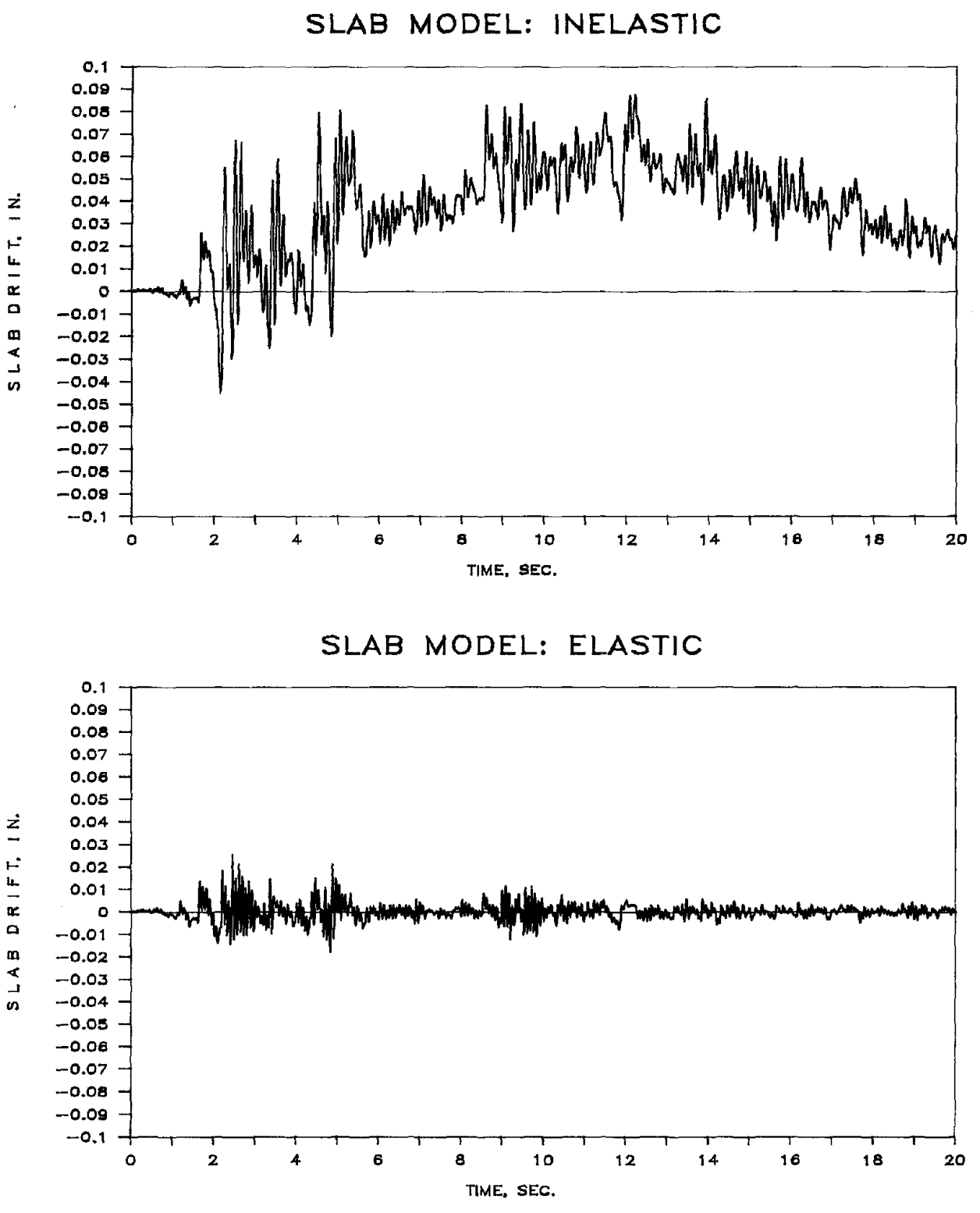

FIGURE 5-7 The Relative Displacement Between The Middle Frame and the End Wall (Slab Drift) for 4 Span Structure

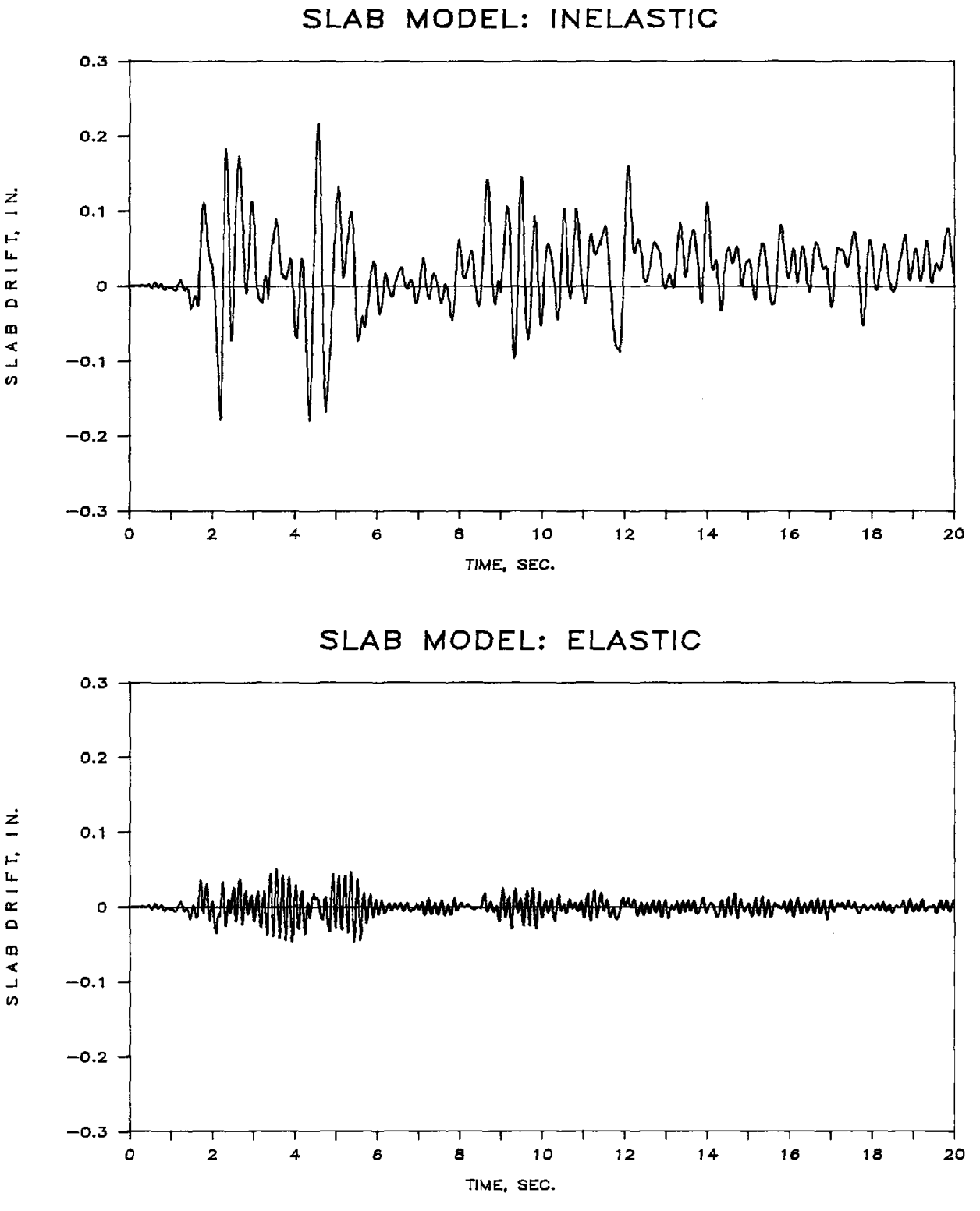

FIGURE 5-8 The Relative Displacement Between The Middle Frame and the End Wall (Slab Drift) for 6 Span Structure

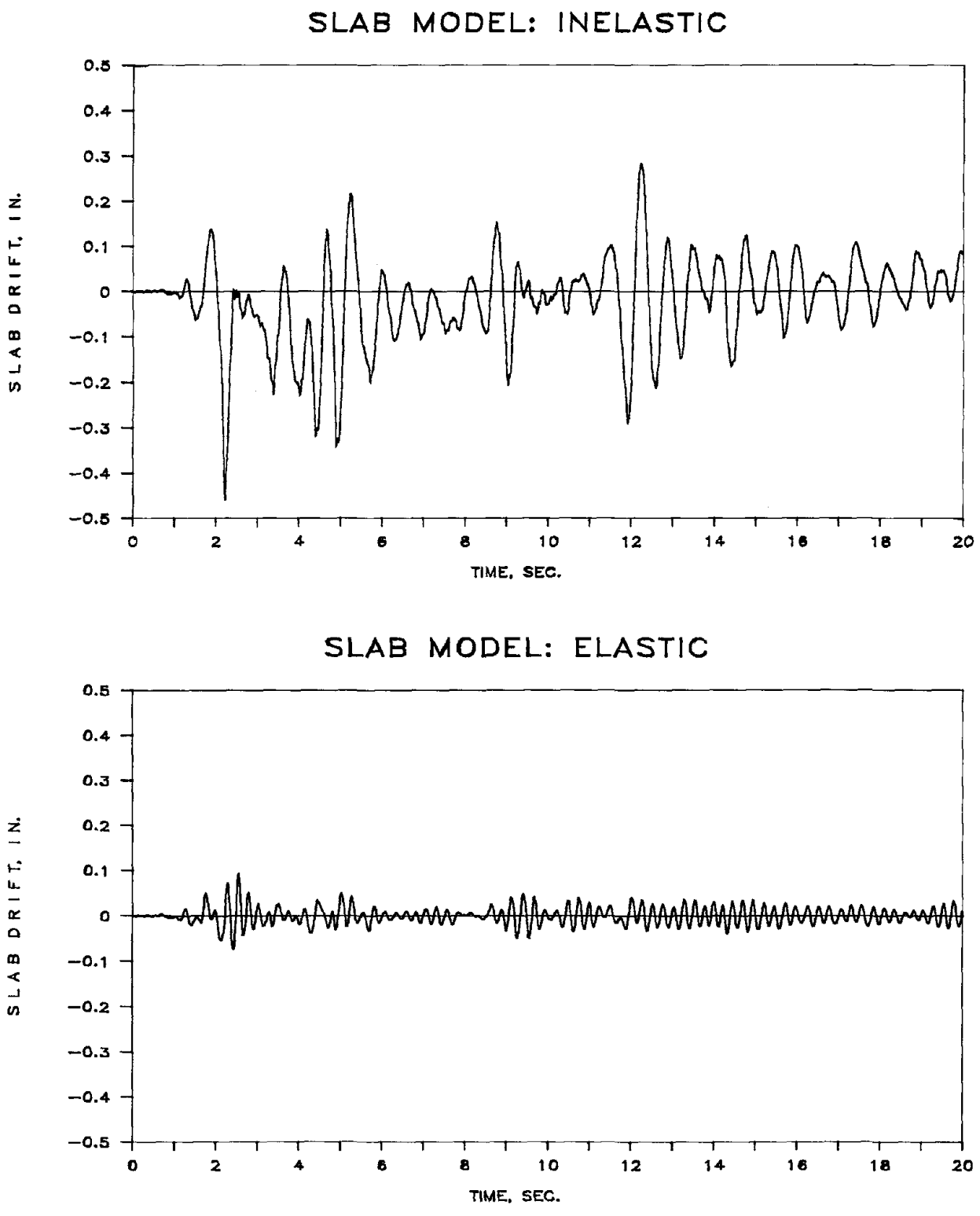

FIGURE 5-9 The Relative Displacement Between The Middle Frame and the End Wall (Slab Drift) for 8 Span Structure

Note that the rigid slab model does not allow for such a relative displacement between the frames.

The maximum in-plane shear forces for the slab floor, which occurs at the end panel, is plotted against the floor slab drift in Fig. 5.10 for inelastic slab model for 4, 6, and 8 span structures. Also, the maximum slab moment histories (in-plane, occurring next to the middle frame) are compared for the three structure in Fig. 5.11 for inelastic slab model. To provide a better understanding of the local inelastic behavior of the slab panel, the moment-curvature hysteresis curves are shown in Fig. 5.12.

Finally, the base shear versus the floor displacement at the middle frame are shown for 4, 6, and 8 span structures in Figs. 5.13, 5.14, and 5.15, respectively. The frame base shear forces and the frame displacements are normalized with respect to the maximum corresponding values obtained from the rigid slab model analysis for each structure.

The importance of recognizing the flexibility of diaphragms is better understood observing the distribution of the maximum base shears in the inner frames of the structures (see Table 5.2).

Although the shear walls carry the larger part of the base shear (Table 5.2 (5)) the assumption of rigid diaphragms underestimates the distribution of shear to the frames (Table 5.2 (7)). In all cases assuming elastic floor diaphragms, the shear distributed to the interior frames is 4, 5, and 4.7 times larger than for the rigid model of test structures with 4, 6 and 8 spans respectively. However, assuming an inelastic model, which simulates more accurately the inplane bending, cracking and shear, the shear distribution to the frames is 8, 10, and 10.3 times greater than the rigid model. The increase in shear distribution is accompanied by a substantial increase in the absolute value of shears in frames when flexible models are assumed. This increase in the case of earthquake excitation (El Centro 1940) is due to the increase in the spectral response caused by a shift of the natural frequencies (Table 5.3(4)) toward larger amplitudes. The effect is more pronounced in longer buildings (8 spans).

The effect of inelastic diaphragm behavior is reflected in smaller magnitude of total base shears, than for elastic behavior (compare FE and FI in Table 5.2). This is due to the energy absorption in the hysteretic behavior of slabs. At the same time, however, the frames are responsible to carry larger shears when the diaphragm yields during an inelastic response (see Table 5.2(7)). All the effects mentioned above more accentuated in diaphragms with larger aspect ratios.

Neglecting the inelastic response of diaphragms with large aspect ratios is unconservative for the design of frames in shear-wall-frame systems. This will lead to severe damage of frames and eventaully to the loss of the vertical load carrying capacity with disastrous consequences.

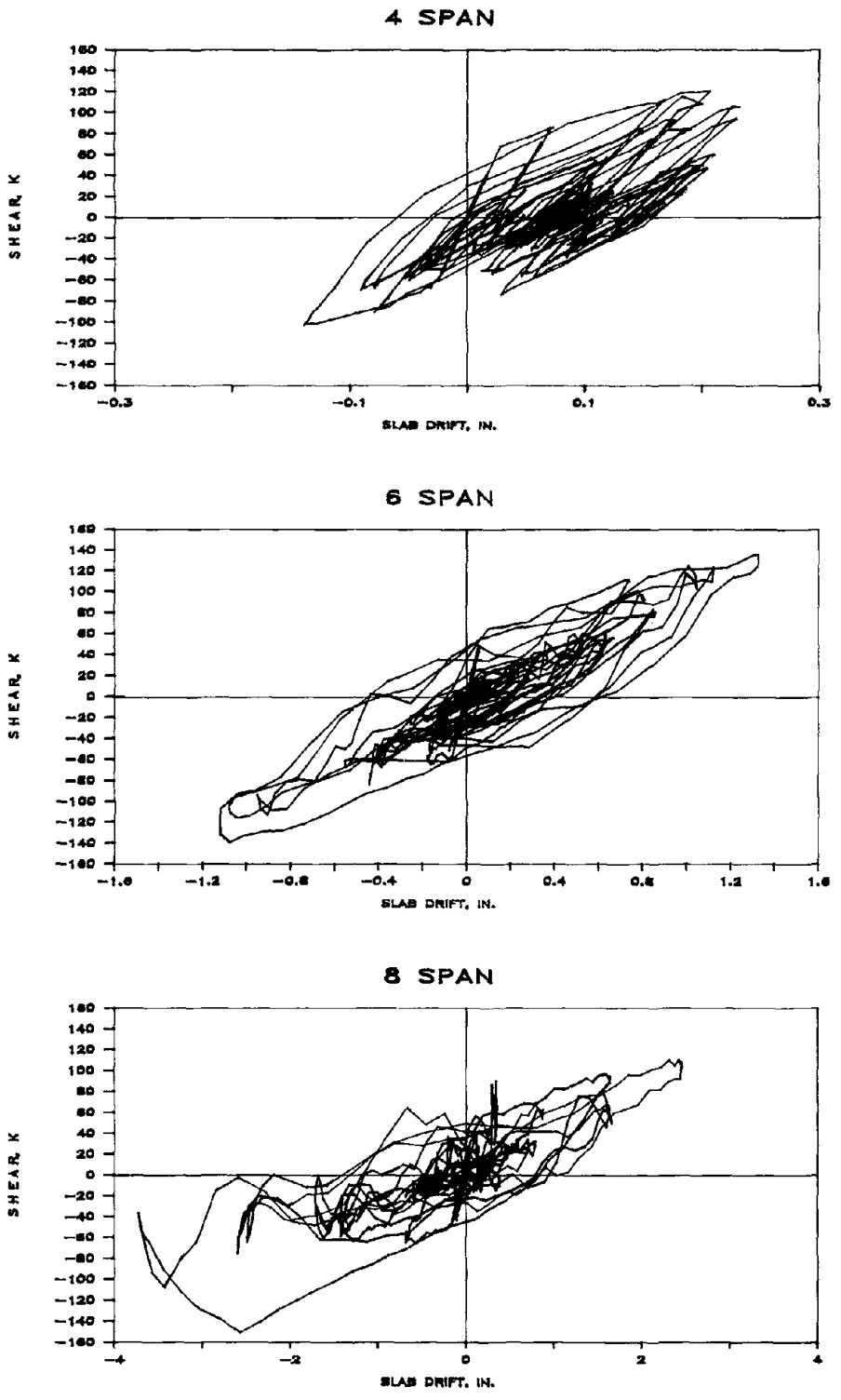

FIGURE 5-10 End Panel Slab Shear Force (in-plane) Vs. Slab Drift for the Multi-Span Structure Using Inelastic Slab Model

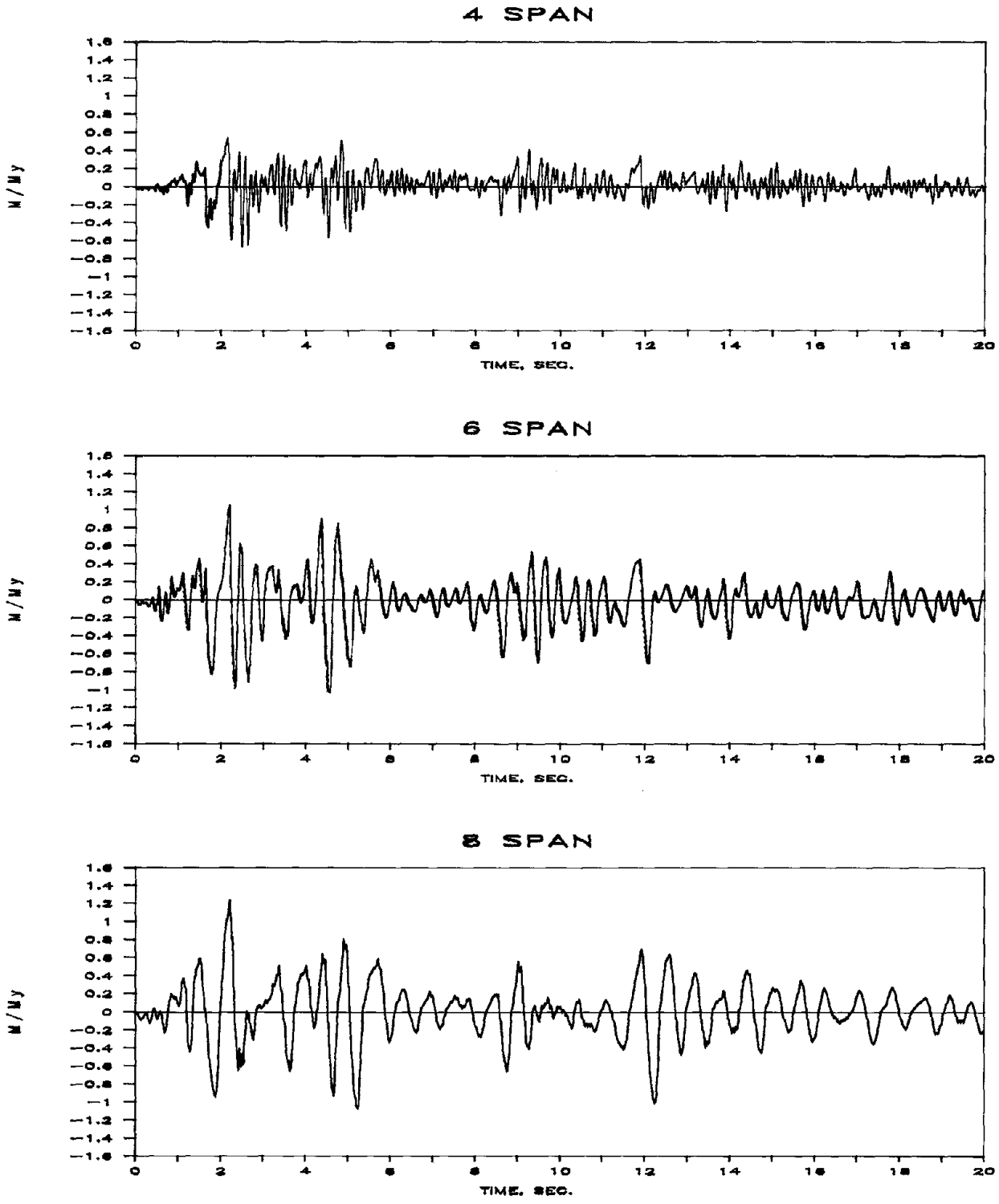

FIGURE 5-11 Maximum Slab Moment (in-plane) for the Multi-Span Structure Using Inelastic Slab Model

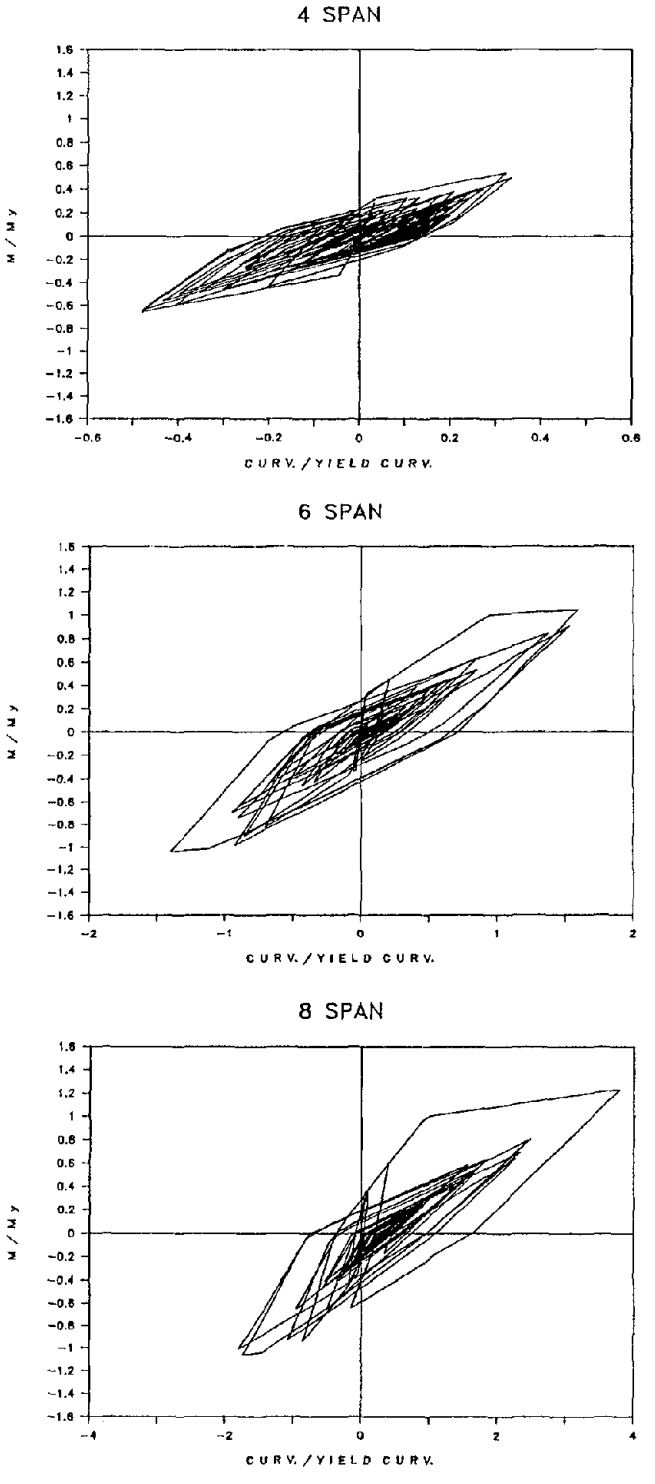

FIGURE 5-12 Slab Moment-Curvature Curves for the Multi-Span Structure Using Inelastic Slab Models

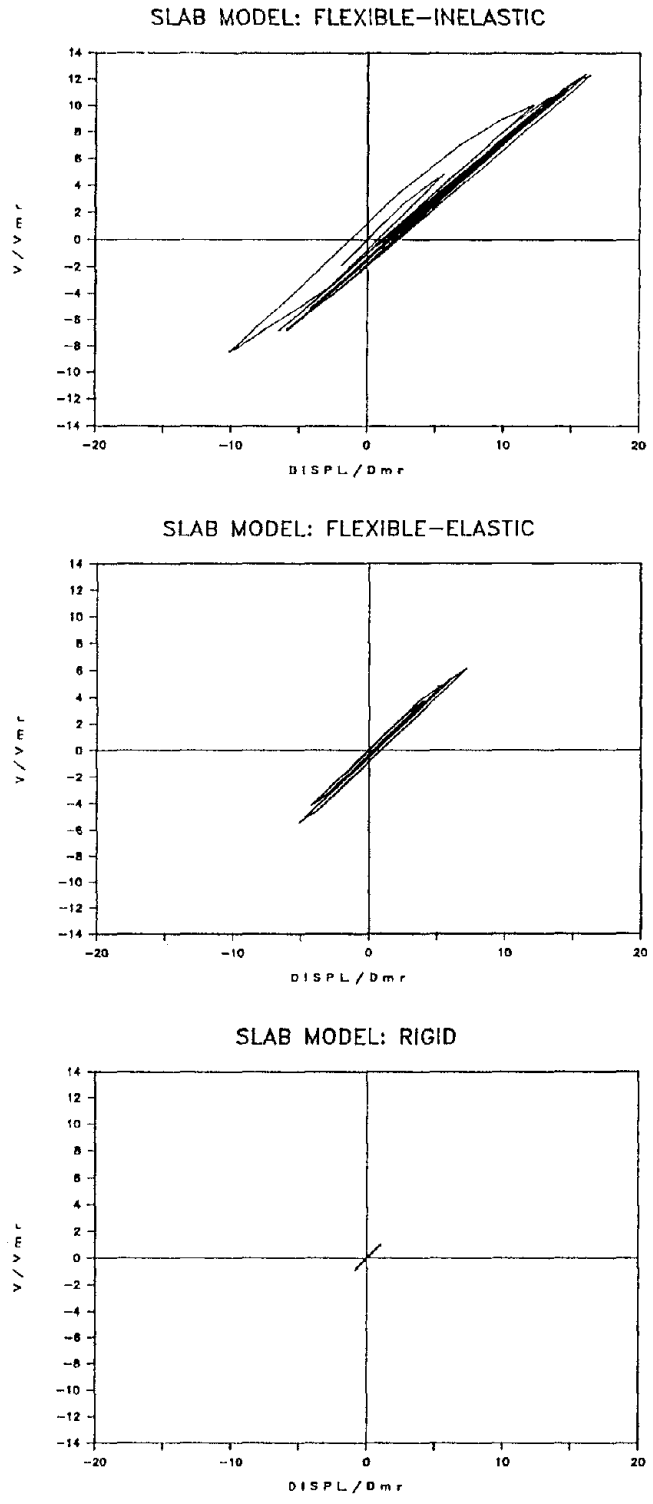

FIGURE 5-13 Base Shear Force Vs. Frame Displacement Curves for the Middle Frame for 4 Span Structure

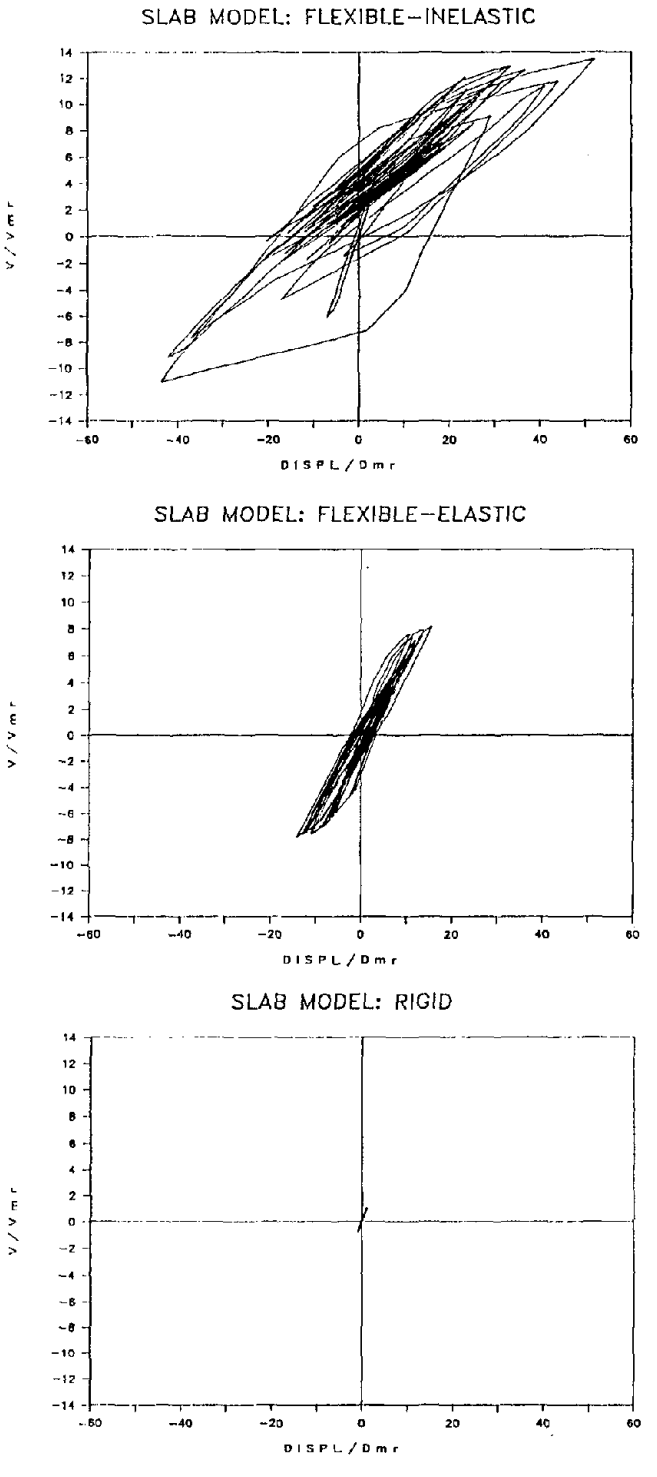

FIGURE 5-14 Base Shear Force Vs. Frame Displacement Curves for the Middle Frame for 6 Span Structure

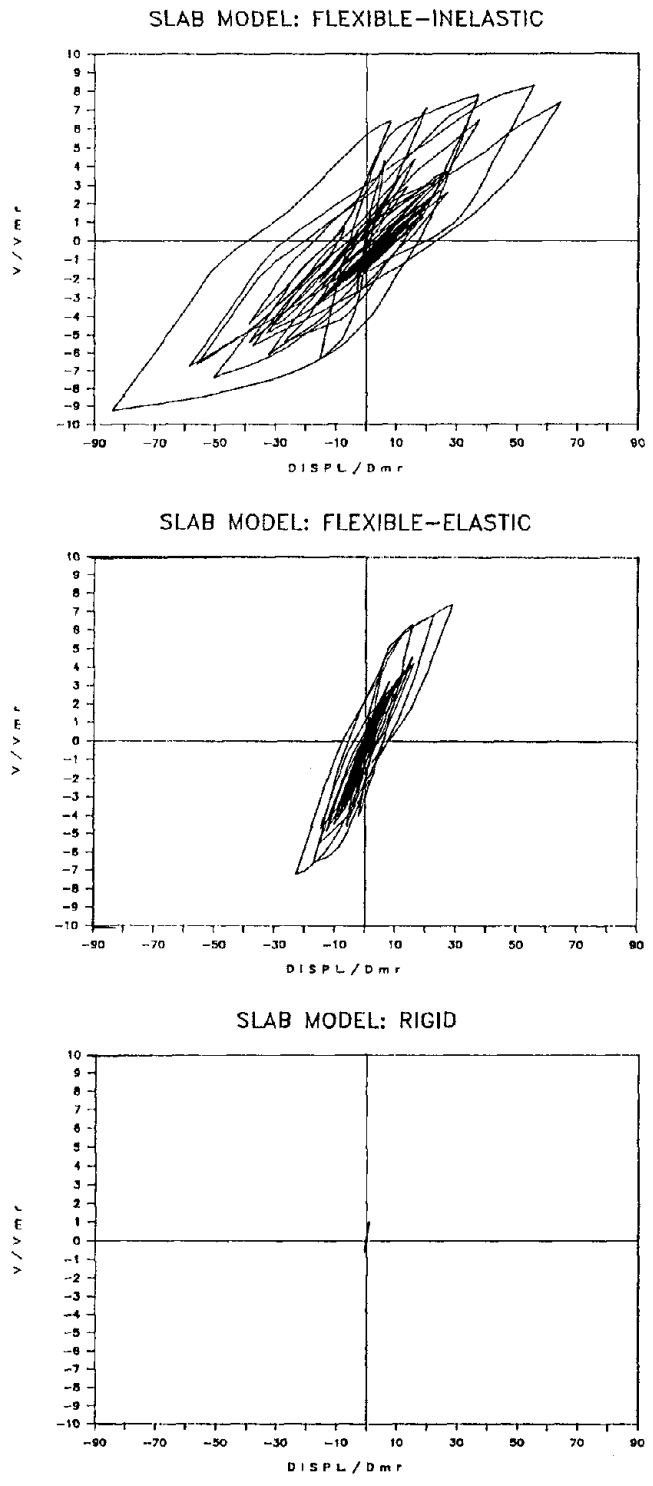

FIGURE 5-15 Base Shear Force Vs. Frame Displacement Curves for the Middle Frame for 8 Span Structure

TABLE 5-2 Maximum Base Shear Distribution

No. of Spans	Slab Model*	Total Shear (kips)	End Walls		Interior Frames	
			Shear (kips)	% of Total	Shear (kips)	% of Total
(1)	(2)	(3)	(4)	(5)	(6)	(7)
4	R	400.3	396.8	99	3.50	1
	FE	526.8	508.0	96	18.8	4
	FI	402.6	371.2	92	31.4	8
6	R	711.2	700.2	98	11.0	2
	FE	778.5	704.6	90	73.9	10
	FI	470.0	375.2	80	98.4	20
8	R	885.8	860.8	97	25.2	3
	FE	1139.0	978.6	86	160.4	14
	FI	611.9	419.8	69	192.1	31

* R : Rigid, FE : Flexible Elastic, FI : Flexible Inelastic

TABLE 5-3 Natural Frequency of Dominant Mode

No. of Spans	Slab Model*	Frequency (Hz)	Period (Seconds)
(1)	(2)	(3)	(4)
4	R	27.0	.037
	FE	16.9	.060
	FI	16.9	.060
6	R	22.7	.045
	FE	9.43	.110
	FI	9.43	.110
8	R	19.6	.050
	FE	6.28	.160
	FI	6.28	.160

* R : Rigid, FE : Flexible Elastic, FI : Flexible Inelastic

SECTION 6
ANALYTICAL PREDICTIONS OF SHAKING TABLE RESPONSE OF A SINGLE STORY 1:6 SCALED MODEL STRUCTURE

This chapter presents the analytical studies prepared for the design and planning of a shaking table test of a 1:6 scale model. The study was done using the analytical model developed in the previous sections. General description of the prototype and the scaled model structures are described first, followed by a parametric study of the collapse mechanism of the model structure, which serves as a guiding tool for modification of the model structure, to obtain the desired response during the shaking table test. Finally, the predicted response of the model structure on the shaking table is presented.

6.1 Description of Prototype and Scaled Model Structures

The geometry of the prototype used is similar to the 4 span single story structure analyzed in Chapter 5, except instead of a full length (25 ft.) wall at the ends, a stiff frame which consisted of two 10 ft. long walls coupled by a 12 ft. long beam with the same dimensions as the other beams is used. This design would provide better interaction between the end and interior frames, while it still preserves the relative high stiffness of the end frame with respect to the floor slab panel system. Also, the natural period of the structure is greater, which results in an increase in the response amplification of the structure, in comparison to the structure with full walls.

The prototype structure design satisfies the same specification and load conditions described in Sec. 5.1. Grade 50 reinforcements are used for the columns, the walls, and the beams, while Grade 40 reinforcements are used for the slabs and hoop ties for all of the frame members. A concrete strength of 4000 psi is adopted for the entire structure.

In accordance with the geometry and capacity of the shaking table at SUNY/Buffalo [8], a 1:6 scale is chosen for the 4-span single story structure. The model structure is designed to comply with the similitude requirements for a direct reduced scale model. This means that the model material properties are assumed to be similar to the prototype material properties, while additional non-structural mass is used to correct the similitude requirement governing the mass density for the structure. The overall geometry of the scaled model is shown in Fig. 6.1a.

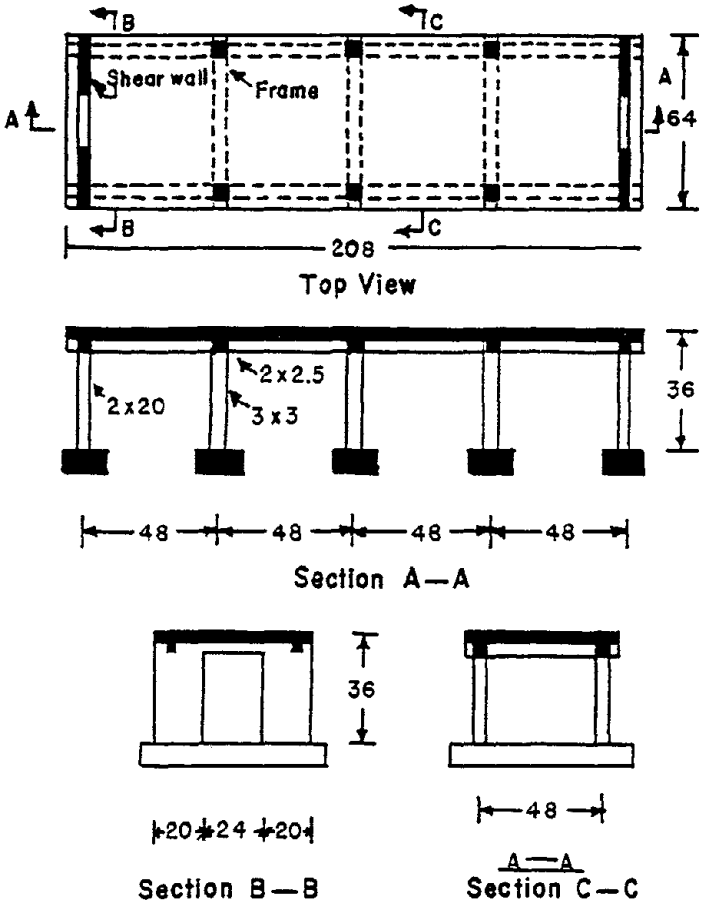

(a) Overall Geometry

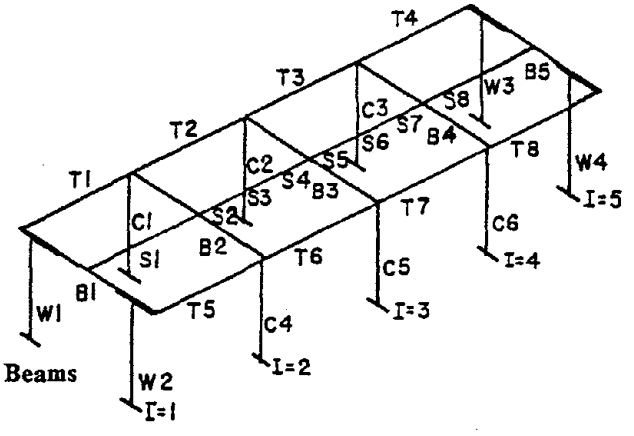

Member Notations

W1-W4 = Walls
C1-C6 = Columns
B1-B5 = Beams
T1-T8 = Transverse Beams
S1-S8 = Slabs

(b) Discretization of the Structure

FIGURE 6-1 1:6 Scaled Single Story Model Used for Shaking Table Test

6.2 Discretization of the Model Structure

The discretization of the model structure is done similarly to the structures analyzed in Chapter 5 with one major difference; the interior slab panels are further divided into three regions in the longitudinal direction (see Fig. 6.1b). This is done to reflect the distribution of the slab reinforcement in longitudinal direction (between positive and negative moment regions). Also, it provides a better lumped mass distribution and a more accurate representation of the yield penetration along the interior slab panels.

It should be noted that for the model response prediction, the actual properties of the model material are used. The detailed list of the input information for the analysis, are given in the output sample given in Appendix B.

6.3 The Collapse Mechanism Study under Monotonically Increasing Lateral Loads

The collapse mode analysis performed by the IDARC2 program is used to identify the failure mechanism for the model structure. For this purpose the structure is loaded uniformly along the floor slab in the transverse direction. The gravity load due to self weight is included by applying them along the transverse beams. The yielding sequence of the structural members are obtained as the lateral load is increased incrementally up to failure; i.e., the failure is defined when the maximum lateral displacement reaches 2% of the structure height.

The initial analysis indicated that the yielding of the end frames at a total lateral load of 12.69 kips dominates the early nonlinear behavior of the model, followed by the yielding of the beams and columns of the interior frames. The structure failure occurs at 16.24 kips , see Table 6.1 (Case 1). This clearly shows that the minimum reinforcement required by the design, is not adequate to insure inelastic behavior in the slab. Since the main objective of the shaking table test is to cause extensive inelastic damage in the slab panels (so that the correlation of the test results with the computed prediction are utilized for calibration of the analytical method), it is found necessary to increase the yielding capacity of the end frames. This is done by changing the amount and distribution of the wall reinforcement, and increasing the amount of steel in the connecting beam.

TABLE 6-1 Yielding Sequence Obtained from Collapse Mechanism Analysis

Case No.	End Frame Member Reinforcement Area *		Member Yield Sequence	
	Wall	Beam	Base shear Force, k	Member Yielding **
1	.184 uniformly distrib.	Top = .04 Bot.= .04	12.70 13.29 13.88 14.17 14.47 15.06 15.06 15.06	W1, W2, W3, W4 (Bottom) B1, B5 (Left) B3 (Right) B2, B4 (Right) C4, C5, C6 (Bottom) B1, B5 (Right) C1, C2, C3 (Bottom) Structure Failure
2	.336 60% at edges	Top = .04 Bot.= .04	14.76 20.67 21.55 21.85 22.14 22.44 22.73 22.73 22.73 23.03 23.62 23.92	B1, B5 (Left) S3, S6 (Right) B3 (Right) B2, B4 (Right) C5 (Bottom) C4, C6 (Bottom) C2 (Bottom) W1, W2 (Bottom) W3, W4 (Bottom) C1, C3 (Bottom) B1, B5 (Right) Structure Failure
3	.336 60% at edges	Top = .08 Bot.= .08	20.67 21.55 22.14 22.14 22.44 22.73 23.32 23.62 24.80 25.10 25.10	S3, S6 (Right) B3 (Right) C5 (Bottom) B2, B4 (Right) C4, C6 (Bottom) C2 (Bottom) C1, C3 (Bottom) W1, W2, W3, W4 (Bottom) B1, B5 (Left) B1, B5 (Right) Structure Failure

* -- Unit: square inch;
** -- See Fig.6.1_b for member notations

Table 6.1 summarizes the the results of the analyses for 3 different cases. Increasing the wall reinforcement from 0.46% to 0.85% (of the gross wall area), and placing of 60% of it at the wall edges, increases the capacity of the wall by 76%, This allows for the yielding in the slab to occur prior to the yielding of the end walls (Case 2). The slab panel yields at a lateral load of 20.66 kips. Then at a lateral load of 22.73 kips, the walls yield, and eventually the structure fails at a load of 23.92 kips. It is noted that the connecting beam experiences an extensive amount of deformation since it yields at a load of 14.76 kips prior to the slab members (see Table 6.1).

To prevent premature local failure of the connecting beam between the walls, the reinforcing of the connecting beam is increased by a factor of two in Case 3. This changes the member yielding sequence slightly, and the structure failure occurs at a load of 25.1 kips. Due to an increase in the lateral loads required to cause yielding the end frame and structure failure, larger amount of ductility is experienced in the interior frames and the slab panels. Consequently, the Case 3 design is selected for the shaking table test. This model structure with varying amount of live load (in addition to the non-structural mass used to correct the density similitude requirement), have been analyzed, for different ground motions. The predicted responses are presented in the following section.

6.4 Results of Seismic Response Analysis

The main goal of the experimental study is to test a single story structure with inelastic floor diaphragm action using simulated earthquake motion. To obtain this objective within the capacity limitation of the shaking table, a parametric study is conducted using the seismic response analysis of the IDARC2 program.

6.4.1 Parametric Study

The main variables studied are:

1) The amount of the live load to be included on the floor panels.

2) The scaled earthquake accelerogram applied to the base of the model structure.

Five cases (Cases A, B, C, D, and E) are considered where the live load considered varies between 0.0% to 100% of the total floor area, distributed symmetrically about the center of the structure. The amount and pattern of the live load considered are shown in Fig. 6.2.

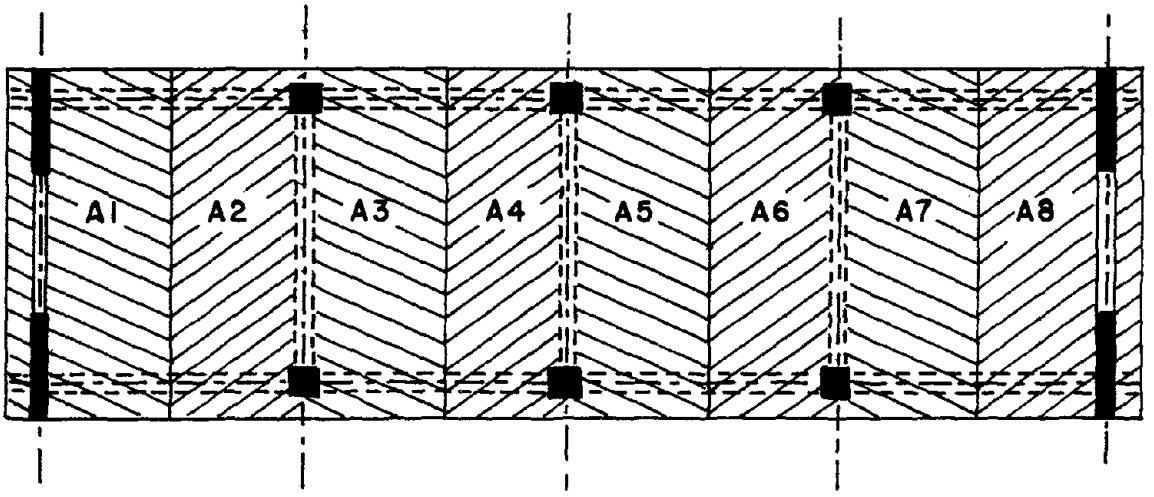

Case	Slab Areas with Live Load
A	None
B	A4-A5
C	A3-A6
D	A2-A7
E	A1-A8

FIGURE 6-2 **Contributory Area for the Live Loads Used for the Parametric Study of the Model Structure**

Inelastic dynamic analysis of the model structure subjected to the normalized and scaled Taft 1952 and El Centro 1940 earthquakes for five different cases of live loads considered has been conducted. Fig. 6.3 shows the scaled accelerograms used in the analysis. The maximum acceleration is limited to 0.95g due to shaking table capacity limitation dictated by the size of the model used. The time scale is compressed by dividing it by the square root of the scale factor for the model to confirm with the similitude requirement.

The summary of the maximum response predicted by the analyses is presented in Table 6.2. When no live load is included, Case A (Fig. 6.2), it is observed that the internal forces caused by the El Centro earthquake, are larger than the values obtained from the Taft earthquake. Also, most of the structural members are either in the elastic range or experienced only cracking. As the amount of the live load increases, the overall response of the structure increase. The interior slab panels yield due to in-plane bending for the loading Case C (where the live load for the interior two panels are considers), for both Taft and El Centro earthquakes. It is noted that, after the slab experiences severe inelastic cracking or yielding, the maximum in-plane moment for the interior slab panels, and the maximum displacement for the middle frame are larger for the Taft earthquake than the corresponding values obtained from the El Centro earthquake. This is mainly due to the wider range of frequencies present in the Taft accelerogram, which excites the floor diaphragm action of the model structure after in-plane slab flexibility becomes more evident, when the slab yields.

To cause adequate amount of inelastic damage in the slab panels without risking of sudden type failure due to a lack of ductility of the slab panel, the use of live load Case C with the scaled Taft accelerogram is found to be satisfactory. The detail of the results of this analysis is presented and discussed next.

6.4.2 Analytical Prediction of the Shaking Table Test

The predicted response of the 1:6 scale model using the scaled Taft earthquake motion with a maximum acceleration of 0.95g (see Fig. 6.3) for the live load Case C (Fig. 6.2) is presented in this section. Time history plots of the displacement, base shear, and The corresponding hysteresis curves for the middle and end frame are given in Figs. 6.4 and 6.5, respectively. It is noted that the middle frame peak displacement is about five times that of the end frame, which indicates that the inelastic floor flexibility plays an important role in the dynamic response of the model structure.

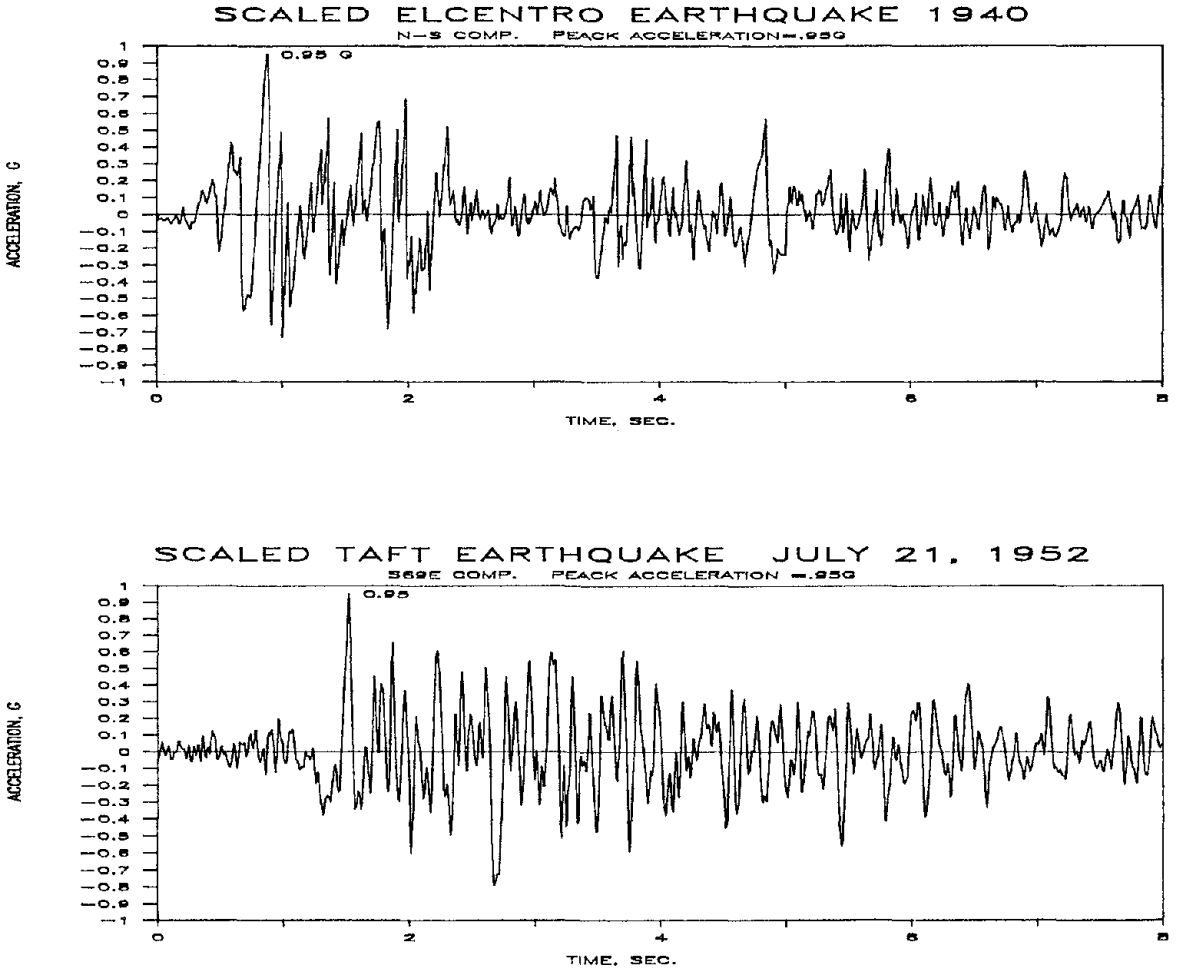

FIGURE 6-3 Scaled Accelerograms used for the Parametric Study of the Model Structure Response

TABLE 6-2 Summary of the Seismic Response Analysis for the Model Structure

Earthquake Record *	Live load Included *	Max. Displacement, in.		Max. Base Shear, k			Max. Slab Response		T
		End Wall	Middle Frame	Structure	End Wall	Middle Frame[1]	Vs	Ms/Mys	Sec/Cycl.
0	1	2	3	4	5	6	7	8	9
Elcentro	Case A	.012 (.883)	.059 (1.02)	12.11 (.882)	5.54 (.883)	.505 (1.09)	4.11 (1.03)	.717 (.922)	.034
	Case B	.018 (.937)	.093 (.932)	14.53 (.936)	6.55 (.935)	.466 (.932)	5.04 (.930)	.936 (.930)	.037
	Case C	.026 (2.05)	.138 (.104)	15.92 (2.05)	7.31 (2.05)	.525 (.938)	6.02 (.104)	1.09 (1.04)	.040
	Case D	.029 (2.05)	.161 (.943)	17.14 (.934)	7.81 (.934)	.572 (.943)	6.38 (.940)	1.11 (.940)	.042
	Case E	.035 (7.25)	.172 (.945)	19.32 (.882)	8.95 (.881)	.589 (.945)	6.49 (.940)	1.13 (.950)	.044
Taft	Case A	.009 (3.13)	.040 (1.88)	10.90 (1.53)	5.00 (1.53)	.390 (3.13)	3.44 (1.88)	.580 (1.88)	.034
	Case B	.024 (2.69)	.102 (3.77)	16.35 (2.69)	7.51 (2.69)	.486 (1.89)	5.03 (2.69)	.924 (3.72)	.037
	Case C	.032 (6.47)	.167 (3.84)	18.09 (2.70)	8.22 (2.70)	.516 (1.89)	5.99 (3.84)	1.14 (3.84)	.040
	Case D	.041 (2.70)	.247 (2.71)	20.58 (2.70)	9.52 (2.70)	.824 (7.18)	7.17 (2.71)	1.25 (2.71)	.042
	Case E	.047 (5.24)	.255 (2.71)	22.51 (2.71)	10.44 (2.71)	.890 (6.14)	7.06 (2.72)	1.22 (3.85)	.044

(Number in parenthesis = Time at which the max. response is reached)

* See Fig.6.2 & 6.3 for the amount and distribution of the floor, live load and earthquake accelerograms used.

Notations:

Vs --- Maximum in-plane shear in the end panel slab;

Ms --- Maximum in-plane moment in the mid-panel slab;

Mys --- Yield moment for the interior slab (Mys = 367 k-in.);

T --- Fundamental period of the structure.

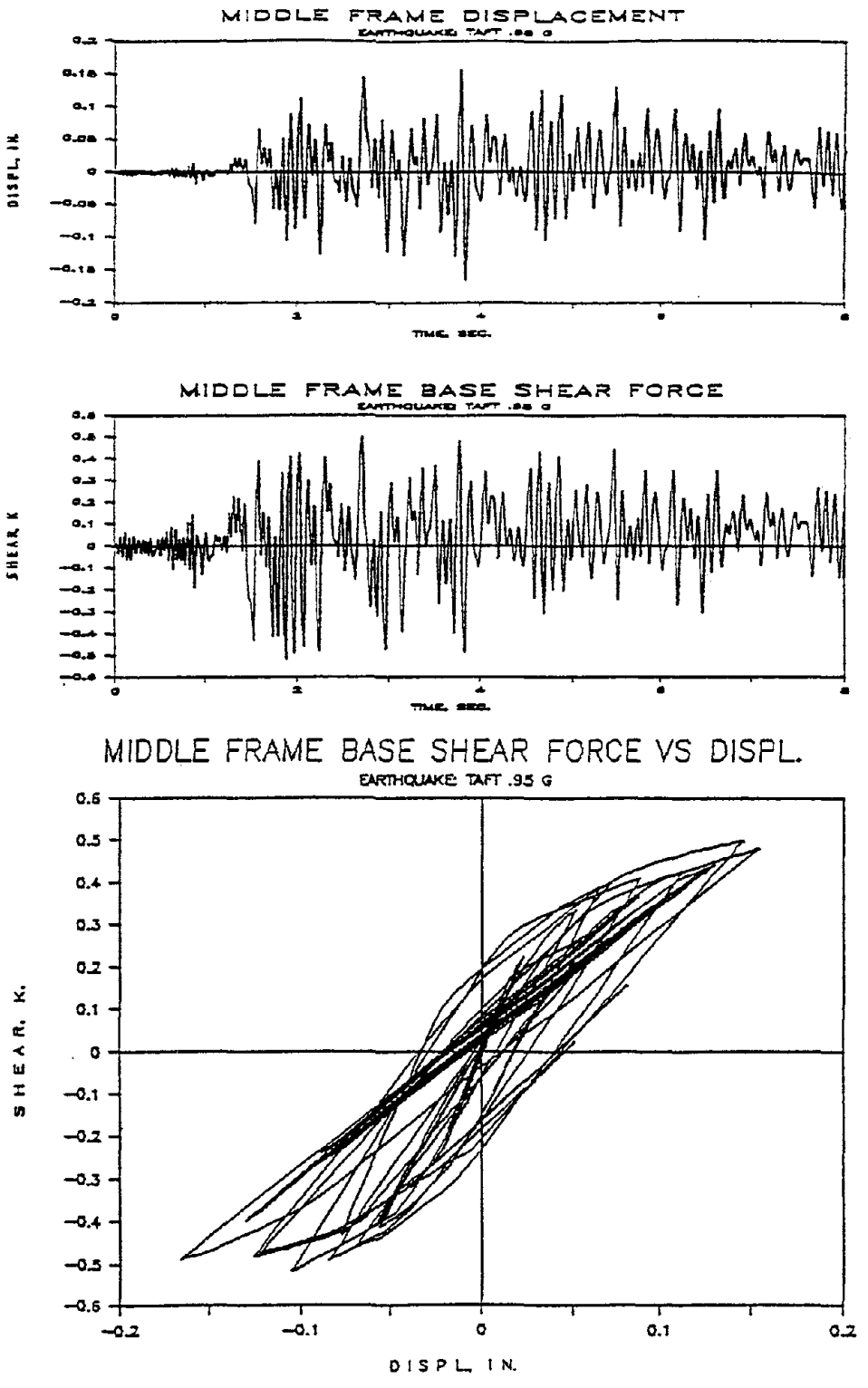

FIGURE 6-4 **Displacement and Base Shear Force of the Middle Frame for the Scaled Model Structure**

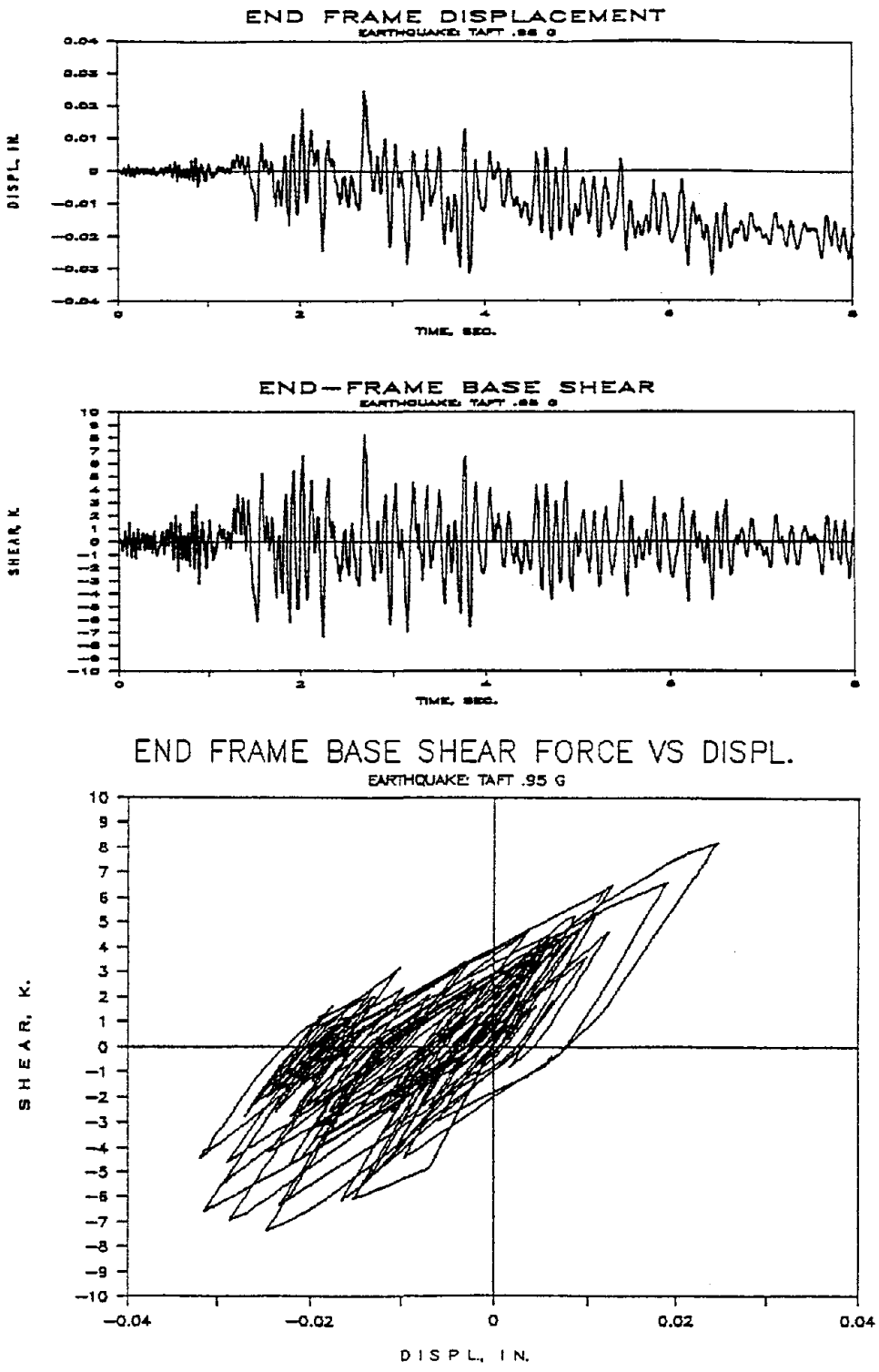

FIGURE 6-5 Displacement and Base Shear Force of the End Frame for the Scaled Model Structure

To illustrate the inelastic behavior of the floor slab system, the horizontal slab drift (the relative displacement between the middle and end frame) and the maximum in-plane slab shear history, which occurs at the end panel, is shown in Fig. 6.6. Also, the hysteresis relationship between the in-plane maximum slab shear and the slab drift is shown in Fig. 6.6. Since the non-linear behavior of the slab panels is mainly due to the in-plane bending of the interior panels, the slab moment history and the moment curvature plots give a local presentation of this action, shown in Fig. 6.7.

Finally, the structure is analyzed using an elastic slab and rigid slab model. The predicted response of the structure with inelastic slab. Plots of displacement and base shear histories for the middle and end frames are shown in Figs. 6.8-6.11.

The hysteresis curves of the middle frame base shear vs. displacement, normalized with respect to the peak values obtained from the rigid slab model analysis are compared in Fig. 6.12. The *maximum displacement* predicted by the inelastic and elastic slab models are 4.95 and 1.69 times the value obtained from rigid analysis, respectively. The *peak base shear forces* predicted by the inelastic slab model is 1.8 and 1.4 the value computed using elastic and rigid slab model, respectively. Thus, it can be concluded that, although the elastic slab model provides a better representation of the test structure behavior in comparison with rigid assumptions, it underestimates both the ductility and strength demands of the interior frames by factors of 2.9 and 1.3, respectively.

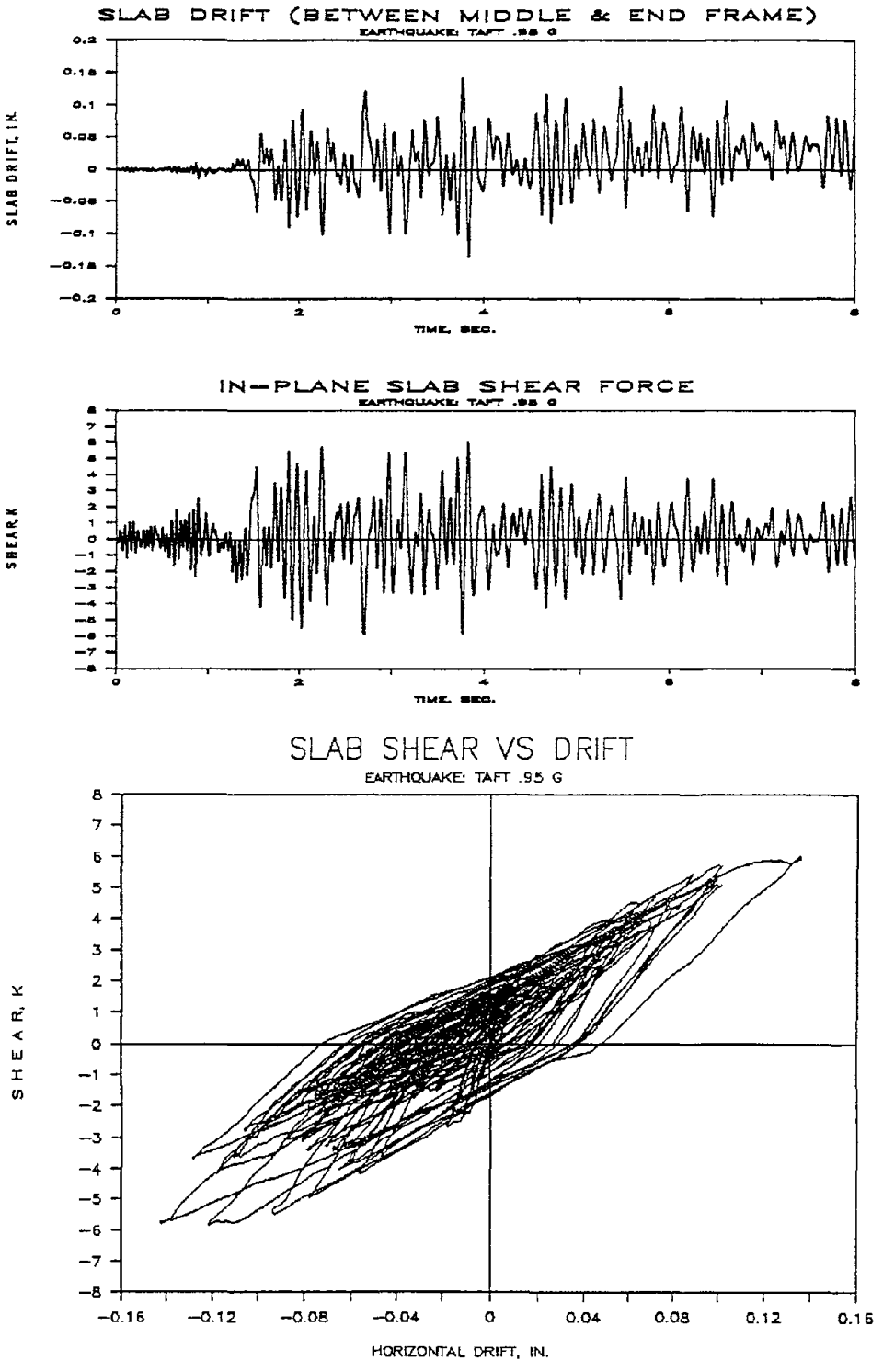

FIGURE 6-6 Slab Drift (Relative Displ. Between Middle and End Frame) and the In-plane Slab Shear Force at the End Panel for the Scaled Model Structure

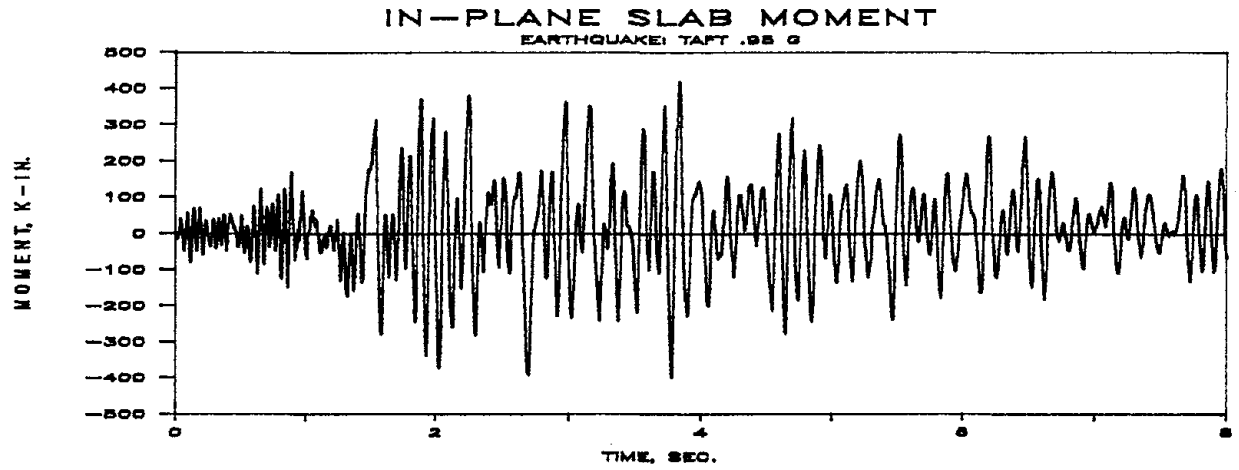

FIGURE 6-7a Slab Moment at Mid-region of the interior panel for the Scaled Model Structure

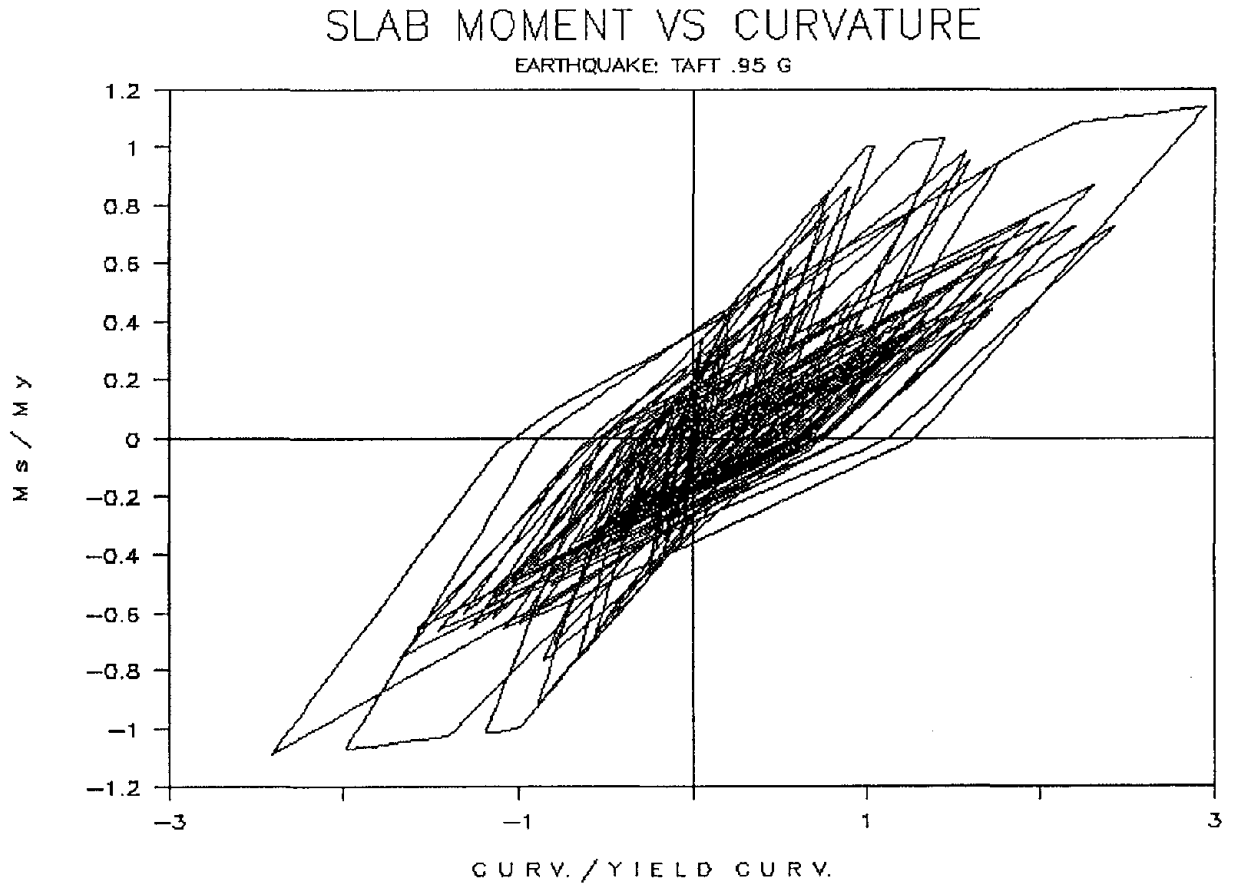

FIGURE 6-7b Moment-Curvature Plot at Mid-region of the interior panel for the Scaled Model Structure

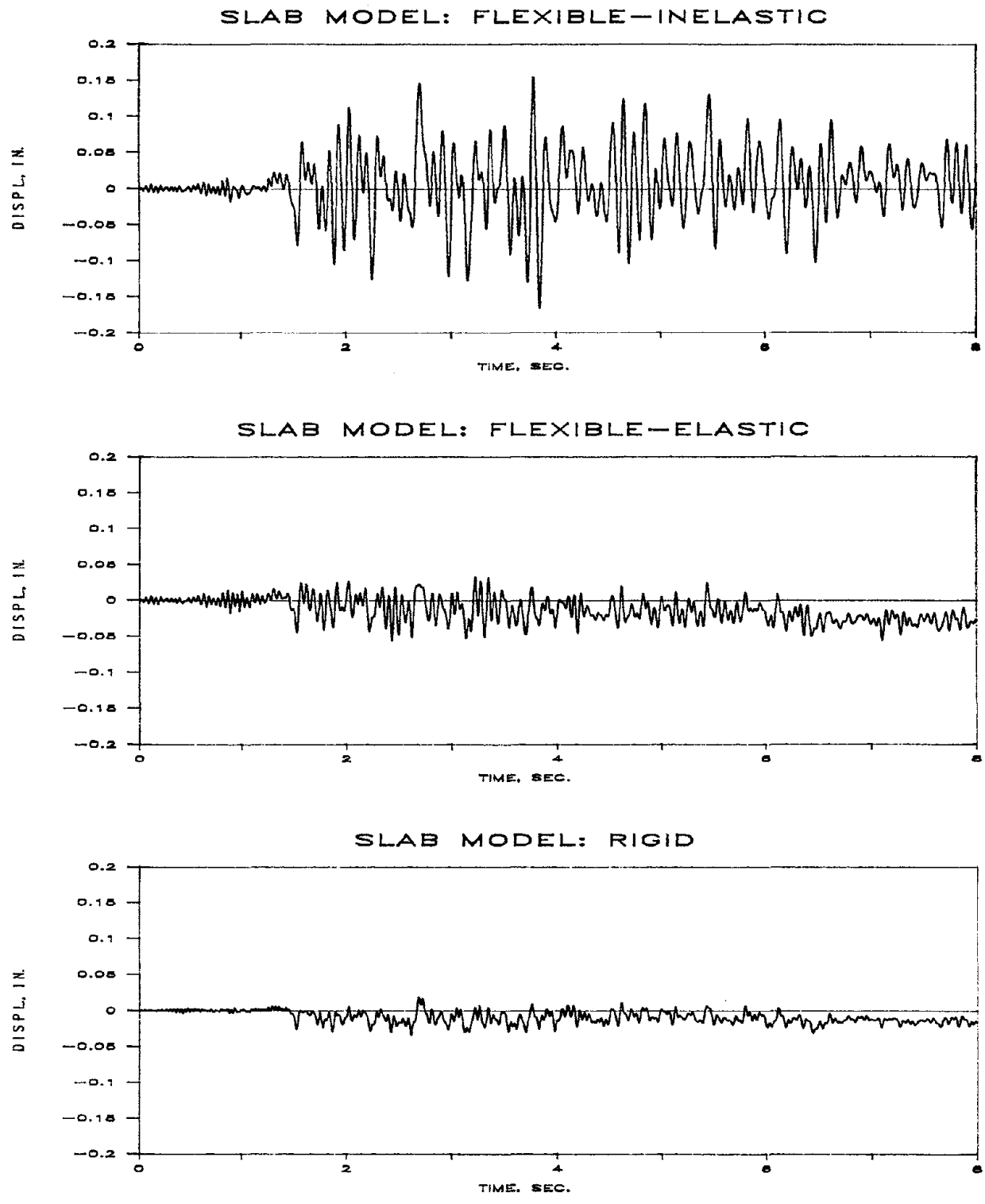

FIGURE 6-8 Lateral Displacement at Middle Frame for the Scaled Model Structure

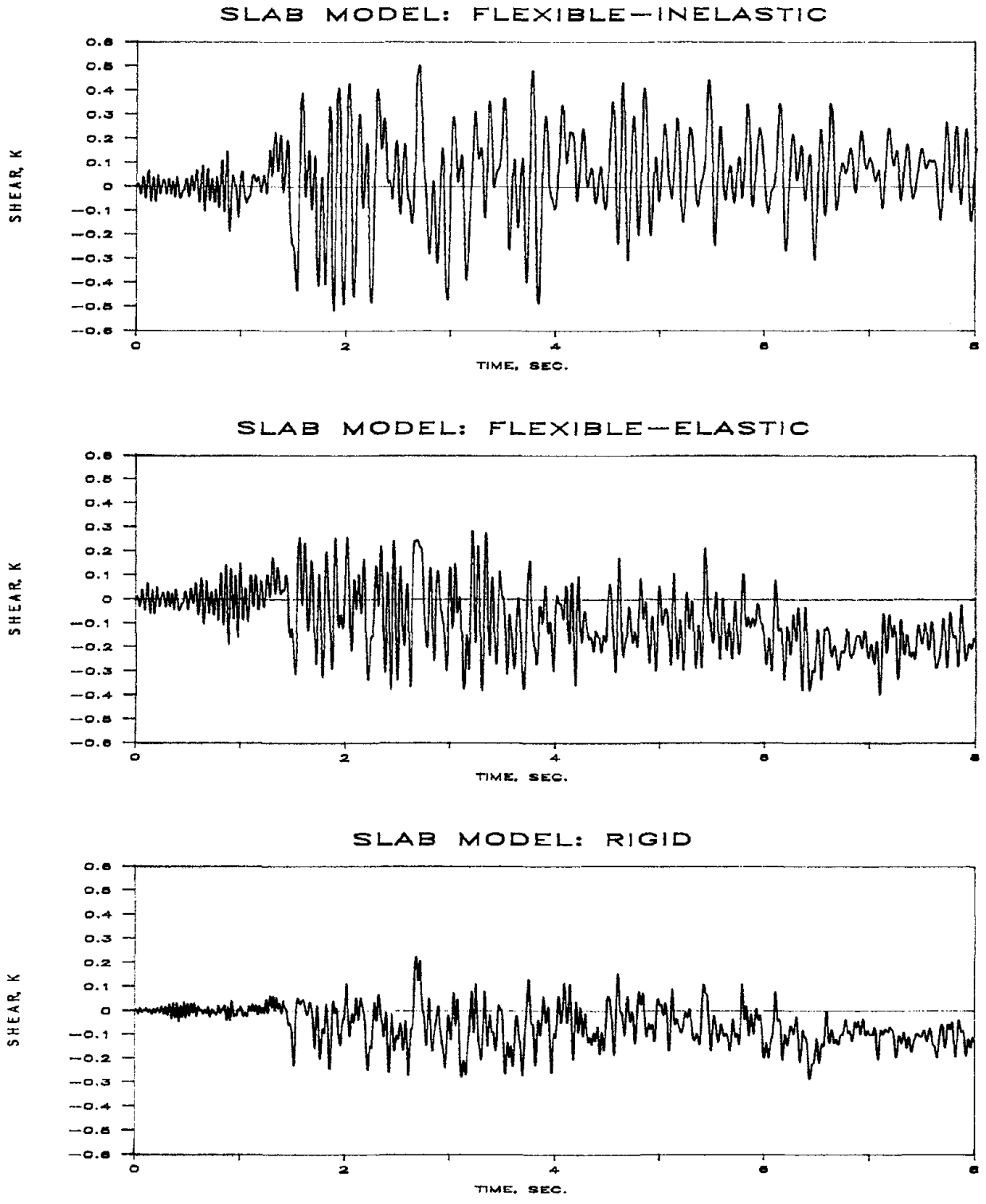

FIGURE 6-9 Base Shear Force Of the Middle Frame for the Scaled Model Structure

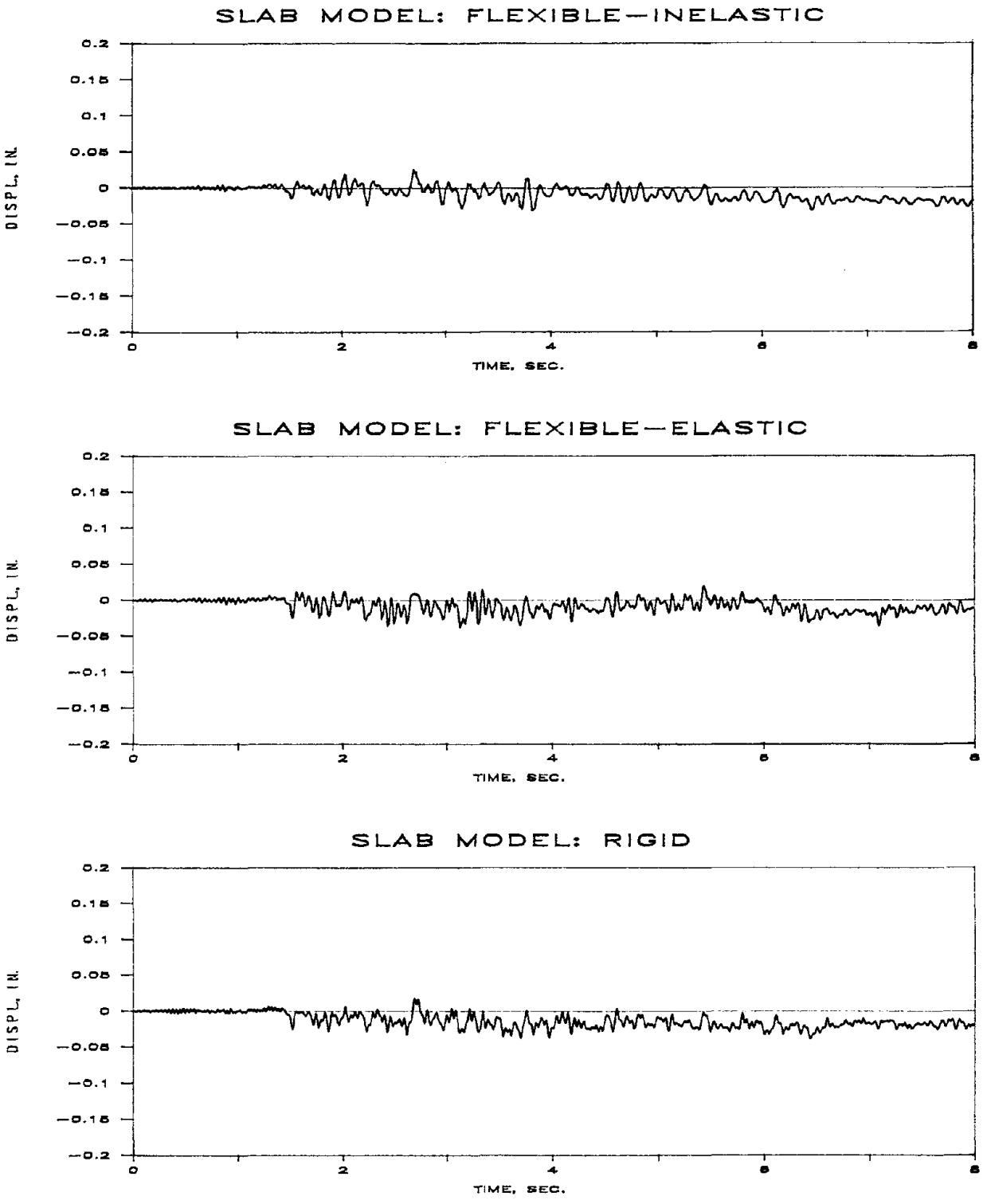

FIGURE 6-10 Lateral Displacement at the End Frame for the Scaled Model Structure

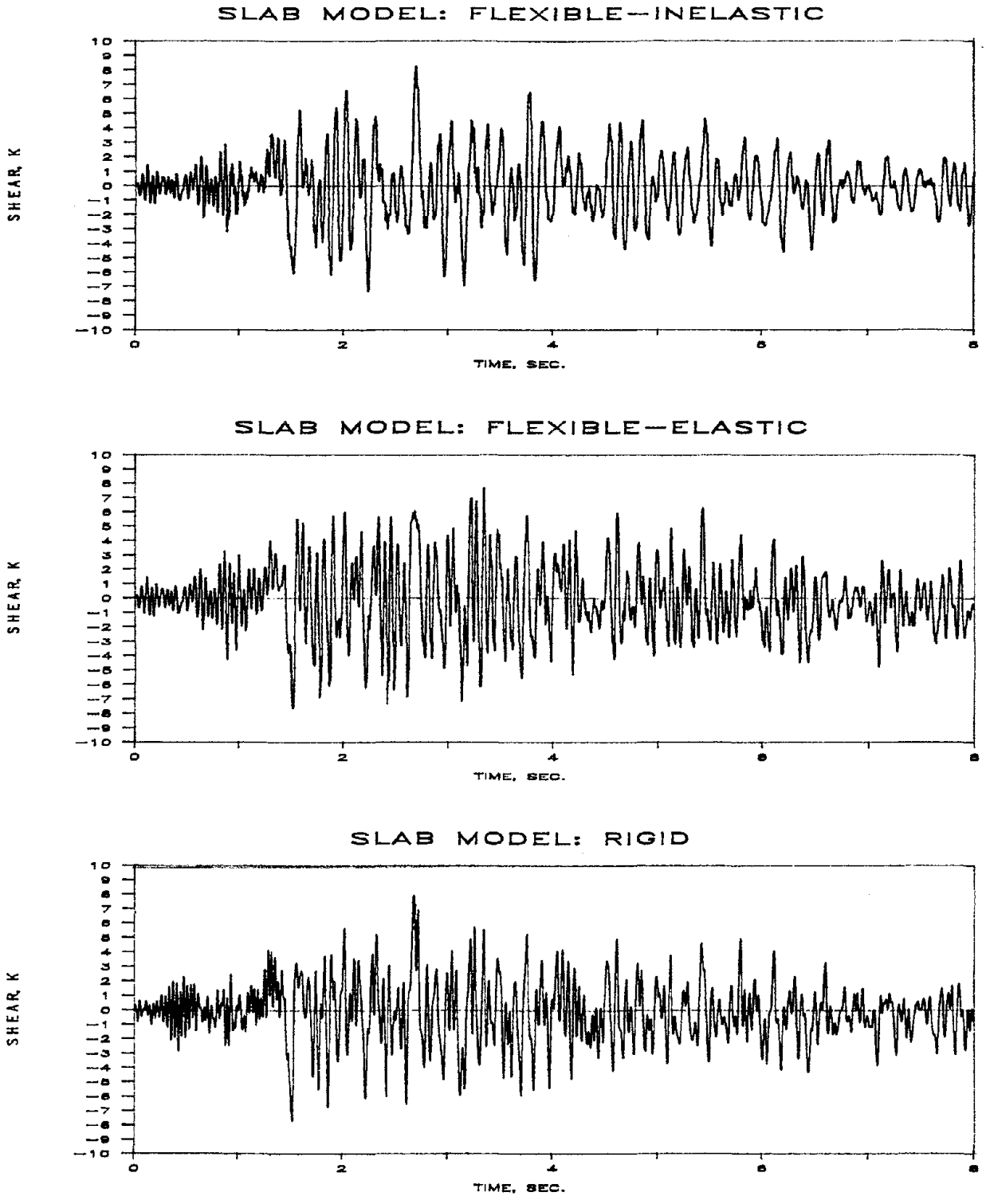

FIGURE 6-11 Base Shear Force of the End Frame for the Scaled Model Structure

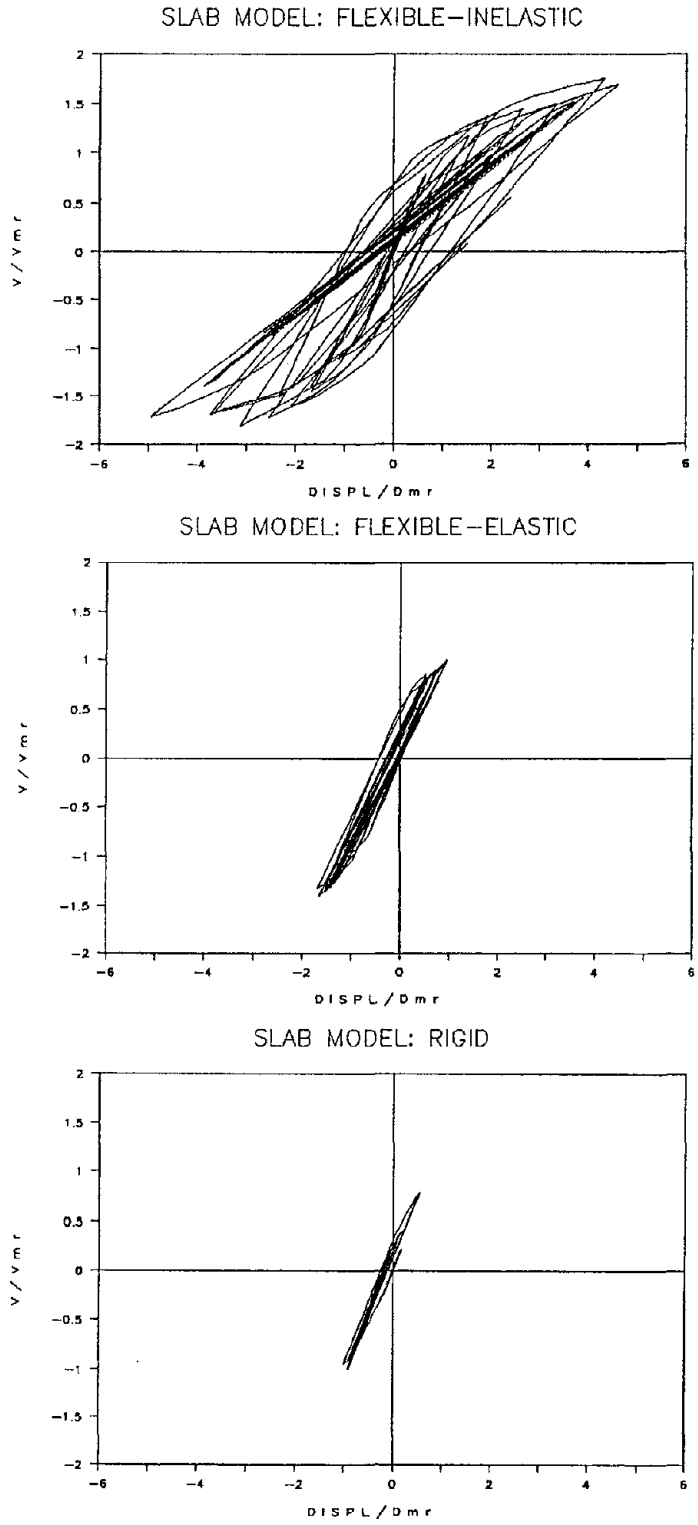

FIGURE 6-12 Comparison of the Base Shear Vs. Lateral Displacement Plots of the Middle Frame Normalized with Respect to the Peak Values Obtained From The Rigid Slab Model Analysis

SECTION 7
SUMMARY AND CONCLUSIONS

An enhanced computer program has been developed for the inelastic analysis and seismic damage evaluation of three-dimensional R/C structures, which accounts for the inelastic in-plane deformations of floor-slab systems.

A macro-model approach was adopted to minimize the amount of input data and reduce the input to the essential quantities which govern structural behavior. Other existing approaches are either over-abundant in input and output information, such as the micro-models of finite element procedures, or are lacking consideration of important effects, such as the variation of properties and behavior in the inelastic range.

The suggested model accounts for the variation of the flexibility of the slab during the inelastic response caused by changes in the plastic regions. The computational scheme allows for modeling slabs with variable thickness and reinforcement. It also enables the consideration of three-dimensional effects due to frame torsion.

The slab model includes influences of both in-plane shear and flexural bending. The influences are considered separately and are combined in the analysis stage to allow for a more accurate capture of the slab effects.

A generalized technique for the evaluation of the flexural capacity of floor slabs is also developed. The analytical envelope is modified based on observed experimental data to fit a trilinear curve which enables the subsequent hysteretic component modeling. Shear capacity computations are derived from empirical models originally developed for shear walls. Inelastic bending and shear are modeled using the *three-parameter hysteretic model* developed in Ref. [17].

The model considers the out-of-plane effects of gravity loads in a macro-behavioral model determined from experimental information. Improvement of such an approach is the subject of a further investigation within the framework of this ongoing project.

The computational model which includes frames, shear-walls, and transverse elements produces information on the force distribution between the structural elements and calculates a composite damage index for each of the principal members to estimate the expected seismic response in the presence of flexible floor slabs.

The suggested model has already been incorporated into an existing program for inelastic damage assessment of R/C buildings [17]. The new version (IDARC2) has several improved features in comparison with the original version. Some of the highlights of the new version are:

1. The program can handle the specification of floor slabs in an extremely versatile manner to account for considerable variation in slab properties across the length and depth of the slab.

- the slab can be subdivided into smaller segments along its length by means of dummy frames. A criterion for the discretization along the length is the change in the distribution of reinforcement in the floor slab system which is generally non-uniform.

- the slab system can be discretized in any arbitrary manner along its depth to facilitate a more realistic fiber model analysis. It is also possible to specify different steel grades for each region.

The program is also capable of modeling the floor diaphragm either as a rigid or as an elastic system for the purpose of comparative studies. The test model structure, presented in Section 6, uses all of these features extensively.

2. A single-step force equilibrium check has been incorporated into the dynamic analysis routine. This procedure is expected to reduce the magnitude of errors due to branch changes in the hysteretic routines. Such a technique may not satisfy equilibrium precisely but has been previously used [11] to reduce the cost of fully iterative procedures.

3. Several output features have been incorporated into the program to give the user a clear understanding of response computations:

- the stress states of components is recorded during the progressive collapse mode analysis. The sequence of failure of components is established.

- the peak component forces and their time of occurrence during various critical stages of loading (such as maximum frame displacement, maximum slab and wall moments) is recorded.

The analytical model developed herein was used for analyzing the importance of flexibility of floor diaphragms and in particular the importance of inelastic response near collapse.

Using the one-story test structures (Section 5) with diaphragms having increasing aspect ratios (long rectangular slabs) it was determined that: (a) The assumption of rigid floor diaphragms leads to underestimating of base shear in flexible frames by factors of 8 to 10. Such an increase may impose a large strength demand which obviously is not forseen in design practice; (b) The deflections of the diaphragms during the inelastic excursions reach magnitudes which impose large ductility requirements in the columns of frames. Such ductilities are usually in excess of the ductility capacity of regular columns.

Neglecting the inelastic response of diaphragms with large aspect ratios may be nonconservative for the design of frames in a frame-shear-wall system. This can lead to severe damage in the frames and eventually to loss of vertical carrying capacity with disastrous consequences.

As a results of these preliminary studies, a 1:6 scale model of a typical single story structure has been designed and constructed for testing under seismic loadings (using the earthquake simulator at SUNY/Buffalo). The inelastic analysis procedure developed in this report was used to predict the response of such a model. The results of the preliminary analyses indicated that a damaging mechanism is obtained if the model is loaded with larger amount of temporary load (live load) in the middle panels, and subjected to large earthquake intensities.

The damaging mechanism consists in an initial yielding of floor slab in flexure in the middle section with subsequent failure of beams and columns in the interior frames. This mechanism is continued by failure of shear walls at the bottom and severe damage to the inner frames.

An experimental program was developed based on these predictions. Subsequently, the test results will be used for the improvement of the computational model. This calibration is an essential step in development of construction/design specifications based on parametric studies using the developed computational tool. The development of such specifications is the eventual scope of this project.

SECTION 8
REFERENCES

1. AMERICAN CONCRETE INSTITUTE, "Building Code Requirements for Reinforced Concrete", ACI-318-83, Detroit, 1983.

2. BLUME, J.A., SHARPE, R.L. AND ELSESSER, E., "A Structural Dynamic Investigation of Fifteen School Buildings Subjected to Simulated Earthquake Motion", Division of Architecture, Sacremento, California, 1961.

3. BOPPANA, R.R. AND NAEIM, F., "Modeling of Floor Diaphragms in Concrete Shear Wall Buildings", Concrete International, ACI, July, 1985.

4. BUTTON, M.R., KELLY, T.E. AND JONES, L.R., "The Influence of Diaphragm Flexibility on the Seismic Response of Buildings", 8th WCEE, Vol.IV, San Francisco, 1984.

5. CHEN, S-J., "Reinforced Concrete Floor Slabs Under In-Plane Monotonic and Cyclic Loading", Ph.D. Dissertation, Lehigh University, Pennsylvania, 1986.

6. COULL, A. AND ADAMS, N.M., "A Simple Method of Analysis of the Load Distribution in Multistory Shear Wall Structures", in *Response of Multistory Concrete Structures to Lateral Forces*, pp.187-207, ACI, Detroit, 1973.

7. GOLDBERG, J.E. AND HERNESS, E.D., "Vibration of Multistory Buildings Considering Floor and Wall Deformations", Bulletin of the Seismological Society of America, Vol.55, No.1, 1965.

8. HWANG, J.S., CHANG, K.C. AND LEE, G.C., "The System Characteristics and Performance of a Shaking Table", Technical Report No. NCEER-87-0004, National Center for Earthquake Engineering Research, SUNY at Buffalo, 1987.

9. JAIN, S.K. AND JENNINGS, P.C., "Analytical Models for Low-Rise Buildings with Flexible Floor Diaphragms", Earthquake Engineering and Structural Dynamics, Vol.13, No.2, 1985.

10. KABEYASAWA, T., SHIOHARA, H., OTANI, S. AND AOYAMA, H., "Analysis of the Full-Scale Seven-Story Reinforced Concrete Test Structure", Journal of the Faculty of Engineering, University of Tokyo, Vol.XXXVII, No.2, 1983.

11. KANAAN, A.E. AND POWELL, G.H., "DRAIN-2D - A General Purpose Computer Program for Dynamic Analysis of Inelastic Plane Structures", Report No.UCB/EERC/73/06 and 73/22, University of California, Berkeley, 1973.

12. KARADOGAN, H.F., "Earthquake Analysis of 3D Structures with Flexible Floors", 7th WCEE, Vol.5, Istanbul, Turkey, 1980.

13. KARADOGAN, H.F., NAKASHIMA, M., HUANG, T. NAD LU, L.W., "Static and Dynamic Analysis of Buildings Considering the Effect of Floor Deformation - A State-of-the-Art Survey", Fritz Engineering Laboratory Report, No.422.2, Lehigh University, Pennsylvania, 1978.

14. MANDER, J.B., "Seismic Design of Bridge Piers", Ph.D. Dissertation, Department of Civil Engineering, University of Cantebury, Christchurch, New Zealand, 1984.

15. MUTO, K., "Aseismic Design Analysis of Buildings", Maruzen, Tokyo, 1974.

16. NAKASHIMA, M., HUANG, T. AND LU, L.W., "Seismic Resistance Characteristics of Reinforced Concrete Beam-Supported Floor Slabs in Building Structures", Fritz Engineering Laboratory Report, No.422.9, Lehigh University, Pennsylvania, 1981.

17. PARK, Y.J., REINHORN, A.M., KUNNATH, S.K., "IDARC: Inelastic Damage Analysis of Reinforced Concrete Frame - Shear-Wall Structures", Technical Report No. NCEER-87-0008, National Center for Earthquake Engineering Research, SUNY at Buffalo, 1987.

18. SHEN, S.Z. AND LU, L.W., "Substructure Analysis of Multistory Buildings with Flexible Floors", Fritz Engineering Laboratory Report, No.422.13, Lehigh University, Pennsylvania, 1985.

19. RUTENBERG, A., "Laterally Loaded Flexible Diaphragm Buildings", Journal of Structural Division, ASCE, Vol.106, ST9, 1980.

20. UNEMORI, A.L., ROESSET, J.M. AND BECKER, J.M., "Effect of In-Plane Floor Slab Flexibility on the Response of Crosswall Buildings", in *Reinforced Concrete Buildings Subjected to Wind and Earthquake Forces*, ACI-SP63, 1980.

21. WIGHT, J.K. (EDITOR), "Earthquake Effects on Reinforced Concrete Structures", U.S.-Japan Research, ACI Special Publication SP-84, 1985.

22. WU, Z.S. AND HUANG, T., "An Elastic Analysis of a Cantilever Slab Panel Subjected to an In-Plane End Shear", Fritz Engineering Laboratory Report, No.481.1, Lehigh University, Pennsylvania, 1983.

23. UNIFORM BUILDING CODE, (UBC), International Conference of Building Officials, Whittier, California, 1985.

APPENDIX A: USER INPUT GUIDE TO IDARC2

A1. INPUT FORMAT

A free format is used to read all input data. Hence, conventional delimiters (comma, blank) may be used to separate data items. Standard FORTRAN variable format is used to distinguish integers and floating point numbers. Input data must, therefore, conform to the specified variable type.

NOTE: NO BLANK LINES ARE TO BE INPUT
AND ALL UNITS MUST BE IN KIPS, INCHES

VARIABLES	*DESCRIPTION*

SET A:
CARD #1: Title of Problem

TITLE	Alpha-numeric title, upto 80 characters.

CARD #2: Control Information

NSO,NFR,MCON,MSTL	NSO = No. of stories NFR = No. of frames MCON = No. of different concrete material properties. MSTL = No. of types of steel reinforcement properties.

NOTES: *(a) The number of stories refers to the total number of floor levels excluding the base level.*

(b) A structure is idealized as a set of plane frames interconnected by transverse beams and flexible floor diaphragms. Fig.6.1a shows an example of a three-dimensional single story structure composed of 5 frames. Fig.6.1b shows the discretized structure with input notation.

(c) The different concrete properties refer to the different types of concrete used in the construction of the various elements. A concrete belongs to the same type if it has the same stress- strain curve (to be input in SET C).

(d) The number of types of steel reinforcement refers to strength parameters and not the size of bars used. All steel bars with the same stress-strain curve (input in SET D) belong to the same steel type.

CARD #3 : ELEMENT TYPES

MCOL,MBEM,MWAL,MEDG, MTRN,MSLB	MCOL = No. of types of columns MBEM = No. of types of beams

MWAL = No. of types of shear walls
MEDG = No. of types of edge columns
MTRN = No. of types of transverse beams
MSLB = No. of types of slabs

NOTES: *The number of types of a particular element is meant to group together a set of similar elements with identical properties. Hence data is required only for a set of elements with identical properties (dimensions, material properties, reinforcements, etc.)*

CARD #4 : ELEMENT DATA

NCOL,NBEM,NWAL,NEDG,
NTRN,NSLB

NCOL = No. of columns
NBEM = No. of beams
NWAL = No. of shear walls
NEDG = No. of edge columns
NTRN = No. of transverse beams
NSLB = No. of slabs

NOTES: *This input refers to the total number of each of the elements in the building. Using the frame in Fig.6.1, NCOL=6, NBEM=5, NWAL=4, NEDG=0, NTRN=8, NSLB=4.*

CARD #5 : BASE SHEAR ESTIMATE

PMAX

Estimate of base shear strength coefficient
(as ratio of shear strength to total weight)

NOTES: *The program uses this information only to determine the load steps for the static analysis under monotonic loading. An initial value of 1.0 may be input for the first run using the static analysis option (to be input later). The true base shear coefficient is computed by program IDARC based on this initial estimate. Use this value for subsequent dynamic and damage analysis.*

CARD #6 : FLOOR ELEVATIONS

HIGT(I),I=1,NSO

Elevation of each story from the base,
beginning with the first floor level.

CARD #7 : FLOOR WEIGHTS

WIGT(1,J),J=1,NFR
.
.
WIGT(NSO,J),J=1,NFR

Weight of floor associated with each
frame for each story level (Fig.A.1).

CARD #8 : CONFIGURATION OF PLAN

NVLN(I),I=1,NFR	Number of j-coordinate points in each frame. (see Fig.A.1)

NOTES: A set of NVLN points for each frame should define completely the j-coordinates necessary to specify every vertical element in that frame.

SET B:
J-COORDINATE LOCATIONS

SPANX(1,1) .. SPANX(1,NVLN(1))	For each frame:
.	input the 'distance' of each of the
.	NVLN points from any reference axis.
.	
SPANX(NFR,1)....SPANX(NFR,NVLN(NFR))	

NOTES: Choose a reference line, preferably to the left of the leftmost j-coordinate point. Another convenient location for the reference line would be along the leftmost j-coordinate location itself. However, there is no restriction as to where this line is located as long as it is perpendicular to the loading axis.

The x-coordinate refers to the distance of each j-coordinate location from this reference line (Fig.A.2).

SET C:
CONCRETE PROPERTIES

I,FC(I),EC(I),ECR(I),	Characteristics of concrete stress-
. EPSO(I),TAUM(I)	strain curve (see Fig.A.3):
.	I = Concrete type number
.	FC = Concrete compressive strength
.	EC = Initial Modulus
MCON,FC(MCON)....	[default=57*(1000*FC)$^{0.5}$]
....TAUM(MCON)	ECR = Tensile cracking strain
	[default=-0.1*FC/EC]
	EPS0= Strain at maximum strength
	[default=0.2%]
	TAUM= Bond strength [default=1.2]

NOTES: For each of the 'MCON' types of concrete, relevant parameters describing the stress-strain curve (as listed above) are necessary. Fig.A.3 shows the stress-strain curve along with the parameters needed to fully define the curve. The equation of the non-linear function is used primarily in the fiber model analysis of shear walls and slabs.

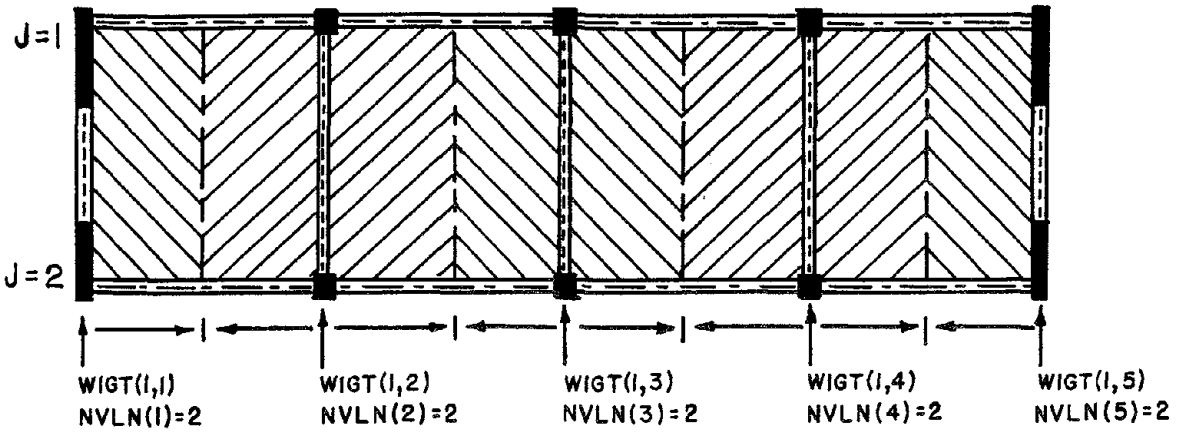

FIGURE A-1 Tributary Areas to be Included in Floor Weight Computation and Determination of J-Coordinate Points

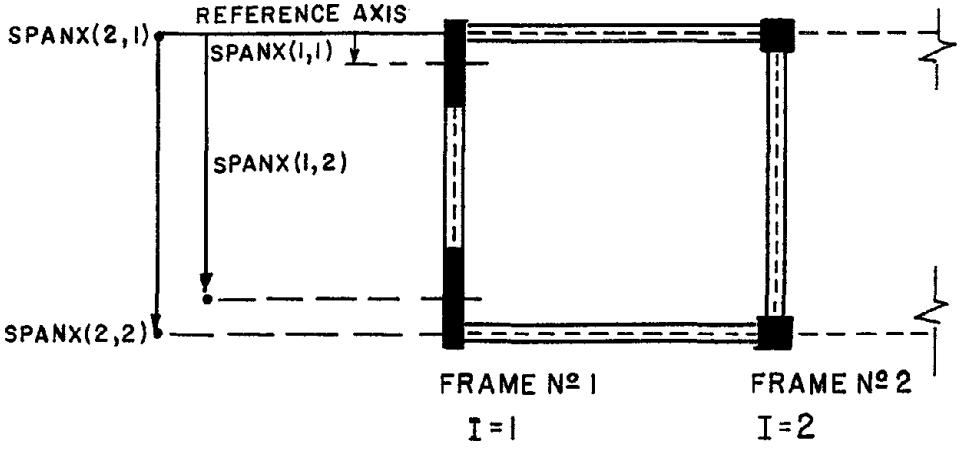

FIGURE A-2 Span Length Determination

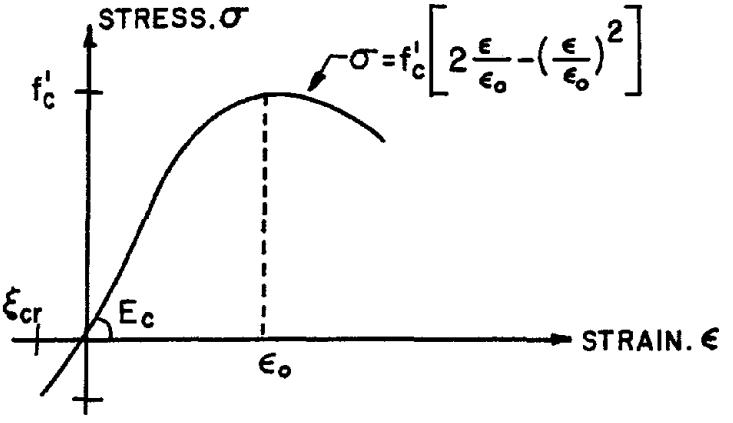

FIGURE A-3 Concrete Stress-Strain Curve

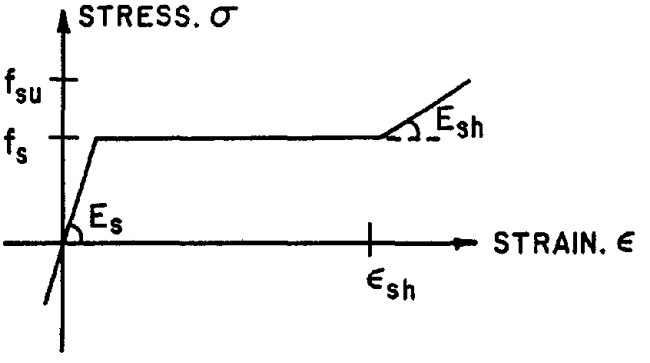

FIGURE A-4 Stress-Strain Input for Steel

Unless otherwise specified (using the tensile cracking strain option), it is assumed that the concrete can resist tension upto 1/10 of its strength in compression.
The bond strength of concrete is obtained typically from experimental testing, however, the program uses a default value of 1.2 ksi if such data is unavailable.

SET D :
PROPERTIES OF REINFORCEMENT

I,FS(I),FSU(I),ES(I),	Characteristics of steel stress-strain
ESH(I), EPSH(I)	for each steel type. (see Fig.A.4):
.	I = Steel type number
.	FS = Yield strength
MSTL,FS(MSTL)	FSU = Ultimate strength
...EPSH(MSTL)	ES = Modulus of elasticity (default: 29000 ksi)
	ESH = Modulus of strain hardening (default: 500 ksi)
	EPSH= Strain at start of hardening (%) (default: 3%)

NOTES: *A trilinear curve (as shown in Fig.A.4) is used to define the stress-strain characteristics of the steel reinforcement. The properties are assumed to be identical in both tension and compression.*
A set of MSTL cards is required in this input as specified in card #2 of set A.

SET E:
COLUMN PROPERTIES

SKIP THIS INPUT IF THE STRUCTURE HAS NO COLUMNS

M,IMC,IMS,AN,SIGCB(M),	Properties of each column type
SIGCT(M),D,B,BC,AT,PE,	(see Fig.A.5):
PW,RW,AMLC(M),	M = Column type number
RAMC1(M),RAMC2(M)	IMC = Concrete type number
.	IMS = Steel type number
.	AN = Axial load
.	SIGCB = Initial moment at bottom
.	SIGCT = Initial moment at top
MCOL,IMC,IMS.....	D = Depth of column
PW,RW.....	B = Width of column
RAMC2(MCOL)	BC = Distance from centroid of reinforcement to face of column
	AT = Area of tension reinforcement
	PE = Total perimeter of all tension reinf.
	PW = Web reinforcement ratio (%)
	RW = Confinement ratio (%)
	AMLC = Center-to-center column height
	RAMC1 = Rigid zone length at bottom
	RAMC2 = Rigid zone length at top

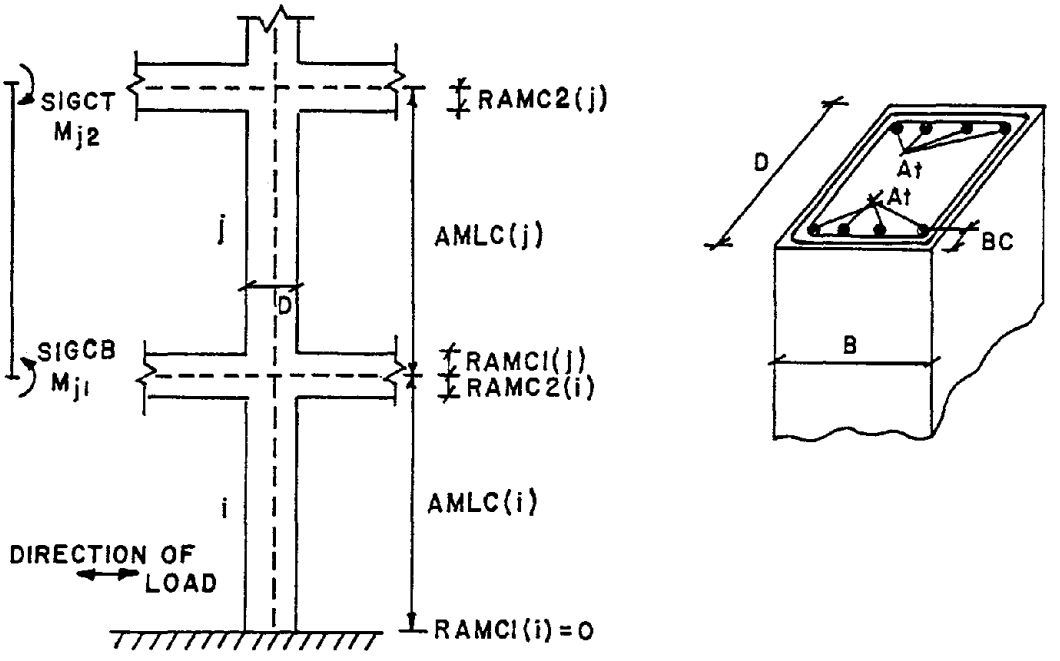

FIGURE A-5 Column Input Details

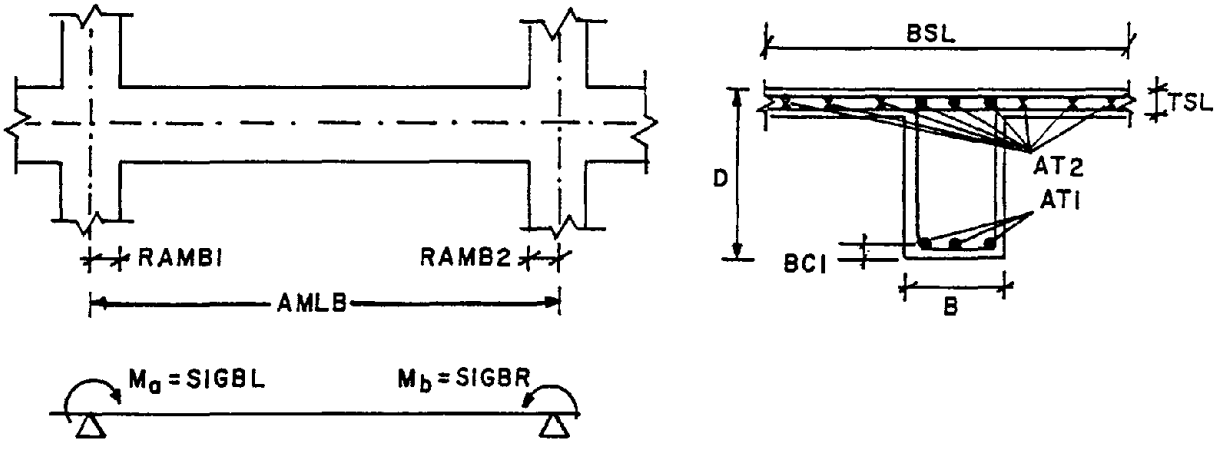

FIGURE A-6 Beam Input Details

NOTES: *The basic properties of each of the MCOL columns (input in card #3) is required in this input section.*

IMC and IMS refer to the concrete and steel stress-strain curves respectively, that are to be used in establishing the strength parameters of the column.

The axial load is determined from the effective vertical load acting on the column. The initial moments input here are in addition to the dead and live load moments computed later using input data SET . The user can ignore inputs for initial loading (which are somewhat approximate) and instead input the actual initial moment values in this section (possibly from another static analysis program in which true 3-d effects are reflected).

The length AMLC of a column is normally the center-to-center length.

The parameter 'AT' is the total area of the tension reinforcement. The analysis, however, assumes that the area of the tension and compression reinforcement are equal. The confinement ratio 'RW' is the volumetric ratio of the hoops to the core concrete.

SET F:

BEAM PROPERTIES

SKIP THIS INPUT IF THE STRUCTURE HAS NO BEAMS

M,IMC,IMS,SIGBL(M),SIGBR(M),
D,B,BSL,TSL,BC1,AT1,AT2,
PE1,PE2,PW,RW,AMLB(M),
RAMB1(M),RAMB2(M)
.
.
.
MBEM,IMC,IMS.....
D,B,BSL.....
RAMB1(MBEM),RAMB2(MBEM)

Properties of each beam type (see Fig.A.6):

M = Beam type number
IMC = Concrete type number
IMS = Steel type number
SIGBL = Initial bending moment at left section
SIGBR = Initial bending moment at right section
D = Overall depth
B = Lower width
BSL = Effective slab width
TSL = Slab thickness
BC1 = Distance from bottom bars to lower face
AT1 = Area of bottom bars
AT2 = Area of top bars
PE1 = Perimeter of bottom bars
PE2 = Perimeter of top bars
PW = Web reinforcement ratio (%)
RW = Confinement ratio (%)
AMLB = Member length
RAMB1 = Rigid zone length (left)
RAMB2 = Rigid zone length (right)

NOTES: *The above input is required for each of the 'MBEM' beams input in card #3.*
IMC and IMS define the concrete and steel stress-strain properties previously input in set C and set D respectively.
SIGBL and SIGBR are the initial bending moments at the left and right section respectively. The sign convention for the bending moments is shown in Fig.A.6 where a positive value indicates compression in the top fibers and tension in the bottom fibers. As with the columns, these moments are additive to the dead and live load moments computed by the program if loading is specified in SET .
For beam-slab elements, BSL refers to the effective width of the slab. For simple frame structures without slab units:

- *BSL and B assume the same value;*
- *TSL is input as the cover distance from the top bars to the upper face of the beam element*

SET G:
SHEAR WALL PROPERTIES

SKIP THIS INPUT IF THE STRUCTURE HAS NO SHEAR WALLS

M,IMC,IMS,AN,D,B,PT,PW,	Shear wall properties: (Fig.A.7)
DC,BC,AG,AMLW(M)	M = Shear wall type number
.	IMC = Concrete type number
.	IMS = Steel type number
.	AN = Axial load
MWAL,IMC,IMS.....	D = Length of shear wall
DC,BC,AG,AMLW(M)	B = Wall thickness
	PT = Vertical reinforcement ratio (%)
	PW = Horizontal reinf ratio (%)
	DC = Depth of edge column
	BC = Width of edge column
	AG = Gross steel area of edge columns
	AMLW = Height of shear wall

NOTES: *The above input is required for each of the MWAL shear walls (input in card #3 of set A).*

Two types of shear walls are possible:
(a) shear walls with edge columns
(b) shear walls without edge columns

Details of typical shear wall elements are shown in Fig.A.7. In the absence of any edge columns set the input parameters BC, DC and AG to zero.

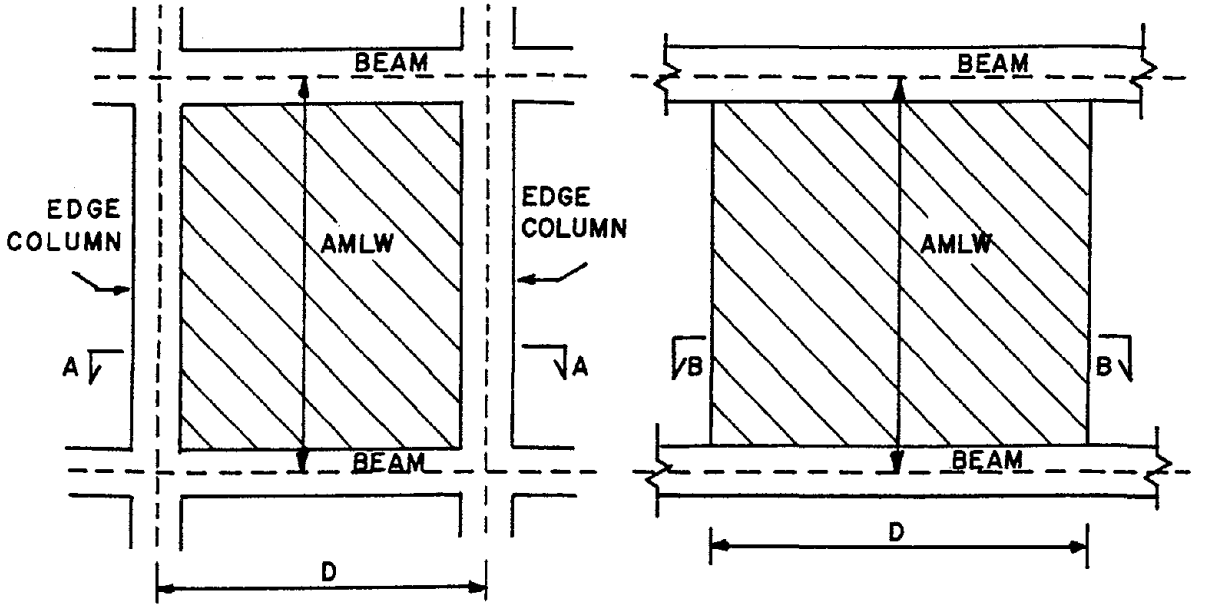

(a) Shear Wall with Edge Columns

(b) Shear Wall without Edge Columns

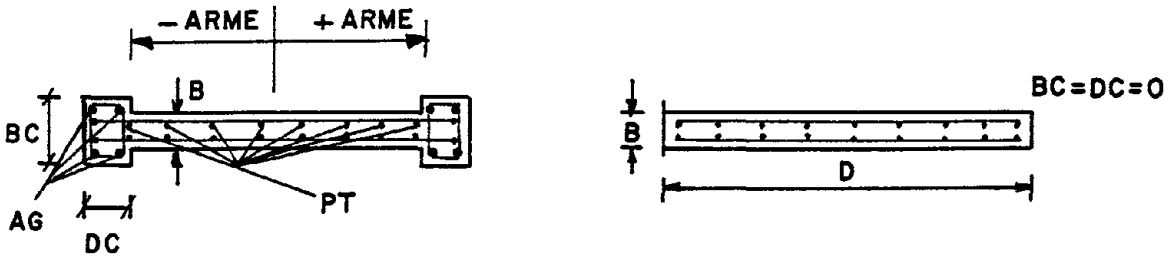

PLAN A-A

PLAN B-B

FIGURE A-7 Shear Wall and Edge Column Input Details

SET H:
EDGE COLUMN PROPERTIES

SKIP THIS INPUT IF THE STRUCTURE HAS NO EDGE COLUMNS

M,IMC,IMS,AN,D,B,AG,	Edge column properties (Fig.A.7):
AMLE,ARME(M)	M = Edge column type number
.	IMC = Concrete type number
.	IMS = Steel type number
.	AN = Axial load
MEDG,IMC,IMS.....	DC = Depth of edge column
...ARME(MEDG)	BC = Width of edge column
	AG = Gross area of main bars
	AMLE = Member length
	ARME = Arm length

NOTES: *Input is required of each of the MEDG edge columns (as specified in card #3 of set A).*

AMLE refers to the center-to-center height of the edge column, while AG is the total area of all the reinforcing bars in the edge column.

In writing the arm length of an edge column, it is important to consider the sign convention used. The arm length is the distance from the interior face of the edge column to the center of the shear wall to which it is anchored.

SET I:
TRANSVERSE BEAM PROPERTIES

THIS INPUT NOT REQUIRED IF STRUCTURE HAS NO TRANSVERSE BEAMS

M,AKV(M),ARV(M),ALV(M)	Transverse beam properties:
.	M = Transverse beam type number
.	AKV = Vertical Stiffness
.	ARV = Torsional Stiffness
.	ALV = Arm length
MTRN,AKV(MTRN)....ALV(MTRN)	

NOTES: *Two types of transverse beams can be defined:*

(a) beam-to-wall connections
(b) beam-to-beam connections

Details of both types of transverse elements are shown in Fig.A.8. The arm length, for beam-to-wall connections, refers to the distance from the beam to the center of the shear wall to which it is connected. This parameter is set to zero for beam-to-beam connections.

The details of the stiffness computations is also shown graphically in Fig.A.8. However, any suitable procedure may be used to arrive at these stiffness values depending upon the nature of the connection.

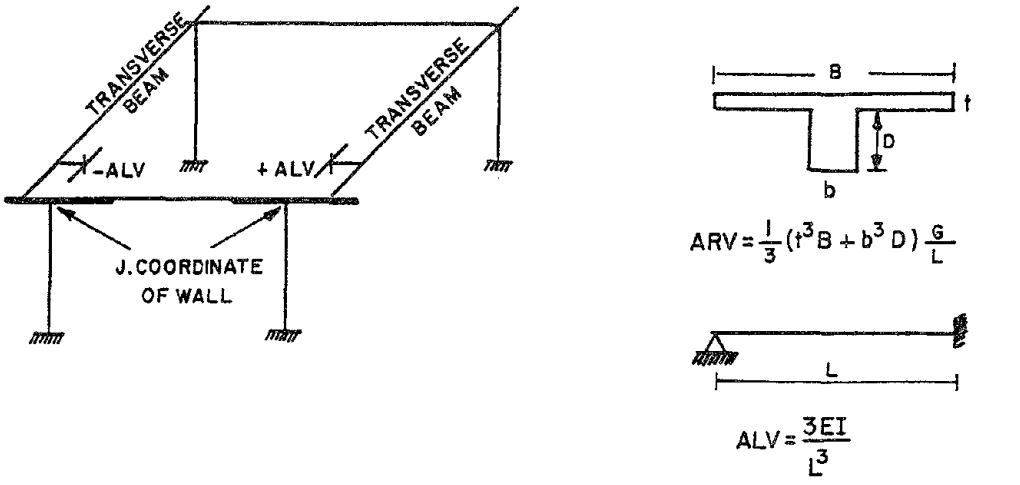

FIGURE A-8 Input Details for Transverse Beams

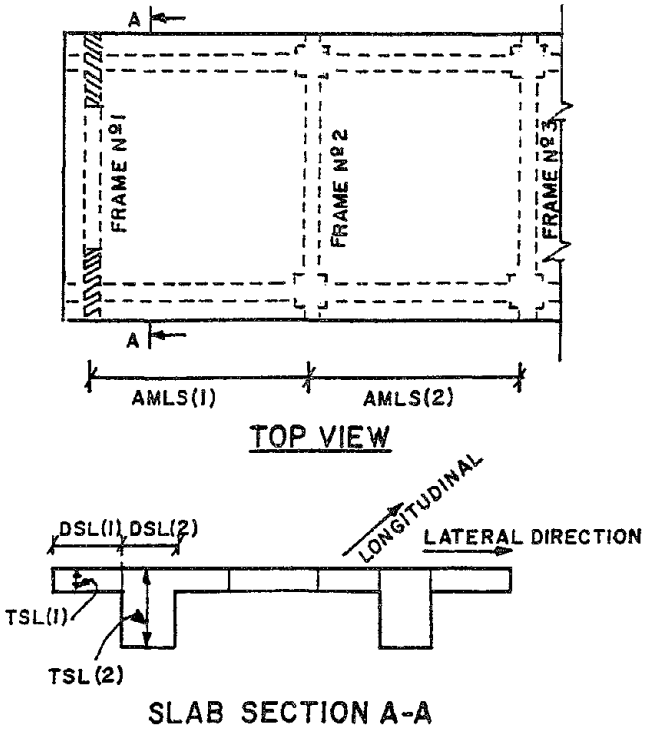

FIGURE A-9 Slab Input Details

SET J:
SLAB PROPERTIES

JSTYP — Modeling of slab types
= 0, Inelastic flexible slab
= 1, Elastic slab
= 2, Rigid slab

For each of the MSLB slab elements, input the following two data sets:

M,IMC,AMLS(M),NSECT
M = Slab type number
IMC = Concrete type number
AMLS = Slab length (frame-to-frame)
NSECT = Number of sections for fiber model analysis

For each of the NSECT sections:

IMS,TSL,DSL,PT,PW,NFIB
IMS = Steel type number
TSL = Thickness of section
DSL = Depth of section
PT = Longitudinal reinforcement ratio
PW = Lateral reinforcement ratio
NFIB = Number of fibers for fiber model analysis

REPEAT ABOVE TWO DATA SETS FOR EACH SLAB TYPE

Note: *Fig.A.9 shows a section of the slab for the sample building. The length of the slab refers to the center-to-center distance between parallel frames.*

A slab strip can be divided into a number of sections, the divisions being representative of the variation of reinforcement across the depth of the slab. This permits a more realistic fiber model analysis for determination of the flexural envelop curve (see Section 3.1).

The user also has the ability to specify the number of fibers to be used in the fiber model analysis for each section. A finer mesh near the ends and a coarser mesh toward the middle is recommended.

ELEMENT CONNECTIVITY INPUT

NOTE: Element connectivity is established through 3 coordinate positions. The *i* coordinate varies from 1 to the number of frames; the *j* coordinate varies from 1 to the number of NVLN positions for each frame; and the *l* coordinate varies from 0 to the number of stories.

SET K:
COLUMN CONNECTIONS

SKIP THIS INPUT IF THE STRUCTURE HAS NO COLUMNS

M,ITC(M),IC(M),JC(M),	Column connectivity data:
LBC(M),LTC(M)	M = Column number
.	ITC = Column type number
.	IC = I-Coordinate
NCOL,ITC(NCOL).....	JC = J-Coordinate
LBC(NCOL),LTC(NCOL)	LBC = Bottom L-coordinate
	LTC = Top L-coordinate

NOTES: IC refers to the frame number, or the i'th coordinate position of the column. JC is the j'th coordinate position of the column (where 'j' varies from 1 to NVLN(i)). LBC and LTC are the bottom and top L-coordinate position of the column respectively.

SET L:
BEAM CONNECTIVITY

SKIP THIS INPUT IF STRUCTURE HAS NO BEAMS

M,ITB(M),LB(M),IB(M),	Beam connectivity data:
JLB(M),JRB(M)	M = Beam number
.	ITB = Beam type number
.	LB = L-Coordinate
.	IB = I-Coordinate
NBEM,ITB(NBEM).....	JLB = Left J-Coordinate
JLB(NBEM),JRB(NBEM)	JRB = Right J-Coordinate

NOTES: Input is required for each NBEM beams as specified in card #4 of set A.

SET M:
SHEAR WALL CONNECTIVITY

SKIP THIS INPUT IF STRUCTURE HAS NO SHEAR WALLS

M,ITW(M),IW(M),JW(M),	Shear wall connectivity data:
LBW(M),LTW(M)	M = Shear wall number
.	ITW = Shear wall type number
.	IW = I-Coordinate
.	JW = J-Coordinate
NWAL,ITW(NWAL).....	LBW = Bottom L-Coordinate
LBW(NWAL),LTW(NWAL)	LTW = Top L-Coordinate

NOTES: Input is required for each of the NWAL shear walls.

SET N:
EDGE COLUMN CONNECTIVITY

SKIP THIS INPUT IF STRUCTURE HAS NO EDGE COLUMNS

M,ITE(M),IE(M),JE(M),	Edge column connectivity data:
LBE(M),LTE(M)	M = Edge column number
.	ITE = Edge column type number
.	IE = I-Coordinate
.	JE = J-Coordinate
NEDG,ITE(NEDG).....	LBE = Bottom L-Coordinate
LBE(NEDG),LTE(NEDG)	LTE = Top L-Coordinate

NOTES: Input is required for each of the NEDG edge columns.

SET O:
TRANSVERSE BEAM CONNECTIVITY

SKIP THIS INPUT IF STRUCTURE HAS NO TRANSVERSE BEAMS

M,ITT(M),LT(I),IWT(M),	Transverse beam connectivity data:
JWT(M),IFT(M),JFT(M)	M = Transverse beam number
	ITT = Transverse beam type number
	LT = L-Coordinate
	IWT = I-Coordinate of origin of transverse beam*
	JWT = J-Coordinate of origin of transverse beam*
NTRN,ITT(NTRN).....	IFT = I-Coordinate of connecting
JWT(NTRN)...JFT(NTRN)	wall or column
	JFT = J-Coordinate of connecting wall or column

NOTES: *NTRN cards are required in this input section*

* *FOR BEAM-WALL CONNECTIONS, IWT AND JWT REFER TO THE I,J COORDINATE LOCATIONS OF THE SHEAR WALL.*

SET P:

SLAB CONNECTIVITY

M,ITS,LSL,ISL1,ISL2

M = Slab number
ITS = Slab type number
LSL = Story number
ISL1 = Starting frame number
ISL2 = Ending frame number

NOTE: *It is imperative that atleast one slab be defined between a set of parallel frames. Therefore, unless dummy frames are defined, the number of slabs is one less than the number of frames.*

SET Q: STATIC ANALYSIS FOR INITIAL LOADS

CARD #1

NLU,NLJ,NLM

NLU = No of uniformly loaded beams
NLJ = No of laterally loaded joints
NLM = No of specified nodal moments

NOTE: *Initial loading may be specified through beams that are uniformly loaded. Specified lateral loads may also be input at floor levels. In the presence of overhanging beams, not accounted for in the analysis, an external nodal moment may be applied at the end of each beam.*

All initial moments are carried forward to the dynamic analysis.

CARD SET #2:

SKIP THIS INPUT IF NLU .EQ. 0

I,IBN(I),FU(I)
.
.
NLU .... FU(NLU)

I = Load number
IBN = Beam number
FU = Load value (k/in)

NOTE: NLU cards required in this section

CARD SET #3:

SKIP THIS INPUT IF NLJ .EQ. 0

I,LF(I),IF(I),FL(I)	I = Load number
.	LF = Story number
.	IF = Frame number
.	FL = Load value
NLJ .... FL(NLJ)	

NOTE: NLU cards required in this section

CARD SET #4:

SKIP THIS INPUT IF NLM .EQ. 0

I,IBM(I),FM1(I),FM2(I)	I = Load number
.	IBM = Beam number
.	FM1 = Moment value (left)
.	FM2 = Moment value (right)
NLM .... FM2(NLM)	

NOTE: NLU cards required in this section

NEXT CARD: DYNAMIC ANALYSIS OPTION

IDYN	Dynamic analysis option
	= 0 , STOP (Do not perform dynamic analysis)
	= 1 , CONTINUE (Dynamic analysis)

THE REMAINING CARDS NEED BE INPUT ONLY IF IDYN .EQ. 1

SET R:
DYNAMIC ANALYSIS CONTROL PARAMETERS

CARD #1

GMAXH,GMAXV,DTCAL,	Control parameters for dynamic analysis:
TDUR,DAMP	GMAXH = Peak horizontal acceleration (g's)
	GMAXV = Peak vertical acceleration (g's)
	DTCAL = Time step for response analysis (secs)
	TDUR = Total duration of analysis (secs)
	DAMP = Damping coefficient (% of critical)

NOTES: The input accelerogram is scaled uniformly to achieve the specified peak acceleration. Set GMAXV to zero if the vertical component of the acceleration is not input.

DTCAL is the user controlled time step for the response analysis. DTCAL should not exceed the time interval of the input wave. It may be necessary to use smaller time steps depending upon the complexity of the structure and the magnitude of the input wave. However, an extremely small time step may also lead to accumulation of round-off and truncation errors.

TDUR must be less than or equal to the total time duration of the input wave.

CARD #2 : INPUT WAVE

IWV,NDATA,DTINP	IWV = 0, Vertical component of acceleration not included = 1, Vertical component of acceleration included NDATA = No. of points in earthquake wave DTINP = Time interval of input wave

CARD #3 : WAVE TITLE

NAMEW	Alpha-numeric title for input wave upto 80 characters

SET S : WAVE DATA - HORIZONTAL COMPONENT

WINPH(I),I=1,NDATA	Horizontal component of earthquake wave (NDATA points)

This data is read from file WAVEH.DAT

SET T : WAVE DATA - VERTICAL COMPONENT

SKIP THIS INPUT IF IWV .EQ. 0

WINPV(I),I=1,NDATA	Vertical component of earthquake wave (NDATA points)

This data is read from file WAVEV.DAT

NOTES: *Accelerogram data may be input in any system of units. The accelerogram is scaled uniformly to achieve the specified peak value in card #1 of set 'O'.*

Since data is read in free format, as many cards as necessary to read the entire wave must be input. The data points of the input wave may, therefore, be entered sequentially until the last (or NDATA) point.

SET U : HYSTERETIC RULE

CARD #1:

NHYS	Number of types of hysteretic rules

CARD SET #2:

HYSTERETIC MODEL PARAMETERS

HC(M),HS(M),HB(M),HP(M) . . . HC(NHYS)..... HP(NHYS)	HC = Degrading coefficient HS = Slippage coefficient HB = Deteriorating coefficient HP = Post-yielding stiffness ratio

NOTES: HC refers to the parameter which defines the stiffness degradation. HS refers to the slippage or pinching coefficient. If pinching effects are to be ignored, input a large value for HS (>1) which then forces the yield strength value to be the new maximum point. HB is the rate of strength degradation.

THE PROGRAM COMPUTES THE VALUE OF THE PARAMETER HB FOR EACH INELASTIC COMPONENT USING THE FORMULATION DESCRIBED IN SECTION 4.3.2. ANY INPUT FOR THIS VALUE WILL OVERRIDE THE DEFAULTS COMPUTED BY THE PROGRAM. IF THE USER SHOULD CHOOSE TO USE THE DEFAULTS THEN A ZERO INPUT IS NECESSARY FOR HB.

Finally, HP defines the post-yielding stiffness ratio. Typical values of this parameter for reinforced concrete vary from 0.01 to 0.05.

NEXT CARD : COLUMN PARAMETERS

SKIP THIS INPUT IF THE STRUCTURE HAS NO COLUMNS

KHYSC(I),I=1,NCOL — Type of hysteretic property for each column

NOTES: For each of NCOL columns, input the number corresponding to the hysteresis rule that is to be used from the hysteretic model parameters input in set #2 above.

NEXT SET: BEAM PARAMETERS

SKIP THIS INPUT IF STRUCTURE HAS NO BEAMS

KHYSB(I),I=1,NBEM — Type of hysteretic property for each beam

NOTES: Specify the hysteresis rule to be used for each of the NBEM beams.

NEXT SET: SHEAR WALL PARAMETERS

SKIP THIS INPUT IF STRUCTURE HAS NO SHEAR WALLS

KHYSW(I,1),KHYSW(I,2) — Type of hysteretic property
. for flexure and shear respectively
.
KHYSW(NWAL,1),KHYSW(NWAL,2)

NOTES: For each of the NWAL shear walls in the structure, 2 hysteretic rules are to be defined. The first defines the flexural behavior while the second defines the shear behavior.

NEXT SET: SLAB PARAMETERS

SKIP THIS INPUT IF STRUCTURE HAS NO SHEAR WALLS

KHYSS(I,1),KHYSS(I,2) — Type of hysteretic property
. for flexure and shear respectively
.
KHYSS(NSLB,1),KHYSS(NSLB,2)

NOTES: For each of the NSLB slabs in the structure, 2 hysteretic rules are prescribed, for flexure and shear respectively.

SET V: OUTPUT CONTROL

NSOUT,DTOUT

NSOUT = No of output histories
DTOUT = Output time interval

NEXT SET:

IFRNO(I),ISTNO(I)
.
.
IFRNO(NSOUT),ISTNO(NSOUT)

IFRNO = Frame number
ISTNO = Story number

NOTES: A set of NSOUT cards define the frame and story level for which an output history is desired. A typical history is created in four files containing displacement, frame-drifts, story drifts and story shear information. See Section A.3 for more information on output details.

NEXT SET:

Note: These outputs produce a moment-curvature history for the specified set of elements. Upto two elements under each type as listed below is possible. For walls and columns, the history refers to the bottom section, for beams the history of the left section is produced while for slabs the history corresponding to the ISL1 coordinate is generated.

JCOLOUT

= 0 , No column output desired
= 1 , PRINT column output

SKIP NEXT CARD IF JCOLOUT .EQ. 0

INUMC1, INUMC2

INUMC1 = Column number 1
INUMC2 = Column number 2

NEXT CARD:

JBEMOUT

= 0 , No beam output desired
= 1 , PRINT beam output

SKIP NEXT CARD IF JBEMOUT .EQ. 0

INUMB1, INUMB2

INUMB1 = Beam number 1
INUMB2 = Beam number 2

NEXT CARD:

JWALOUT

= 0 , No wall output desired
= 1 , PRINT wall output

SKIP NEXT CARD IF JWALOUT .EQ. 0

INUMW1, INUMW2	INUMW1 = Wall number 1 INUMW2 = Wall number 2

NEXT CARD:

SKIP NEXT CARD IF JSLBOUT .EQ. 0

JSLBOUT	= 0 , No slab output desired = 1 , PRINT slab output
INUMS1, INUMS2	INUMS1 = Slab number 1 INUMS2 = Slab number 2

NEXT CARD:

ISTLEVEL,IFRSH,IEND1,IEND2	Story level at which shear-drift history is desired specified as follows:

ISTLEVEL: refers to the story level
IFRSH: frame at specified story for which shear history is recorded
(shear refers to slab shear)
IEND1 and IEND2 refer to the 2 frame numbers between which the relative drift is measured.

END OF INPUT

A.2. CURRENT PROGRAM LIMITS

The present version of program IDARC2 is available for use on DEC/VAX operating systems.

IDARC2 uses variable dimensions for all the main arrays. The current settings for these dimensions are as follows:

- upto 60 beam elements, 60 column elements, 60 transverse beams, 60 edge columns and 30 shear walls;
- upto 200 global degrees of freedom
- a maximum of 10 stories;
- a maximum of 10 j-coordinate locations per frame
- a maximum of 10 frames (i.e. NFR=10)
- upto 10 different concrete types and 10 different steel types

For buildings with more elements than specified above, it is necessary to change the dimensions of the appropriate arrays.

For convenience, all variable arrays are placed in an isolated routine called IDARCS_DEFN.FOR. Necessary parameters may be changed here.

Two additional parameters that must be checked are the half-band width of the global stiffness matrix and the total number of degrees of freedom of the structure. Current limits are 200 degrees of freedom and a half-band width of 50.

Degrees of freedom = NST * [{NVLN(I) * 2 + 2} + {2 * No. of dummy frames}]

where NST is the number of stories.

The overall stiffness matrix is stored in the array OST(M,N) where:

M = 200, degrees of freedom
N = 50, half-band width

This array dimension must be changed to the values computed (as described above) if M > 200 or N > 50.

Exact values can be easily determined by numbering the degrees of freedom

A.3. Files

Data is read from a sequential input file where the data elements are separated by conventional delimiters. The following convention is adopted:

A fixed input filename IDARC.DAT is used for the sequential input (format details listed in Appendix A.1).
Earthquake data is read from files WAVEH.DAT (for horizontal component) and WAVEV.DAT (for vertical component, if used).

Several output files are generated:

IDARC.OUT containing the descriptive input listing; and the results of the static, dynamic and damage analysis.

The reamining files are created depending on the number of output histories requested:

DISPL.PRN ..... is created for displacement histories
FRDRF.PRN ..... is created for frame-drift histories
STDRF.PRN ..... is created for story-drift histories
SHEAR.PRN ..... is created for story-shear histories

Story drifts are computed relative to the lower story level. Frame drifts are, likewise, computed relative to the (i-1)th frame.

COL.PRN ..... is created for column moment-curvature histories
BEM.PRN ..... is created for beam moment-curvature histories
WAL.PRN ..... is created for wall moment-curvature histories
SLB.PRN ..... is created for slab moment-curvature histories

SHDRF.PRN ..... is created for the shear-drift history specified by the user.

APPENDIX B: SAMPLE SUMMARY OF INPUT AND OUTPUT

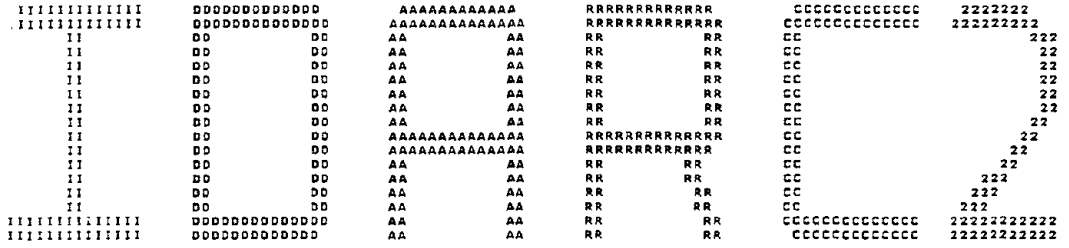

INELASTIC DAMAGE ANALYSIS OF REINFORCED CONCRETE STRUCTURES
WITH FLEXIBLE FLOOR DIAPHRAGMS

STATE UNIVERSITY OF NEW YORK AT BUFFALO
DEPARTMENT OF CIVIL ENGINEERING

JUNE 1988

INPUT DATA:

TITLE: 4 SPAN STRUCTURE WITH END WALLS (1-STORY)

********** BUILDING CONFIGURATION AND MATERIAL INFORMATION **********

NUMBER OF STORIES 1
NUMBER OF FRAMES 5

NO. OF TYPES OF CONCRETE 1
NO. OF TYPES OF STEEL 1

********** ELEMENT INFORMATION **********

NO. OF TYPES OF COLUMNS 1
NO. OF TYPES OF BEAMS 1
NO. OF TYPES OF SHEAR WALLS 1
NO. OF TYPES OF EDGE COLUMNS 0
NO. OF TYPES OF TRANSVERSE BEAMS 3
NO. OF TYPES OF SLABS 2

NUMBER OF COLUMNS 6
NUMBER OF BEAMS 3
NUMBER OF SHEAR WALLS 2
NUMBER OF EDGE COLUMNS 0
NUMBER OF TRANSVERSE BEAMS 8
NUMBER OF SLAB ELEMENTS 4

ESTIMATED BASE SHEAR COEFFICIENT : 1.0
(% OF TOTAL WEIGHT)

SYSTEM OF UNITS: INCH, KIPS

********** STORY HEIGHT AND FLOOR WEIGHTS **********

STORY HEIGHT FLOOR

	FROM BASE	WEIGHT				
1	212.500	97.360	103.020	103.020	103.020	97.360

********** X CO-ORDINATE DISTANCE OF COLUMN FROM REFERENCE POINT **********

FRAME	COLUMN COORDINATE (IN ORDER)	
1	144.00	
2	0.00	288.00
3	0.00	288.00
4	0.00	288.00
5	144.00	

********** CONCRETE PROPERTIES **********

TYPE	STRENGTH	MODULUS	STRAIN AT TENSION CRACK	STRAIN AT MAX STRENGTH (%)	BOND STRENGTH
1	4.000	3600.000	-0.000111	0.200	0.800

********** REINFORCEMENT PROPERTIES **********

TYPE	YIELD STRENGTH	ULTIMATE STRENGTH	YOUNGS MODULUS	MODULUS AT HARDENING	STRAIN AT HARDENING
1	40.000	55.000	29000.000	300.000	3.000

********** COLUMN TYPES **********

COLUMN TYPE	CONCRETE TYPE	STEEL TYPE	DEPTH	WIDTH	COVER	LENGTH	RIGID ZONE (BOT)	RIGID ZONE (TOP)
1	1	1	18.000	18.000	2.500	212.500	0.000	18.500

***** AXIAL LOAD AND REINFORCEMENT OF COLUMNS *****

TYPE	AXIAL LOAD	MOMENT (BOT)	MOMENT (TOP)	STEEL AREA	PERIMETER OF BARS	WEB REINF RATIO	CONFINEMENT RATIO
1	51.510	0.000	0.000	2.000	7.0700	1.1100	1.6700

********** BEAM TYPES **********

BEAM TYPE	CONCRETE TYPE	STEEL TYPE	DEPTH	WIDTH	SLAB WIDTH	SLAB THICKNESS	COVER	MEMBER LENGTH	RIGID ZONE (LEFT)	RIGID ZONE (RIGHT)
1	1	1	22.000	12.000	42.000	7.000	3.000	288.000	9.000	9.000

***** INITIAL MOMENTS AND REINFORCEMENT OF BEAMS *****

BEAM TYPE	MOMENT (LEFT)	MOMENT (RIGHT)	STEEL AREA (BOTTOM)	STEEL AREA (TOP)	PERIMETER OF BARS (BOT)	PERIMETER OF BARS (TOP)	WEB REINF RATIO	CONFINEMENT RATIO
1	0.000	0.000	1.580	2.370	6.2800	9.4200	0.700	1.6000

********** SHEAR WALL TYPES **********

WALL TYPE	CONCRETE TYPE	STEEL TYPE	DIST BET. EDGE COLS	WALL THICKNESS	DEPTH OF EDGE COL	WIDTH OF EDGE COL	DEPTH OF WALL
1	1	1	300.000	12.000	0.000	0.000	212.500

***** AXIAL LOAD AND REINFORCEMENT OF SHEAR WALLS *****

WALL TYPE	AXIAL LOAD	VERTICAL REINF RATIO	HORIZONTAL REINF RATIO	GROSS STEEL AREA IN EDGE COL
1	97.360	0.6670	0.2500	0.0000

********** TRANSVERSE BEAMS **********

TYPE	STIFFNESS	STIFFNESS (TORSIONAL)	ARM LENGTH
1	8.183	67210.000	-144.000
2	8.183	67210.000	144.000
3	8.183	67210.000	0.000

********** SLAB PROPERTIES **********

TYPE	CONC TYPE	LENGTH
1	1	288.0000

DATA FOR 7 SECTIONS:

SECTION	STEEL TYPE	THICKNESS	DEPTH	MAIN REINF	LATERAL REINF	FIBERS
1	1	7.0000	42.0000	0.001428	0.002008	10
2	1	22.0000	12.0000	0.010530	0.002008	8
3	1	7.0000	66.0000	0.001888	0.002008	10
4	1	7.0000	144.0000	0.003175	0.002008	10
5	1	7.0000	66.0000	0.001888	0.002008	10
6	1	22.0000	12.0000	0.010530	0.002008	8
7	1	7.0000	42.0000	0.001428	0.002008	10

TYPE	CONC TYPE	LENGTH
2	1	288.0000

DATA FOR 7 SECTIONS:

SECTION	STEEL TYPE	THICKNESS	DEPTH	MAIN REINF	LATERAL REINF	FIBERS
1	1	7.0000	42.0000	0.001428	0.002332	10
2	1	22.0000	12.0000	0.010530	0.002332	8
3	1	7.0000	66.0000	0.001888	0.002332	10
4	1	7.0000	144.0000	0.003175	0.002332	10
5	1	7.0000	66.0000	0.001888	0.002332	10
6	1	22.0000	12.0000	0.010530	0.002332	8
7	1	7.0000	42.0000	0.001428	0.002332	10

ACTIVE OPTION FOR SLAB TYPE: FLEXIBLE

********** NODAL CONNECTIVITY INFORMATION **********

********** COLUMN ELEMENTS **********

COL. NO.	TYPE	I-COORD	J-COORD	L-COORD (BOT)	L-COORD (TOP)
1	1	2	1	0	1
2	1	3	1	0	1
3	1	4	1	0	1
4	1	2	2	0	1
5	1	3	2	0	1
6	1	4	2	0	1

********** BEAM ELEMENTS **********

BEAM NO.	TYPE	L-COORD	I-COORD	J-COORD (LEFT)	J-COORD (RIGHT)
1	1	1	2	1	2
2	1	1	3	1	2
3	1	1	4	1	2

********** SHEAR WALL ELEMENTS **********

WALL NO.	TYPE	I-COORD	J-COORD	L-COORD (BOTTOM)	L-COORD (TOP)
1	1	1	1	0	1
2	1	5	1	0	1

********** TRANSVERSE BEAM ELEMENTS **********

NO.	TYPE	L-COORD	I-COORD ----(WALL//COL)----	J-COORD	I-COORD ------(COLUMN)-----	J-COORD
1	1	1	1	1	2	1
2	3	1	2	1	3	1
3	3	1	3	1	4	1
4	1	1	5	1	4	1
5	2	1	1	1	2	2
6	3	1	2	2	3	2
7	3	1	3	2	4	2
8	2	1	5	1	4	2

********** SLAB ELEMENTS **********

SLAB NO.	SLAB TYPE	L-COORD	I-COORD FRAME I	I-COORD FRAME J
1	1	1	1	2
2	2	1	2	3
3	2	1	3	4
4	1	1	4	5

********** CONFIGURATION OF PLAN **********

PLAN OF FRAME 5:

PLAN OF FRAME 4:

PLAN OF FRAME 3:

PLAN OF FRAME 2:

PLAN OF FRAME 1:

********** FRAME ELEVATION AND ELEMENT TYPES **********

ELEVATION OF FRAME NO. 1

NOTATION:

-	=	BEAM	NUMBERS INDICATE ELEMENT TYPES
!	=	COLUMN	COLUMN TYPE NUMBERS ON RIGHT
W	=	SHEAR WALL	SHEAR WALL NUMBERS ON LEFT, AND
I	=	EDGE COLUMN	EDGE COLUMN NUMBERS BELOW COLUMN TYPES

ELEVATION OF FRAME NO. 2

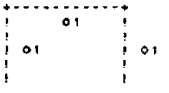

NOTATION:

-	=	BEAM	NUMBERS INDICATE ELEMENT TYPES
!	=	COLUMN	COLUMN TYPE NUMBERS ON RIGHT
W	=	SHEAR WALL	SHEAR WALL NUMBERS ON LEFT, AND
I	=	EDGE COLUMN	EDGE COLUMN NUMBERS BELOW COLUMN TYPES

ELEVATION OF FRAME NO. 3

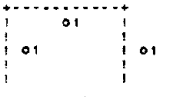

NOTATION:

-	=	BEAM	NUMBERS INDICATE ELEMENT TYPES
!	=	COLUMN	COLUMN TYPE NUMBERS ON RIGHT
W	=	SHEAR WALL	SHEAR WALL NUMBERS ON LEFT, AND
I	=	EDGE COLUMN	EDGE COLUMN NUMBERS BELOW COLUMN TYPES

ELEVATION OF FRAME NO. 4

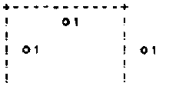

NOTATION:

-	=	BEAM	NUMBERS INDICATE ELEMENT TYPES
!	=	COLUMN	COLUMN TYPE NUMBERS ON RIGHT
W	=	SHEAR WALL	SHEAR WALL NUMBERS ON LEFT, AND
I	=	EDGE COLUMN	EDGE COLUMN NUMBERS BELOW COLUMN TYPES

ELEVATION OF FRAME NO. 5

NOTATION:

-	=	BEAM	NUMBERS INDICATE ELEMENT TYPES
!	=	COLUMN	COLUMN TYPE NUMBERS ON RIGHT
W	=	SHEAR WALL	SHEAR WALL NUMBERS ON LEFT, AND
I	=	EDGE COLUMN	EDGE COLUMN NUMBERS BELOW COLUMN TYPES

********** LOADING DATA **********

NO. OF UNIFORMLY LOADED BEAMS 3
NO. OF LATERAL LOADING POINTS 0
NO. OF APPLIED NODAL MOMENTS 3

UNIFORM LOAD DATA:

LOAD NO.	BEAM NO.	LOAD VALUE
1	1	0.231
2	2	0.231
3	3	0.231

NODAL MOMENTS DATA:

LOAD NO.	BEAM NO.	LEFT MOMENT	RIGHT MOMENT
1	1	-265.680	265.680
2	2	-265.680	265.680
3	3	-265.680	265.680

********** O U T P U T O F R E S U L T S **********

OUTPUT NOTATION:

AXIAL STIFFNESS = (E A)/L : KIP/IN
FLEXURAL STIFFNESS = (EI) : KSI

********** COLUMN PROPERTIES **********

NO.	MEMBER LENGTH	AXIAL STIFFNESS	CRACKING MOMENT	YIELD MOMENT	INITIAL FLEXURAL STIFFNESS	POST YIELDING STIFFNESS	YIELD CURVATURE
1	0.1940E+03	0.5489E+04	0.9360E+03	0.1488E+04	0.3506E+06	0.1753E+06	0.2562E-03
2	0.1940E+03	0.5489E+04	0.9360E+03	0.1488E+04	0.3506E+06	0.1753E+06	0.2533E-03
3	0.1940E+03	0.5489E+04	0.9360E+03	0.1488E+04	0.3506E+06	0.1753E+06	0.2562E-03
4	0.1940E+03	0.5489E+04	0.9360E+03	0.1488E+04	0.3506E+06	0.1753E+06	0.3270E-03
5	0.1940E+03	0.5489E+04	0.9360E+03	0.1488E+04	0.3506E+06	0.1753E+06	0.3246E-03
6	0.1940E+03	0.5489E+04	0.9360E+03	0.1488E+04	0.3506E+06	0.1753E+06	0.3270E-03

********** BEAM PROPERTIES ********** ***** POSITIVE MOMENTS,CURVATURES *****

BEAM NO.	MEMBER LENGTH	INITIAL MOMENT (LEFT)	INITIAL MOMENT (RIGHT)	CRACKING MOMENT (+)	YIELD MOMENT (+)	CRACK CLOSING MOMENT	INITIAL FLEXURAL STIFFNESS	POST YIELDING STIFFNESS (+)	YIELD CURVATURE (+)
1	0.2700E+03	-0.3935E+02	-0.1585E+04	0.8784E+03	0.1154E+04	-0.1154E+04	0.8265E+06	0.3133E+06	0.1832E-03
2	0.2700E+03	-0.3935E+02	-0.1585E+04	0.8784E+03	0.1154E+04	-0.1154E+04	0.8265E+06	0.3133E+06	0.1832E-03
3	0.2700E+03	-0.3935E+02	-0.1585E+04	0.8784E+03	0.1154E+04	-0.1154E+04	0.8265E+06	0.3133E+06	0.1832E-03

***** NEGATIVE MOMENTS, CURVATURES *****

BEAM NO.	CRACKING MOMENT (-)	YIELD MOMENT (-)	POST YIELDING STIFFNESS (-)	YIELD CURVATURE (-)
1	-0.1404E+04	-0.1559E+04	0.3133E+06	-0.1545E-03
2	-0.1404E+04	-0.1559E+04	0.3133E+06	-0.1545E-03
3	-0.1404E+04	-0.1559E+04	0.3133E+06	-0.1545E-03

********** SHEAR WALL PROPERTIES **********

***** FLEXURAL PROPERTIES *****

WALL NO.	MEMBER LENGTH	AXIAL STIFFNESS	CRACKING MOMENT	YIELD MOMENT	INITIAL FLEXURAL STIFFNESS	POST YIELDING STIFFNESS	YIELD CURVATURE
1	0.2125E+03	0.6093E+05	0.8418E+05	0.1318E+06	0.1067E+12	0.2669E+10	0.8761E-05
2	0.2125E+03	0.6093E+05	0.8418E+05	0.1318E+06	0.1067E+12	0.2669E+10	0.8761E-05

***** SHEAR PROPERTIES *****

NOTATION:

SHEAR STIFFNESS = (GA) ; KIPS
SHEAR DEFORMATION = NONDIMENSIONAL AV. STRAIN

WALL NO.	CRACKING SHEAR	YIELD SHEAR	INITIAL SHEAR STIFFNESS	POST YIELD SHEAR STIFFNESS	YIELD SHEAR DEFORMATION
1	0.1174E+04	0.1304E+04	0.5184E+07	0.2592E+05	0.1184E-02
2	0.1174E+04	0.1304E+04	0.5184E+07	0.2592E+05	0.1184E-02

********** TRANSVERSE BEAM PROPERTIES **********

NO.	STIFFNESS (VERTICAL)	STIFFNESS (TORSIONAL)	ARM LENGTH
1	0.81830E+01	0.67210E+05	-0.14400E+03
2	0.81830E+01	0.67210E+05	0.00000E+00
3	0.81830E+01	0.67210E+05	0.00000E+00
4	0.81830E+01	0.67210E+05	-0.14400E+03
5	0.81830E+01	0.67210E+05	0.14400E+03
6	0.81830E+01	0.67210E+05	0.00000E+00
7	0.81830E+01	0.67210E+05	0.00000E+00
8	0.81830E+01	0.67210E+05	0.14400E+03

********** SLAB ELEMENT PROPERTIES **********

SLAB	SHEAR PROPERTIES		FLEXURAL PROPERTIES		
	CRACKING SHEAR	YIELD SHEAR	CRACKING MOMENT	YIELD MOMENT	YIELD CURVATURE
1	0.54148E+03	0.87685E+03	0.24897E+05	0.74838E+05	0.38048E-05
2	0.38125E+03	0.45157E+03	0.24897E+05	0.74838E+05	0.38048E-05
3	0.38125E+03	0.45157E+03	0.24897E+05	0.74838E+05	0.38048E-05
4	0.54148E+03	0.87685E+03	0.24897E+05	0.74838E+05	0.38048E-05

********** D Y N A M I C A N A L Y S I S **********

INPUT DATA:

********** DETAILS OF INPUT BASE MOTION **********

MAX SCALED VALUE OF HORIZONTAL COMPONENT (g): 0.700
MAX SCALED VALUE OF VERTICAL COMPONENT (g): 0.000
TIME INTERVAL OF ANALYSIS (SEC): 0.000500
TOTAL DURATION OF RESPONSE ANALYSIS (SEC): 20.000
DAMPING COEFFICIENT (% OF CRITICAL): 2.000

VERTICAL COMPONENT OF BASE MOTION: 0

[=0, NOT INCLUDED; =1, INCLUDED]

WAVE NAME: ELCENTRO EQ WAVE 0.7G

NO. OF POINTS IN INPUT BASE MOTION: 1500

TIME INTERVAL OF INPUT WAVE (SEC): 0.020000

********** PROPERTIES FOR HYSTERETIC RULE **********

NO. OF TYPES OF HYSTERETIC RULES: 5

RULE NO.	DEGRADING COEFFICIENT	SLIPPAGE COEFFICIENT	DETERIORATING COEFFICIENT	POST-YIELD STIFFNESS RATIO
1	2.000	1.000	0.000	0.01500
2	2.000	1.000	0.000	0.01500
3	3.000	1.000	0.000	0.01000
4	0.020	1.000	0.000	0.01000
5	1.000	1.000	0.100	0.01000

********** HYSTERETIC RULE FOR COLUMNS **********

COLUMN NO.	HYSTERESIS RULE NO.
1	1
2	1
3	1
4	1
5	1
6	1

********** HYSTERETIC RULE FOR BEAMS **********

BEAM NO.	HYSTERESIS RULE NO.
1	2
2	2
3	2

********** HYSTERETIC RULE FOR SHEAR WALLS **********

WALL NO.	HYSTERESIS RULE (FLEXURE)	HYSTERESIS RULE (SHEAR)
1	3	4
2	3	4

********** HYSTERETIC RULE FOR SLABS **********

SLAB NO.	HYSTERESIS RULE (FLEXURE)	HYSTERESIS RULE (SHEAR)
1	5	4
2	5	4
3	5	4
4	5	4

********** COMMENCING DYNAMIC ANALYSIS **********

********** MAXIMUM RESPONSE ******* .... FRAME NO. 1

STORY NO.	STORY DRIFT	DISPLACEMENT	VELOCITY	ACCELERATION	STORY SHEAR
1	0.1317E-01	0.1317E-01	0.9926E+00	0.3219E+03	0.1858E+03

********** MAXIMUM RESPONSE ******* .... FRAME NO. 2

STORY NO.	STORY DRIFT	DISPLACEMENT	VELOCITY	ACCELERATION	STORY SHEAR
1	0.1641E+00	0.1641E+00	0.5056E+01	0.3765E+03	0.1079E+02

********** MAXIMUM RESPONSE ******* .... FRAME NO. 3

STORY NO.	STORY DRIFT	DISPLACEMENT	VELOCITY	ACCELERATION	STORY SHEAR
1	0.2435E+00	0.2435E+00	0.7899E+01	0.5079E+03	0.1474E+02

********** MAXIMUM RESPONSE ******* .... FRAME NO. 4

STORY NO.	STORY DRIFT	DISPLACEMENT	VELOCITY	ACCELERATION	STORY SHEAR
1	0.1641E+00	0.1641E+00	0.5056E+01	0.3765E+03	0.1079E+02

********** MAXIMUM RESPONSE ******* .... FRAME NO. 5

STORY NO.	STORY DRIFT	DISPLACEMENT	VELOCITY	ACCELERATION	STORY SHEAR
1	0.1317E-01	0.1317E-01	0.9926E+00	0.3219E+03	0.1858E+03

********** MAX STORY SHEARS **********

STORY	BASE SHEAR	TIME OF OCCURENCE
1	0.40261E+03	0.24995E+01

********** MAXIMUM MOMENTS AND SHEARS **********

(TIME OF OCCURENCE SHOWN IN PARANTHESIS)

***** COLUMNS *****

COL NO.	** MAXIMUM MOMENTS ** BOT	TOP	MAX SHEAR
1	-.8120E+03 [2.17]	0.9889E+03 [2.17]	-0.9283E+01 [2.17]
2	-.9383E+03 [2.16]	0.1047E+04 [2.16]	-0.1023E+02 [2.16]
3	-.8120E+03 [2.17]	0.9889E+03 [2.17]	-0.9283E+01 [2.17]
4	0.9411E+03 [4.54]	-.1034E+04 [4.54]	0.1018E+02 [4.54]
5	0.9915E+03 [5.05]	-.1080E+04 [4.54]	0.1068E+02 [5.05]
6	0.9411E+03 [4.54]	-.1034E+04 [4.54]	0.1018E+02 [4.54]

***** BEAMS *****

BEAM NO.	** MAXIMUM MOMENTS ** LEFT	RIGHT	MAX SHEAR
1	-.1154E+04 (2.17)	-.1214E+04 (4.54)	0.3570E+01 (4.54)
2	-.1188E+04 (2.15)	-.1243E+04 (4.54)	0.4886E+01 (5.05)
3	-.1154E+04 (2.17)	-.1214E+04 (4.54)	0.3570E+01 (4.54)

***** WALLS *****

WALL NO.	** MAXIMUM MOMENTS ** BOT	TOP	MAX SHEAR
1	0.3946E+05 (2.50)	0.3259E+02 (5.05)	0.1856E+03 (2.50)
2	0.3946E+05 (2.50)	0.3259E+02 (5.05)	0.1856E+03 (2.50)

***** SLABS *****

SLAB NO.	** MAXIMUM MOMENTS ** FRAME I	FRAME J	MAX SHEAR
1	0.2523E-10 (10.72)	-.3491E+05 (2.51)	0.1231E+03 (2.51)
2	-.3491E+05 (2.51)	-.4978E+05 (2.51)	0.8173E+02 (2.85)
3	-.4978E+05 (2.51)	-.3491E+05 (2.51)	-0.8173E+02 (2.85)
4	-.3491E+05 (2.51)	-.4939E-10 (16.95)	-0.1231E+03 (2.51)

INELASTIC DAMAGE ANALYSIS OF REINFORCED CONCRETE STRUCTURES
WITH FLEXIBLE FLOOR DIAPHRAGMS

STATE UNIVERSITY OF NEW YORK AT BUFFALO
DEPARTMENT OF CIVIL ENGINEERING

JUNE 1988

INPUT DATA:

TITLE: SCALED MODEL WITH STIFF END FRAMES (50% LL)

********** BUILDING CONFIGURATION AND MATERIAL INFORMATION **********

NUMBER OF STORIES 1
NUMBER OF FRAMES 9

NO. OF TYPES OF CONCRETE 1
NO. OF TYPES OF STEEL 2

********** ELEMENT INFORMATION **********

NO. OF TYPES OF COLUMNS 2
NO. OF TYPES OF BEAMS 2
NO. OF TYPES OF SHEAR WALLS 1
NO. OF TYPES OF EDGE COLUMNS 0
NO. OF TYPES OF TRANSVERSE BEAMS 1
NO. OF TYPES OF SLABS 3

NUMBER OF COLUMNS 8
NUMBER OF BEAMS 5
NUMBER OF SHEAR WALLS 4
NUMBER OF EDGE COLUMNS 0
NUMBER OF TRANSVERSE BEAMS 8
NUMBER OF SLAB ELEMENTS 8

ESTIMATED BASE SHEAR COEFFICIENT : 1.0
(% OF TOTAL WEIGHT)

SYSTEM OF UNITS: INCH, KIPS

********** STORY HEIGHT AND FLOOR WEIGHTS **********

STORY	HEIGHT FROM BASE	FLOOR WEIGHT							
1	35.440	2.252 2.252	1.854	1.434	1.434	1.274	1.434	1.434	1.854

********** X CO-ORDINATE DISTANCE OF COLUMN FROM REFERENCE POINT **********

FRAME	COLUMN COORDINATE (IN ORDER)	
1	2.00	46.00
2	0.00	48.00
3	0.00	48.00
4	0.00	48.00
5	0.00	48.00
6	0.00	48.00
7	0.00	48.00
8	0.00	48.00
9	2.00	46.00

********** CONCRETE PROPERTIES **********

TYPE	STRENGTH	MODULUS	STRAIN AT TENSION CRACK	STRAIN AT MAX STRENGTH (%)	BOND STRENGTH
1	4.000	3000.000	0.000133	0.300	1.200

********** REINFORCEMENT PROPERTIES **********

TYPE	YIELD STRENGTH	ULTIMATE STRENGTH	YOUNGS MODULUS	MODULUS AT HARDENING	STRAIN AT HARDENING
1	40.000	50.000	28000.000	300.000	2.000
2	50.000	80.000	28000.000	300.000	1.500

********** COLUMN TYPES **********

COLUMN TYPE	CONCRETE TYPE	STEEL TYPE	DEPTH	WIDTH	COVER	LENGTH	RIGID ZONE (BOT)	RIGID ZONE (TOP)
1	1	2	3.000	3.000	0.400	35.440	0.000	3.085
2	1	2	3.000	3.000	0.400	35.440	0.000	3.085

***** AXIAL LOAD AND REINFORCEMENT OF COLUMNS *****

TYPE	AXIAL LOAD	MOMENT (BOT)	MOMENT (TOP)	STEEL AREA	PERIMETER OF BARS	WEB REINF RATIO	CONFINEMENT RATIO
1	1.640	0.000	0.000	0.050	1.3800	1.2500	2.0500
2	2.070	0.000	0.000	0.050	1.3800	1.2500	2.0500

********** BEAM TYPES **********

BEAM TYPE	CONCRETE TYPE	STEEL TYPE	DEPTH	WIDTH	SLAB WIDTH	SLAB THICKNESS	COVER	MEMBER LENGTH	RIGID ZONE (LEFT)	RIGID ZONE (RIGHT)
1	1	2	3.670	2.000	7.000	1.187	0.500	44.000	10.000	10.000
2	1	2	3.670	2.000	7.000	1.187	0.500	48.000	1.500	1.500

***** INITIAL MOMENTS AND REINFORCEMENT OF BEAMS *****

BEAM TYPE	MOMENT (LEFT)	MOMENT (RIGHT)	STEEL AREA (BOTTOM)	STEEL AREA (TOP)	PERIMETER OF BARS (BOT)	PERIMETER OF BARS (TOP)	WEB REINF RATIO	CONFINEMENT RATIO
1	0.000	0.000	0.080	0.080	2.0000	2.0000	1.000	2.7800
2	0.000	0.000	0.040	0.050	1.0000	1.2500	0.857	1.8500

********** SHEAR WALL TYPES **********

WALL TYPE	CONCRETE TYPE	STEEL TYPE	DIST BET. EDGE COLS	WALL THICKNESS	DEPTH OF EDGE COL	WIDTH OF EDGE COL	DEPTH OF WALL
1	1	2	17.000	2.000	3.000	2.000	35.440

***** AXIAL LOAD AND REINFORCEMENT OF SHEAR WALLS *****

WALL TYPE	AXIAL LOAD	VERTICAL REINF RATIO	HORIZONTAL REINF RATIO	GROSS STEEL AREA IN EDGE COL
1	1.125	0.4000	0.2600	0.1000

********** TRANSVERSE BEAMS **********

TYPE	STIFFNESS	STIFFNESS (TORSIONAL)	ARM LENGTH
1	1.140	259.000	-2.000
2	1.140	259.000	2.000
3	1.140	259.000	0.000

********** SLAB PROPERTIES **********

TYPE	CONC TYPE	LENGTH
1	1	24.0000

DATA FOR 7 SECTIONS:

SECTION	STEEL TYPE	THICKNESS	DEPTH	MAIN REINF	LATERAL REINF	FIBERS
1	1	1.1870	7.0000	0.001420	0.003340	10
2	2	3.6700	2.0000	0.011000	0.003340	8
3	1	1.1870	11.0000	0.001420	0.003340	10
4	1	1.1870	24.0000	0.003560	0.003340	20
5	1	1.1870	11.0000	0.001420	0.003340	10
6	2	3.6700	2.0000	0.011000	0.003340	8
7	1	1.1870	7.0000	0.001420	0.003340	10

TYPE	CONC TYPE	LENGTH
2	1	48.0000

DATA FOR 7 SECTIONS:

SECTION	STEEL TYPE	THICKNESS	DEPTH	MAIN REINF	LATERAL REINF	FIBERS
1	1	1.1870	7.0000	0.001420	0.002600	10
2	2	3.6700	2.0000	0.011000	0.002260	8
3	1	1.1870	11.0000	0.001420	0.002600	10
4	1	1.1870	24.0000	0.004270	0.002600	20
5	1	1.1870	11.0000	0.001420	0.002600	10
6	1	3.6700	2.0000	0.011000	0.002600	8
7	1	1.1870	7.0000	0.001420	0.002600	10

TYPE	CONC TYPE	LENGTH
3	1	12.0000

DATA FOR 7 SECTIONS:

SECTION	STEEL TYPE	THICKNESS	DEPTH	MAIN REINF	LATERAL REINF	FIBERS
1	1	1.1870	7.0000	0.002100	0.003340	10
2	2	3.6700	2.0000	0.013600	0.003340	8
3	1	1.1870	11.0000	0.002100	0.003340	10
4	1	1.1870	24.0000	0.006400	0.003340	20
5	1	1.1870	11.0000	0.002100	0.003340	10
6	2	3.6700	2.0000	0.013600	0.003340	8
7	1	1.1870	7.0000	0.002100	0.003340	10

ACTIVE OPTION FOR SLAB TYPE: FLEXIBLE

********** NODAL CONNECTIVITY INFORMATION **********

********** COLUMN ELEMENTS **********

COL.	TYPE	I-COORD	J-COORD	L-COORD	L-COORD

NO.				(BOT)	(TOP)
1	1	2	1	0	1
2	2	5	1	0	1
3	1	8	1	0	1
4	1	2	2	0	1
5	2	5	2	0	1
6	1	8	2	0	1

********** BEAM ELEMENTS **********

BEAM NO.	TYPE	L-COORD	I-COORD	J-COORD (LEFT)	J-COORD (RIGHT)
1	1	1	1	1	2
2	2	1	2	1	2
3	2	1	5	1	2
4	2	1	8	1	2
5	1	1	9	1	2

********** SHEAR WALL ELEMENTS **********

WALL NO.	TYPE	I-COORD	J-COORD	L-COORD (BOTTOM)	L-COORD (TOP)
1	1	1	1	0	1
2	1	1	2	0	1
3	1	9	1	0	1
4	1	9	2	0	1

********** TRANSVERSE BEAM ELEMENTS **********

NO.	TYPE	L-COORD	I-COORD (WALL//COL)	J-COORD (WALL//COL)	I-COORD (COLUMN)	J-COORD (COLUMN)
1	1	1	1	1	2	1
2	3	1	2	1	5	1
3	3	1	5	1	8	1
4	1	1	9	1	8	1
5	2	1	1	2	2	2
6	3	1	2	2	5	2
7	3	1	5	2	8	2
8	2	1	9	2	8	2

********** SLAB ELEMENTS **********

SLAB NO.	SLAB TYPE	L-COORD	I-COORD FRAME I	I-COORD FRAME J
1	2	1	1	2
2	3	1	2	3
3	1	1	3	4
4	3	1	4	5
5	3	1	5	6
6	1	1	6	7
7	3	1	7	8
8	2	1	8	9

********** CONFIGURATION OF PLAN **********

PLAN OF FRAME 9: ***O*********O*

PLAN OF FRAME 8: O*********O

PLAN OF FRAME 7: O*********O

PLAN OF FRAME 6: O*********O

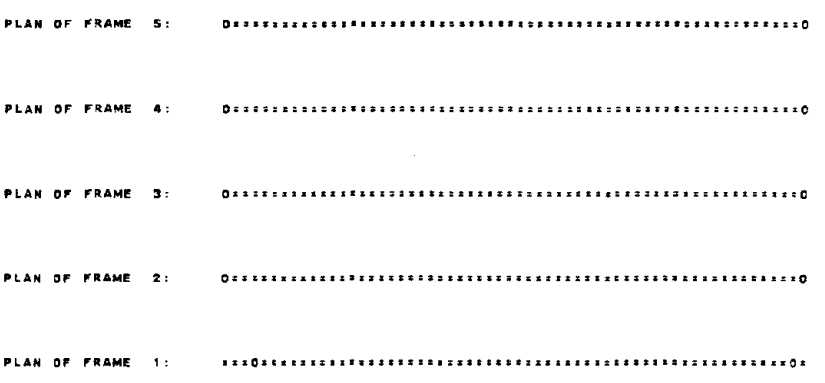

********** FRAME ELEVATION AND ELEMENT TYPES **********

ELEVATION OF FRAME NO. 1

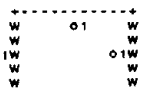

NOTATION:

-	=	BEAM	NUMBERS INDICATE ELEMENT TYPES
!	=	COLUMN	COLUMN TYPE NUMBERS ON RIGHT
W	=	SHEAR WALL	SHEAR WALL NUMBERS ON LEFT, AND
I	=	EDGE COLUMN	EDGE COLUMN NUMBERS BELOW COLUMN TYPES

ELEVATION OF FRAME NO. 2

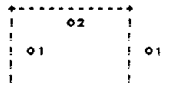

NOTATION:

-	=	BEAM	NUMBERS INDICATE ELEMENT TYPES
!	=	COLUMN	COLUMN TYPE NUMBERS ON RIGHT
W	=	SHEAR WALL	SHEAR WALL NUMBERS ON LEFT, AND
I	=	EDGE COLUMN	EDGE COLUMN NUMBERS BELOW COLUMN TYPES

ELEVATION OF FRAME NO. 3

NOTATION:

-	=	BEAM	NUMBERS INDICATE ELEMENT TYPES
!	=	COLUMN	COLUMN TYPE NUMBERS ON RIGHT
W	=	SHEAR WALL	SHEAR WALL NUMBERS ON LEFT, AND
I	=	EDGE COLUMN	EDGE COLUMN NUMBERS BELOW COLUMN TYPES

ELEVATION OF FRAME NO. 4

NOTATION:

-	=	BEAM	NUMBERS INDICATE ELEMENT TYPES
!	=	COLUMN	COLUMN TYPE NUMBERS ON RIGHT
W	=	SHEAR WALL	SHEAR WALL NUMBERS ON LEFT, AND
I	=	EDGE COLUMN	EDGE COLUMN NUMBERS BELOW COLUMN TYPES

ELEVATION OF FRAME NO. 5

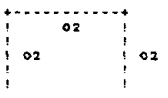

NOTATION:

-	=	BEAM	NUMBERS INDICATE ELEMENT TYPES
!	=	COLUMN	COLUMN TYPE NUMBERS ON RIGHT
W	=	SHEAR WALL	SHEAR WALL NUMBERS ON LEFT, AND
I	=	EDGE COLUMN	EDGE COLUMN NUMBERS BELOW COLUMN TYPES

ELEVATION OF FRAME NO. 6

NOTATION:

-	=	BEAM	NUMBERS INDICATE ELEMENT TYPES
!	=	COLUMN	COLUMN TYPE NUMBERS ON RIGHT
W	=	SHEAR WALL	SHEAR WALL NUMBERS ON LEFT, AND
I	=	EDGE COLUMN	EDGE COLUMN NUMBERS BELOW COLUMN TYPES

ELEVATION OF FRAME NO. 7

NOTATION:

-	=	BEAM	NUMBERS INDICATE ELEMENT TYPES
!	=	COLUMN	COLUMN TYPE NUMBERS ON RIGHT
W	=	SHEAR WALL	SHEAR WALL NUMBERS ON LEFT, AND
I	=	EDGE COLUMN	EDGE COLUMN NUMBERS BELOW COLUMN TYPES

ELEVATION OF FRAME NO. 8

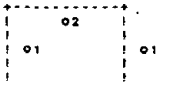

NOTATION:

-	=	BEAM	NUMBERS INDICATE ELEMENT TYPES
!	=	COLUMN	COLUMN TYPE NUMBERS ON RIGHT
W	=	SHEAR WALL	SHEAR WALL NUMBERS ON LEFT, AND
I	=	EDGE COLUMN	EDGE COLUMN NUMBERS BELOW COLUMN TYPES

ELEVATION OF FRAME NO. 9

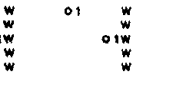

NOTATION:

-	=	BEAM	NUMBERS INDICATE ELEMENT TYPES
!	=	COLUMN	COLUMN TYPE NUMBERS ON RIGHT
W	=	SHEAR WALL	SHEAR WALL NUMBERS ON LEFT, AND
I	=	EDGE COLUMN	EDGE COLUMN NUMBERS BELOW COLUMN TYPES

********** LOADING DATA **********

NO. OF UNIFORMLY LOADED BEAMS 5
NO. OF LATERAL LOADING POINTS 0
NO. OF APPLIED NODAL MOMENTS 5

UNIFORM LOAD DATA:

LOAD NO.	BEAM NO.	LOAD VALUE
1	1	0.018
2	2	0.036
3	3	0.047
4	4	0.036
5	5	0.018

NODAL MOMENTS DATA:

LOAD NO.	BEAM NO.	LEFT MOMENT	RIGHT MOMENT
1	1	-0.881	0.881
2	2	-1.150	1.150
3	3	-1.500	1.500
4	4	-1.150	1.150
5	5	-0.881	0.881

********** O U T P U T O F R E S U L T S **********

ACTIVE SYSTEM OF UNITS: INCH, KIPS

********** FAILURE SEQUENCE **********

YIELDING DETECTED IN BEAM 3 AT BASE SHEAR COEFF VALUE: 0.825

FLEXURAL YIELDING IN SLAB 3 AT BASE SHEAR COEFF VALUE: 1.125
FLEXURAL YIELDING IN SLAB 6 AT BASE SHEAR COEFF VALUE: 1.125

YIELDING DETECTED IN BEAM 2 AT BASE SHEAR COEFF VALUE: 1.150
YIELDING DETECTED IN BEAM 4 AT BASE SHEAR COEFF VALUE: 1.150

YIELDING DETECTED IN COLUMN 5 AT BASE SHEAR COEFF VALUE: 1.200

YIELDING DETECTED IN COLUMN 4 AT BASE SHEAR COEFF VALUE: 1.225
YIELDING DETECTED IN COLUMN 6 AT BASE SHEAR COEFF VALUE: 1.225

YIELDING DETECTED IN COLUMN 2 AT BASE SHEAR COEFF VALUE: 1.275

YIELDING DETECTED IN COLUMN 1 AT BASE SHEAR COEFF VALUE: 1.300
YIELDING DETECTED IN COLUMN 3 AT BASE SHEAR COEFF VALUE: 1.300

FLEXURAL YIELDING IN SLAB 3 AT BASE SHEAR COEFF VALUE: 1.425
FLEXURAL YIELDING IN SLAB 6 AT BASE SHEAR COEFF VALUE: 1.425

********** O U T P U T O F R E S U L T S **********

FUNDAMENTAL PERIOD OF STRUCTURE (SEC): 0.040

MAXIMUM BASE SHEAR COEFFICIENT: 1.425

MAXIMUM DEFORMATION AT TOP ... FRAME 1: 0.039
(% OF BUILDING HEIGHT)
FRAME 2: 1.229
FRAME 3: 1.524
FRAME 4: 1.920
FRAME 5: 1.921
FRAME 6: 1.920
FRAME 7: 1.524
FRAME 8: 1.229
FRAME 9: 0.039

********** PLOT OF BASE SHEAR VS. TOP DEFORMATION ****** FRAME 1

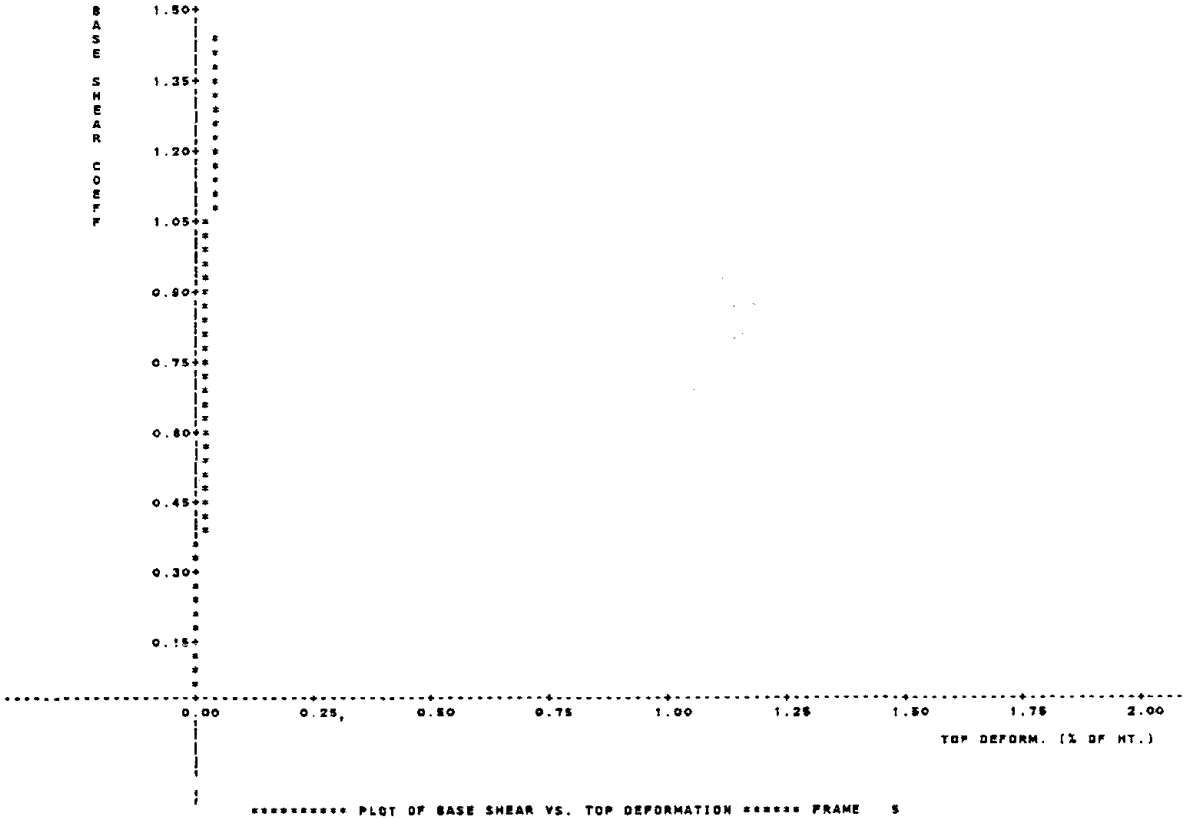

********** PLOT OF BASE SHEAR VS. TOP DEFORMATION ****** FRAME 5

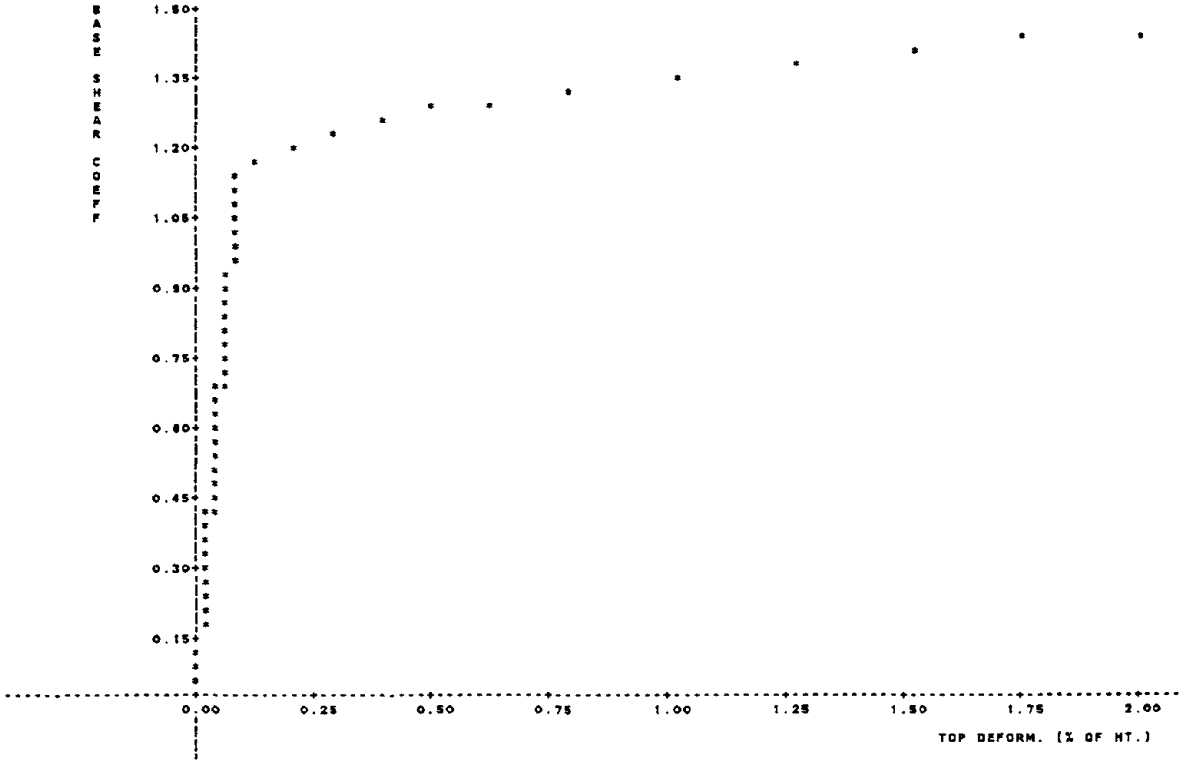

OUTPUT NOTATION:

AXIAL STIFFNESS = (E A)/L : KIP/IN
FLEXURAL STIFFNESS = (EI) : KSI

********** COLUMN PROPERTIES **********

NO.	MEMBER LENGTH	AXIAL STIFFNESS	CRACKING MOMENT	YIELD MOMENT	INITIAL FLEXURAL STIFFNESS	POST YIELDING STIFFNESS	YIELD CURVATURE
1	0.3236E+02	0.7619E+03	0.4474E+01	0.7681E+01	0.2277E+05	0.1139E+03	0.1857E-02
2	0.3236E+02	0.7619E+03	0.4889E+01	0.8160E+01	0.2277E+05	0.1139E+03	0.1668E-02
3	0.3236E+02	0.7619E+03	0.4474E+01	0.7681E+01	0.2277E+05	0.1139E+03	0.1857E-02
4	0.3236E+02	0.7619E+03	0.4474E+01	0.7681E+01	0.2277E+05	0.1139E+03	0.2146E-02
5	0.3236E+02	0.7619E+03	0.4889E+01	0.8160E+01	0.2277E+05	0.1139E+03	0.2182E-02
6	0.3236E+02	0.7619E+03	0.4474E+01	0.7681E+01	0.2277E+05	0.1139E+03	0.2146E-02

********** BEAM PROPERTIES **********

***** POSITIVE MOMENTS,CURVATURES *****

BEAM NO.	MEMBER LENGTH	INITIAL MOMENT (LEFT)	INITIAL MOMENT (RIGHT)	CRACKING MOMENT (+)	YIELD MOMENT (+)	CRACK CLOSING MOMENT	INITIAL FLEXURAL STIFFNESS	POST YIELDING STIFFNESS (+)	YIELD CURVATURE (+)
1	0.2400E+02	0.7999E+01	-0.5901E+01	0.4074E+01	0.1155E+02	-0.1155E+02	0.3689E+05	0.1844E+03	0.2262E-02
2	0.4500E+02	-0.4524E+00	-0.6999E+01	0.4074E+01	0.8002E+01	-0.8002E+01	0.4039E+05	0.2020E+03	0.1298E-02
3	0.4500E+02	-0.4524E+00	-0.6999E+01	0.4074E+01	0.8002E+01	-0.8002E+01	0.4039E+05	0.2020E+03	0.1298E-02
4	0.4500E+02	-0.4524E+00	-0.6999E+01	0.4074E+01	0.8002E+01	-0.8002E+01	0.4039E+05	0.2020E+03	0.1298E-02
5	0.2400E+02	0.7999E+01	-0.5901E+01	0.4074E+01	0.1155E+02	-0.1155E+02	0.3689E+05	0.1844E+03	0.2262E-02

***** NEGATIVE MOMENTS, CURVATURES *****

BEAM NO.	CRACKING MOMENT (-)	YIELD MOMENT (-)	POST YIELDING STIFFNESS (-)	YIELD CURVATURE (-)
1	-0.7601E+01	-0.1070E+02	0.1844E+03	-0.1311E-02
2	-0.6187E+01	-0.8874E+01	0.2020E+03	-0.1097E-02
3	-0.6187E+01	-0.8874E+01	0.2020E+03	-0.1097E-02
4	-0.6187E+01	-0.8874E+01	0.2020E+03	-0.1097E-02
5	-0.7601E+01	-0.1070E+02	0.1844E+03	-0.1311E-02

********** SHEAR WALL PROPERTIES **********

***** FLEXURAL PROPERTIES *****

WALL NO.	MEMBER LENGTH	AXIAL STIFFNESS	CRACKING MOMENT	YIELD MOMENT	INITIAL FLEXURAL STIFFNESS	POST YIELDING STIFFNESS	YIELD CURVATURE
1	0.3544E+02	0.3366E+04	0.8000E+02	0.1737E+03	0.8273E+07	0.1568E+06	0.1427E-03
2	0.3544E+02	0.3366E+04	0.8000E+02	0.1737E+03	0.8273E+07	0.1568E+06	0.1427E-03
3	0.3544E+02	0.3366E+04	0.8000E+02	0.1737E+03	0.8273E+07	0.1568E+06	0.1427E-03
4	0.3544E+02	0.3366E+04	0.8000E+02	0.1737E+03	0.8273E+07	0.1568E+06	0.1427E-03

***** SHEAR PROPERTIES *****

NOTATION:

SHEAR STIFFNESS = (GA) : KIPS
SHEAR DEFORMATION = NONDIMENSIONAL AV. STRAIN

WALL NO.	CRACKING SHEAR	YIELD SHEAR	INITIAL SHEAR STIFFNESS	POST YIELD SHEAR STIFFNESS	YIELD SHEAR DEFORMATION
1	0.1177E+02	0.1307E+02	0.4800E+05	0.2400E+03	0.5639E-03
2	0.1177E+02	0.1307E+02	0.4800E+05	0.2400E+03	0.5639E-03
3	0.1177E+02	0.1307E+02	0.4800E+05	0.2400E+03	0.5639E-03
4	0.1177E+02	0.1307E+02	0.4800E+05	0.2400E+03	0.5639E-03

********** TRANSVERSE BEAM PROPERTIES **********

NO.	STIFFNESS (VERTICAL)	STIFFNESS (TORSIONAL)	ARM LENGTH
1	0.11400E+01	0.25900E+03	-0.20000E+01
2	0.11400E+01	0.25900E+03	0.00000E+00
3	0.11400E+01	0.25900E+03	0.00000E+00
4	0.11400E+01	0.25900E+03	-0.20000E+01
5	0.11400E+01	0.25900E+03	0.20000E+01
6	0.11400E+01	0.25900E+03	0.00000E+00
7	0.11400E+01	0.25900E+03	0.00000E+00

8	0.11400E+01	0.25800E+03	0.20000E+01

********** SLAB ELEMENT PROPERTIES **********

SLAB	SHEAR PROPERTIES		FLEXURAL PROPERTIES		
	CRACKING SHEAR	YIELD SHEAR	CRACKING MOMENT	YIELD MOMENT	YIELD CURVATURE
1	0.15800E+02	0.19750E+02	0.12398E+03	0.37570E+03	0.28634E-04
2	0.14802E+02	0.18502E+02	0.15674E+03	0.47496E+03	0.29015E-04
3	0.11663E+02	0.14588E+02	0.12112E+03	0.36702E+03	0.28575E-04
4	0.83854E+01	0.10482E+02	0.15674E+03	0.47496E+03	0.29015E-04
5	0.83854E+01	0.10482E+02	0.15674E+03	0.47496E+03	0.29015E-04
6	0.11653E+02	0.14588E+02	0.12112E+03	0.36702E+03	0.28575E-04
7	0.14802E+02	0.18502E+02	0.15674E+03	0.47496E+03	0.29015E-04
8	0.15800E+02	0.19750E+02	0.12398E+03	0.37570E+03	0.28634E-04

********** D Y N A M I C A N A L Y S I S **********

INPUT DATA:

********** DETAILS OF INPUT BASE MOTION **********

MAX SCALED VALUE OF HORIZONTAL COMPONENT (g): 0.950

MAX SCALED VALUE OF VERTICAL COMPONENT (g): 0.000

TIME INTERVAL OF ANALYSIS (SEC): 0.000408

TOTAL DURATION OF RESPONSE ANALYSIS (SEC): 5.000

DAMPING COEFFICIENT (% OF CRITICAL): 2.000

VERTICAL COMPONENT OF BASE MOTION: 0

(=0, NOT INCLUDED; =1, INCLUDED)

WAVE NAME: TAFT EARTHQUAKE

NO. OF POINTS IN INPUT BASE MOTION: 1500

TIME INTERVAL OF INPUT WAVE (SEC): 0.004160

********** PROPERTIES FOR HYSTERETIC RULE **********

NO. OF TYPES OF HYSTERETIC RULES: 5

RULE NO.	DEGRADING COEFFICIENT	SLIPPAGE COEFFICIENT	DETERIORATING COEFFICIENT	POST-YIELD STIFFNESS RATIO
1	2.000	1.000	0.000	0.01500
2	2.000	1.000	0.000	0.01500
3	3.000	1.000	0.000	0.01000
4	0.020	1.000	0.000	0.01000
5	1.000	1.000	0.100	0.01000

********** HYSTERETIC RULE FOR COLUMNS **********

COLUMN NO.	HYSTERESIS RULE NO.
1	1
2	1
3	1
4	1
5	1
6	1

********** HYSTERETIC RULE FOR BEAMS **********

BEAM NO.	HYSTERESIS RULE NO.
1	2
2	2
3	2
4	2
5	2

********** HYSTERETIC RULE FOR SHEAR WALLS **********

WALL NO.	HYSTERESIS RULE (FLEXURE)	HYSTERESIS RULE (SHEAR)
1	3	4
2	3	4
3	3	4
4	3	4

********** HYSTERETIC RULE FOR SLABS **********

SLAB NO.	HYSTERESIS RULE (FLEXURE)	HYSTERESIS RULE (SHEAR)
1	5	4
2	5	4
3	5	4
4	5	4
5	5	4
6	5	4
7	5	4
8	5	4

********** COMMENCING DYNAMIC ANALYSIS **********

YIELDING DETECTED IN SLAB NO. 3

YIELDING DETECTED IN SLAB NO. 6

PRINTING FORCES AT TIME..... 1.888592

***** COLUMNS *****

COL NO.	MOMENT (BOT)	MOMENT (TOP)	SHEAR
1	-0.54151E+01	0.54197E+01	-0.33487E+00
2	-0.66265E+01	0.62939E+01	-0.38933E+00
3	-0.54151E+01	0.54197E+01	-0.33487E+00
4	-0.39484E+01	0.98820E+00	-0.15254E+00
5	-0.42941E+01	-0.97843E+00	-0.10575E+00
6	-0.39484E+01	0.98820E+00	-0.15254E+00

***** BEAMS *****

BEAM NO.	MOMENT (LEFT)	MOMENT (RIGHT)	SHEAR
1	-0.45567E+01	0.37841E+01	-0.34795E+00
2	-0.84058E+01	0.10258E+01	-0.18515E+00
3	-0.70004E+01	-0.15811E+01	-0.12043E+00
4	-0.84058E+01	0.10258E+01	-0.18515E+00
5	-0.45567E+01	0.37841E+01	-0.34795E+00

***** WALLS *****

WALL NO.	MOMENT (BOT)	MOMENT (TOP)	SHEAR
1	-0.10120E+03	0.80883E+01	-0.32366E+01
2	-0.72918E+02	0.58360E+01	-0.23199E+01
3	-0.10120E+03	0.80883E+01	-0.32366E+01
4	-0.72918E+02	0.58360E+01	-0.23199E+01

***** SLABS *****

SLAB NO.	MOMENT (FRONT)	MOMENT (REAR)	SHEAR
1	0.16743E-13	0.25391E+03	-0.53772E+01
2	0.25291E+03	0.30562E+03	-0.41965E+01
3	0.30698E+03	0.36709E+03	-0.25921E+01
4	0.36713E+03	0.37456E+03	-0.81599E+00
5	0.37456E+03	0.36713E+03	0.81599E+00
6	0.36709E+03	0.30698E+03	0.25921E+01
7	0.30562E+03	0.25291E+03	0.41965E+01
8	0.25391E+03	0.47111E-13	0.53772E+01

********** MAXIMUM RESPONSE ******* .... FRAME NO. 1

STORY NO.	STORY DRIFT	DISPLACEMENT	VELOCITY	ACCELERATION	STORY SHEAR
1	0.3188E-01	0.3188E-01	0.1762E+01	0.4210E+03	0.8222E+01

********** MAXIMUM RESPONSE ******* .... FRAME NO. 2

STORY NO.	STORY DRIFT	DISPLACEMENT	VELOCITY	ACCELERATION	STORY SHEAR
1	0.1233E+00	0.1233E+00	0.6058E+01	0.8114E+03	0.8773E+00

********** MAXIMUM RESPONSE ******* .... FRAME NO. 3

STORY NO.	STORY DRIFT	DISPLACEMENT	VELOCITY	ACCELERATION	STORY SHEAR
1	0.1423E+00	0.1423E+00	0.8957E+01	0.5601E+03	0.0000E+00

********** MAXIMUM RESPONSE ******* .... FRAME NO. 4

STORY NO.	STORY DRIFT	DISPLACEMENT	VELOCITY	ACCELERATION	STORY SHEAR
1	0.1848E+00	0.1848E+00	0.8175E+01	0.8598E+03	0.0000E+00

********** MAXIMUM RESPONSE ******* .... FRAME NO. 5

STORY NO.	STORY DRIFT	DISPLACEMENT	VELOCITY	ACCELERATION	STORY SHEAR
1	0.1885E+00	0.1885E+00	0.8310E+01	0.7201E+03	0.5181E+00

********** MAXIMUM RESPONSE ******* .... FRAME NO. 6

STORY NO.	STORY DRIFT	DISPLACEMENT	VELOCITY	ACCELERATION	STORY SHEAR
1	0.1848E+00	0.1848E+00	0.8184E+01	0.5715E+03	0.0000E+00

********** MAXIMUM RESPONSE ******* .... FRAME NO. 7

STORY NO.	STORY DRIFT	DISPLACEMENT	VELOCITY	ACCELERATION	STORY SHEAR
1	0.1421E+00	0.1421E+00	0.6983E+01	0.5550E+03	0.0000E+00

********** MAXIMUM RESPONSE ******* .... FRAME NO. 8

STORY NO.	STORY DRIFT	DISPLACEMENT	VELOCITY	ACCELERATION	STORY SHEAR
1	0.1230E+00	0.1230E+00	0.6073E+01	0.5114E+03	0.6476E+00

********** MAXIMUM RESPONSE ******* .... FRAME NO. 9

STORY NO.	STORY DRIFT	DISPLACEMENT	VELOCITY	ACCELERATION	STORY SHEAR
1	0.3150E-01	0.3150E-01	0.1788E+01	0.4210E+03	0.8222E+01

********** MAX STORY SHEARS **********

STORY	BASE SHEAR	TIME OF OCCURENCE
1	0.18091E+02	0.28869E+01

********** MAXIMUM MOMENTS AND SHEARS **********

(TIME OF OCCURENCE SHOWN IN PARANTHESIS)

***** COLUMNS *****

COL NO.	** MAXIMUM MOMENTS ** BOT	TOP	MAX SHEAR
1	-.7022E+01 (3.18)	0.5517E+01 (2.25)	-0.3850E+00 (3.18)
2	-.8894E+01 (3.84)	0.8587E+01 (2.25)	-0.4585E+00 (3.84)
3	-.7022E+01 (3.18)	0.5517E+01 (2.25)	-0.3850E+00 (3.18)
4	0.7202E+01 (5.47)	-.5509E+01 (3.78)	0.3818E+00 (2.70)
5	0.8763E+01 (3.78)	-.8675E+01 (2.70)	0.4723E+00 (3.78)
6	0.7760E+01 (8.63)	-.6788E+01 (8.14)	0.4070E+00 (8.63)

***** BEAMS *****

BEAM NO.	** MAXIMUM MOMENTS ** LEFT	RIGHT	MAX SHEAR
1	-.7780E+01 (2.25)	-.7780E+01 (3.78)	0.5922E+00 (2.70)
2	-.8595E+01 (2.25)	-.8574E+01 (2.70)	-0.2185E+06 (3.84)
3	-.7878E+01 (3.84)	-.7934E+01 (5.47)	0.1457E+00 (3.78)
4	-.8595E+01 (2.25)	-.8574E+01 (2.70)	0.2293E+00 (5.14)
5	-.7780E+01 (2.25)	-.7637E+01 (2.70)	0.5922E+00 (2.70)

***** WALLS *****

WALL NO.	** MAXIMUM MOMENTS ** BOT	TOP	MAX SHEAR
1	-.1331E+03 (3.18)	0.1437E+02 (2.25)	-0.4259E+01 (3.18)
2	0.1528E+03 (2.70)	-.1438E+02 (2.70)	0.4730E+01 (2.70)
3	-.1331E+03 (3.18)	0.1437E+02 (2.25)	-0.4259E+01 (3.18)
4	0.1528E+03 (2.70)	-.1438E+02 (2.70)	0.4730E+01 (2.70)

***** SLABS *****

SLAB NO.	** MAXIMUM MOMENTS ** FRAME I	FRAME J	MAX SHEAR
1	0.5425E-12 (4.84)	0.2881E+03 (3.84)	-0.5988E+01 (3.84)
2	0.2878E+03 (3.84)	-.3427E+03 (3.78)	0.4883E+01 (3.78)
3	-.3430E+03 (3.78)	0.4181E+03 (3.84)	0.3400E+01 (3.78)
4	-.4158E+03 (3.78)	-.4251E+03 (3.78)	-0.1084E+01 (4.70)
5	-.4251E+03 (3.78)	-.4154E+03 (3.78)	0.1145E+01 (4.68)
6	0.4175E+03 (3.84)	-.3424E+03 (2.70)	-0.3422E+01 (3.78)
7	-.3422E+03 (2.70)	-.2861E+03 (2.70)	-0.4899E+01 (3.78)
8	0.2866E+03 (3.84)	-.3528E-12 (4.80)	-0.5974E+01 (2.70)

NATIONAL CENTER FOR EARTHQUAKE ENGINEERING RESEARCH
LIST OF PUBLISHED TECHNICAL REPORTS

The National Center for Earthquake Engineering Research (NCEER) publishes technical reports on a variety of subjects related to earthquake engineering written by authors funded through NCEER. These reports are available from both NCEER's Publications Department and the National Technical Information Service (NTIS). Requests for reports should be directed to the Publications Department, National Center for Earthquake Engineering Research, State University of New York at Buffalo, Red Jacket Quadrangle, Buffalo, New York 14261. Reports can also be requested through NTIS, 5285 Port Royal Road, Springfield, Virginia 22161. NTIS accession numbers are shown in parenthesis, if available.

NCEER-87-0001 "First-Year Program in Research, Education and Technology Transfer," 3/5/87, (PB88-134275/AS).

NCEER-87-0002 "Experimental Evaluation of Instantaneous Optimal Algorithms for Structural Control," by R.C. Lin, T.T. Soong and A.M. Reinhorn, 4/20/87, (PB88-134341/AS).

NCEER-87-0003 "Experimentation Using the Earthquake Simulation Facilities at University at Buffalo," by A.M. Reinhorn and R.L. Ketter, to be published.

NCEER-87-0004 "The System Characteristics and Performance of a Shaking Table," by J.S. Hwang, K.C. Chang and G.C. Lee, 6/1/87, (PB88-134259/AS).

NCEER-87-0005 "A Finite Element Formulation for Nonlinear Viscoplastic Material Using a Q Model," by O. Gyebi and G. Dasgupta, 11/2/87, (PB88-213764/AS).

NCEER-87-0006 "Symbolic Manipulation Program (SMP) - Algebraic Codes for Two and Three Dimensional Finite Element Formulations," by X. Lee and G. Dasgupta, 11/9/87, (PB88-219522/AS).

NCEER-87-0007 "Instantaneous Optimal Control Laws for Tall Buildings Under Seismic Excitations," by J.N. Yang, A. Akbarpour and P. Ghaemmaghami, 6/10/87, (PB88-134333/AS).

NCEER-87-0008 "IDARC: Inelastic Damage Analysis of Reinforced Concrete Frame - Shear-Wall Structures," by Y.J. Park, A.M. Reinhorn and S.K. Kunnath, 7/20/87, (PB88-134325/AS).

NCEER-87-0009 "Liquefaction Potential for New York State: A Preliminary Report on Sites in Manhattan and Buffalo," by M. Budhu, V. Vijayakumar, R.F. Giese and L. Baumgras, 8/31/87, (PB88-163704/AS). This report is available only through NTIS (see address given above).

NCEER-87-0010 "Vertical and Torsional Vibration of Foundations in Inhomogeneous Media," by A.S. Veletsos and K.W. Dotson, 6/1/87, (PB88-134291/AS).

NCEER-87-0011 "Seismic Probabilistic Risk Assessment and Seismic Margins Studies for Nuclear Power Plants," by Howard H.M. Hwang, 6/15/87, (PB88-134267/AS). This report is available only through NTIS (see address given above).

NCEER-87-0012 "Parametric Studies of Frequency Response of Secondary Systems Under Ground-Acceleration Excitations," by Y. Yong and Y.K. Lin, 6/10/87, (PB88-134309/AS).

NCEER-87-0013 "Frequency Response of Secondary Systems Under Seismic Excitation," by J.A. HoLung, J. Cai and Y.K. Lin, 7/31/87, (PB88-134317/AS).

NCEER-87-0014 "Modelling Earthquake Ground Motions in Seismically Active Regions Using Parametric Time Series Methods," by G.W. Ellis and A.S. Cakmak, 8/25/87, (PB88-134283/AS).

NCEER-87-0015 "Detection and Assessment of Seismic Structural Damage," by E. DiPasquale and A.S. Cakmak, 8/25/87, (PB88-163712/AS).

NCEER-87-0016 "Pipeline Experiment at Parkfield, California," by J. Isenberg and E. Richardson, 9/15/87, (PB88-163720/AS).

NCEER-87-0017 "Digital Simulation of Seismic Ground Motion," by M. Shinozuka, G. Deodatis and T. Harada, 8/31/87, (PB88-155197/AS). This report is available only through NTIS (see address given above).

NCEER-87-0018 "Practical Considerations for Structural Control: System Uncertainty, System Time Delay and Truncation of Small Control Forces," J.N. Yang and A. Akbarpour, 8/10/87, (PB88-163738/AS).

NCEER-87-0019 "Modal Analysis of Nonclassically Damped Structural Systems Using Canonical Transformation," by J.N. Yang, S. Sarkani and F.X. Long, 9/27/87, (PB88-187851/AS).

NCEER-87-0020 "A Nonstationary Solution in Random Vibration Theory," by J.R. Red-Horse and P.D. Spanos, 11/3/87, (PB88-163746/AS).

NCEER-87-0021 "Horizontal Impedances for Radially Inhomogeneous Viscoelastic Soil Layers," by A.S. Veletsos and K.W. Dotson, 10/15/87, (PB88-150859/AS).

NCEER-87-0022 "Seismic Damage Assessment of Reinforced Concrete Members," by Y.S. Chung, C. Meyer and M. Shinozuka, 10/9/87, (PB88-150867/AS). This report is available only through NTIS (see address given above).

NCEER-87-0023 "Active Structural Control in Civil Engineering," by T.T. Soong, 11/11/87, (PB88-187778/AS).

NCEER-87-0024 Vertical and Torsional Impedances for Radially Inhomogeneous Viscoelastic Soil Layers," by K.W. Dotson and A.S. Veletsos, 12/87, (PB88-187786/AS).

NCEER-87-0025 "Proceedings from the Symposium on Seismic Hazards, Ground Motions, Soil-Liquefaction and Engineering Practice in Eastern North America," October 20-22, 1987, edited by K.H. Jacob, 12/87, (PB88-188115/AS).

NCEER-87-0026 "Report on the Whittier-Narrows, California, Earthquake of October 1, 1987," by J. Pantelic and A. Reinhorn, 11/87, (PB88-187752/AS). This report is available only through NTIS (see address given above).

NCEER-87-0027 "Design of a Modular Program for Transient Nonlinear Analysis of Large 3-D Building Structures," by S. Srivastav and J.F. Abel, 12/30/87, (PB88-187950/AS).

NCEER-87-0028 "Second-Year Program in Research, Education and Technology Transfer," 3/8/88, (PB88-219480/AS).

NCEER-88-0001 "Workshop on Seismic Computer Analysis and Design of Buildings With Interactive Graphics," by W. McGuire, J.F. Abel and C.H. Conley, 1/18/88, (PB88-187760/AS).

NCEER-88-0002 "Optimal Control of Nonlinear Flexible Structures," by J.N. Yang, F.X. Long and D. Wong, 1/22/88, (PB88-213772/AS).

NCEER-88-0003 "Substructuring Techniques in the Time Domain for Primary-Secondary Structural Systems," by G.D. Manolis and G. Juhn, 2/10/88, (PB88-213780/AS).

NCEER-88-0004 "Iterative Seismic Analysis of Primary-Secondary Systems," by A. Singhal, L.D. Lutes and P.D. Spanos, 2/23/88, (PB88-213798/AS).

NCEER-88-0005 "Stochastic Finite Element Expansion for Random Media," by P.D. Spanos and R. Ghanem, 3/14/88, (PB88-213806/AS).

NCEER-88-0006 "Combining Structural Optimization and Structural Control," by F.Y. Cheng and C.P. Pantelides, 1/10/88, (PB88-213814/AS).

NCEER-88-0007 "Seismic Performance Assessment of Code-Designed Structures," by H.H-M. Hwang, J-W. Jaw and H-J. Shau, 3/20/88, (PB88-219423/AS).

NCEER-88-0008 "Reliability Analysis of Code-Designed Structures Under Natural Hazards," by H.H-M. Hwang, H. Ushiba and M. Shinozuka, 2/29/88, (PB88-229471/AS).

NCEER-88-0009 "Seismic Fragility Analysis of Shear Wall Structures," by J-W Jaw and H.H-M. Hwang, 4/30/88, (PB89-102867/AS).

NCEER-88-0010 "Base Isolation of a Multi-Story Building Under a Harmonic Ground Motion - A Comparison of Performances of Various Systems," by F-G Fan, G. Ahmadi and I.G. Tadjbakhsh, 5/18/88, (PB89-122238/AS).

NCEER-88-0011 "Seismic Floor Response Spectra for a Combined System by Green's Functions," by F.M. Lavelle, L.A. Bergman and P.D. Spanos, 5/1/88, (PB89-102875/AS).

NCEER-88-0012 "A New Solution Technique for Randomly Excited Hysteretic Structures," by G.Q. Cai and Y.K. Lin, 5/16/88, (PB89-102883/AS).

NCEER-88-0013 "A Study of Radiation Damping and Soil-Structure Interaction Effects in the Centrifuge," by K. Weissman, supervised by J.H. Prevost, 5/24/88, (PB89-144703/AS).

NCEER-88-0014 "Parameter Identification and Implementation of a Kinematic Plasticity Model for Frictional Soils," by J.H. Prevost and D.V. Griffiths, to be published.

NCEER-88-0015 "Two- and Three- Dimensional Dynamic Finite Element Analyses of the Long Valley Dam," by D.V. Griffiths and J.H. Prevost, 6/17/88, (PB89-144711/AS).

NCEER-88-0016 "Damage Assessment of Reinforced Concrete Structures in Eastern United States," by A.M. Reinhorn, M.J. Seidel, S.K. Kunnath and Y.J. Park, 6/15/88, (PB89-122220/AS).

NCEER-88-0017 "Dynamic Compliance of Vertically Loaded Strip Foundations in Multilayered Viscoelastic Soils," by S. Ahmad and A.S.M. Israil, 6/17/88, (PB89-102891/AS).

NCEER-88-0018 "An Experimental Study of Seismic Structural Response With Added Viscoelastic Dampers," by R.C. Lin, Z. Liang, T.T. Soong and R.H. Zhang, 6/30/88, (PB89-122212/AS).

NCEER-88-0019 "Experimental Investigation of Primary - Secondary System Interaction," by G.D. Manolis, G. Juhn and A.M. Reinhorn, 5/27/88, (PB89-122204/AS).

NCEER-88-0020 "A Response Spectrum Approach For Analysis of Nonclassically Damped Structures," by J.N. Yang, S. Sarkani and F.X. Long, 4/22/88, (PB89-102909/AS).

NCEER-88-0021 "Seismic Interaction of Structures and Soils: Stochastic Approach," by A.S. Veletsos and A.M. Prasad, 7/21/88, (PB89-122196/AS).

NCEER-88-0022 "Identification of the Serviceability Limit State and Detection of Seismic Structural Damage," by E. DiPasquale and A.S. Cakmak, 6/15/88, (PB89-122188/AS).

NCEER-88-0023 "Multi-Hazard Risk Analysis: Case of a Simple Offshore Structure," by B.K. Bhartia and E.H. Vanmarcke, 7/21/88, (PB89-145213/AS).

NCEER-88-0024 "Automated Seismic Design of Reinforced Concrete Buildings," by Y.S. Chung, C. Meyer and M. Shinozuka, 7/5/88, (PB89-122170/AS).

NCEER-88-0025 "Experimental Study of Active Control of MDOF Structures Under Seismic Excitations," by L.L. Chung, R.C. Lin, T.T. Soong and A.M. Reinhorn, 7/10/88, (PB89-122600/AS).

NCEER-88-0026 "Earthquake Simulation Tests of a Low-Rise Metal Structure," by J.S. Hwang, K.C. Chang, G.C. Lee and R.L. Ketter, 8/1/88, (PB89-102917/AS).

NCEER-88-0027 "Systems Study of Urban Response and Reconstruction Due to Catastrophic Earthquakes," by F. Kozin and H.K. Zhou, 9/22/88, to be published.

NCEER-88-0028 "Seismic Fragility Analysis of Plane Frame Structures," by H.H-M. Hwang and Y.K. Low, 7/31/88, (PB89-131445/AS).

NCEER-88-0029 "Response Analysis of Stochastic Structures," by A. Kardara, C. Bucher and M. Shinozuka, 9/22/88.

NCEER-88-0030 "Nonnormal Accelerations Due to Yielding in a Primary Structure," by D.C.K. Chen and L.D. Lutes, 9/19/88.

NCEER-88-0031 "Design Approaches for Soil-Structure Interaction," by A.S. Veletsos, A.M. Prasad and Y. Tang, 12/30/88.

NCEER-88-0032 "A Re-evaluation of Design Spectra for Seismic Damage Control," by C.J. Turkstra and A.G. Tallin, 11/7/88, (PB89-145221/AS).

NCEER-88-0033 "The Behavior and Design of Noncontact Lap Splices Subjected to Repeated Inelastic Tensile Loading," by V.E. Sagan, P. Gergely and R.N. White, 12/8/88.

NCEER-88-0034 "Seismic Response of Pile Foundations," by S.M. Mamoon, P.K. Banerjee and S. Ahmad, 11/1/88, (PB89-145239/AS).

NCEER-88-0035 "Modeling of R/C Building Structures With Flexible Floor Diaphragms (IDARC2)," by A.M. Reinhorn, S.K. Kunnath and N. Panahshahi, 9/7/88.